

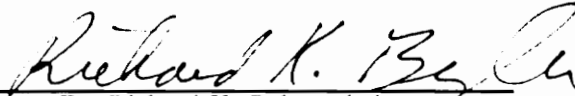
**Development of an Inexpensive Computer Vision System
for Grading Oyster Meats**

by

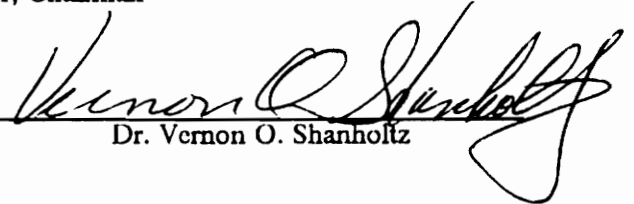
Teck Wah Awa

Thesis submitted to the Faculty of the
Virginia Polytechnic Institute and State University
in partial fulfillment of the requirements for the degree of
Master of Science
in
Agricultural Engineering

APPROVED:


Dr. Richard K. Byler, Chairman


Dr. Kenneth C. Diehl


Dr. Vernon O. Shanholtz

May, 1988

Blacksburg, Virginia

2

LD
5655
V855
1988
A842
C.2

**Development of an Inexpensive Computer Vision System
for Grading Oyster Meats**

by

Teck Wah Awa

Dr. Richard K. Byler, Chairman

Agricultural Engineering

(ABSTRACT)

The objective of this study was to develop an inexpensive automated device for grading raw oyster meats. The automation technique chosen was digital imaging. Typically, a computer vision system contains a microcomputer and a digital camera. An inexpensive digital camera connected to a personal computer was used to measure the projected area of the oyster meats. Physical characteristics of the oyster meats were important in designing a computer vision grading system and the necessary data were not found in the literature. Selected physical characteristics of oyster meats, including the projected area, weight, height, and volume were measured by independent methods. The digital image areas were found to be highly correlated to oyster meat volumes and weights. Currently oysters are marketed on the basis of volume. The results from this study indicated that the relationship between the oyster meat area as measured by computer vision and volume can be used as a grading criterion. The oysters ranged in volume from 3.5 cm³ to 19.4 cm³. A three dimensional image was not required because the height was not important. Tests showed that the system was consistent and successfully graded 5 oysters per second. The system was calibrated, and the prediction equation was validated with an estimated measurement error of ± 3.04 cm³ at a 95% confidence level. The development of automated graders using digital imaging techniques could help improve the quality and consistency of the graded oyster meats.

Acknowledgements

The author expresses his deepest appreciation to his major professor, Dr. R. K. Byler for his valuable suggestions and continued encouragement in dealing with problems during the last two years. Sincere appreciation is extended to Dr. K. C. Diehl and Dr. V. O. Shanholtz for serving in the graduate committee and for their critical reviews. Many thanks to the Gulf and South Atlantic Fisheries Development Foundation, Inc. for supporting the study. The author is thankful to Mr. Peter Hien and Mr. Maarten van Gelder for their previous work and help in building and analyzing the system. And finally, special thanks are due to all those who have given the author the opportunity and the support throughout the graduate study. The author wishes to dedicate his thesis to his mother who has given him the support to come all this way.

Table of Contents

Chapter I. Introduction	1
Chapter II. Objectives	4
Chapter III. Literature Review	5
3.1. General	5
3.2. Digital Imaging Methods	7
3.2.1. Image Sensing	8
3.2.2. Image Analysis	8
3.2.3. Image Interpretation	9
3.3. Illumination Techniques	10
3.4. Agricultural Applications	11
3.5. Commercialized Machine Vision Systems	16
3.6. Oyster Physical Properties and Grading Automation	17
Chapter IV. Measurement of Physical Properties	21
4.1. General	21

4.2. Methodology	23
4.2.1. Projected Area Measurement	23
4.2.2. Weight Measurement	27
4.2.3. Height Measurement	27
4.2.4. Volume Measurement	30
4.3. Statistic Analysis	32
4.4. Conclusion	40
Chapter V. Digital Camera System Testing	43
5.1. General	43
5.2. Lighting Readjustment Test	44
5.3. Replacement Test	45
5.4. Conclusion	46
Chapter VI. Oyster Meat Grading System Development	50
6.1. General	50
6.2. System Components	51
6.2.1. Digital Camera	51
6.2.1.1. Principle of Operation	55
6.2.1.2. Control Hardware	57
6.2.1.3. Command Functions	58
6.2.2. Illumination Technique	60
6.2.3. Conveying Mechanism	62
6.2.3.1. Gearmotor	64
6.2.3.2. Speed Controller	64
6.2.3.3. Rotating Disc	67
6.3. System Software	70

Chapter VII. System Testing and Evaluation	78
7.1. General	78
7.2. Processing Time	79
7.3. Area Calibration at Different Target Velocities	79
7.4. Grading Rate	81
7.5. System Testing	89
7.6. System Evaluation	92
Chapter VIII. System Improvement	95
8.1. General	95
8.2. New Camera Design	95
8.3. Three Images per Exposure	96
Chapter IX. Summary and Conclusion	103
Chapter X. Recommendations	106
Bibliography	109
Appendix A. Digital Camera Calibration Data	112
Appendix B. Physical Properties Data	117
Appendix C. Image Display Software	124
Appendix D. System Software	131
Appendix E. System Calibration Data	139

Appendix F. Cross Validation Data	142
Appendix G. Calibration Data with 6.5 mm Lens	144
Vita	145

List of Illustrations

Figure 1. A Block Diagram of a Typical Image Processing System 6

Figure 2. The Frequently Used Illumination Techniques (Gonzalez, 1983) 12

Figure 3. Absorbance of Oyster Shell and Meat as a Function of Wavelength (Wheaton, et al., 1985) 22

Figure 4. Schematic of the Height Measurement Device 28

Figure 5. Schematic of the Air-Comparison Pycnometer 31

Figure 6. Plot of Volume versus Height 35

Figure 7. Plot of Volume versus Weight 36

Figure 8. Plot of Volume versus Image Area 37

Figure 9. Plot of Image Area versus Photographic Area 38

Figure 10. Plot of Weight versus Image Area 41

Figure 11. Schematic of the Completed System 52

Figure 12. The 256 x 256 Optic RAM and The "Honeycomb" Pixel Arrangement 53

Figure 13. Spectral Response of Photodiodes and an Incandescent Light Source 61

Figure 14. Reciprocal Fluence versus Wavelength for IS32 Optic RAM 63

Figure 15. Diagram of the Gearmotor 65

Figure 16. Diagram of the Speed Controller 66

Figure 17. Physical Dimensions of the Rotating Disc 68

Figure 18. System Flow Chart 74

Figure 19. Overlapping images 75

Figure 20. Display Showing Images of the Metal Targets at Different Speeds 83

Figure 21. Display Showing the Oyster Images Stationary and at 15 RPM 84
Figure 22. A Monitor Display Showing the Sorted Oyster Meats' Category 88
Figure 23. Plots of Volume versus Area for Both the Select and Standard Oysters 94
Figure 24. Three Images per Exposure Displays 99

List of Tables

Table 1. Results of the Linear Regression Model with/without Intercepts	26
Table 2. Pearson Correlation Coefficient Analyses	33
Table 3. The Linear Regression for Volume-Area and Weight-Area Models	42
Table 4. Lighting Readjustment Test Results with Metal Targets.	47
Table 5. Lighting Readjustment Test Results with Oyster Meats	48
Table 6. Replacement Test Results with Oyster Meats.	49
Table 7. Optic RAM Dimension	54
Table 8. Picture Transmission Time (in Milliseconds).	56
Table 9. Friction Coefficient of the Oyster Meats	71
Table 10. Industry Sorting Standards For Eastern Shore Oysters	77
Table 11. Results of the Processing Speed Analysis	80
Table 12. The Linear Statistics at the Different Speeds	82
Table 13. Percent of Image Size Decreases at 15 RPM Compared to Stationary	85
Table 14. Grading Rates at Different Motor Speeds.	87
Table 15. Cross Validation for Determination of Model Performance	90
Table 16. Oyster's Category Standards in Term of Area and Pixels at 15 RPM	91
Table 17. Data Collected and Analyzed for the 25 Oyster Meats	93
Table 18. Linear Regression Results for the 6.5 mm C-mount Lens	97
Table 19. Linear Regression Results for Three Images per Exposure	100
Table 20. F-test and Duncan test Statistics for Three Images per Exposure	102

Chapter I. Introduction

Oysters are one of the most important products of the seafood industry in the Gulf and Atlantic regions. The oyster industry is still dependent exclusively on hand labor for shucking and grading. After shucking, oyster meats are normally graded and sorted into several categories, by hand, based on oyster volume. Rising labor costs, shortage of experienced labor, and increasing operation costs have affected the viability of the oyster industry. In addition, manual grading and sorting are subjective and susceptible to human error. Factors such as eye fatigue, personal bias, and variations in lighting conditions influence the decision of an individual in grading and sorting operations.

Automation of the grading and sorting process would help to solve these problems. Automation of the oyster grading and sorting process would lower labor costs, improve tedious and uncomfortable working environments, increase production rates, and improve performance and quality assurance. Data obtained from automated operations are usually nondestructive, and increasingly affordable as technology improves. Removing human analysis from the grading and sorting lines not only will eliminate error associated with manual techniques but also will increase the analytical precision. The tasks can be repeated in the same way by using software controlled procedures and necessary feedback information from the process can be obtained. The operational flexibility of the system can be increased due to the capability of reprogramming the system software. These ad-

vantages could be achieved by attaching a grading device to a host computer which would allow accurate record keeping of the process.

A preliminary requirement for designing automated devices is a knowledge of the physical properties of the specimen to be graded (i.e., oyster meat). The natural biological variation of living creatures increases the difficulty of developing automated devices for handling agricultural products. There are no commercially available automated machines for shucking or for grading oysters because of the difficulty in handling the oyster meats and the natural variation between individuals. This biological variation has not been controlled, however, this difficulty should not stop the introduction of automation to the oyster industry.

At the present state of technology, there are many automation principles and techniques which can be used, especially with the application of digital electronics. Of all the possibilities, the technique of machine vision has generated the most interest. There are already many examples in the literature on the use of machine vision, but still there is a great potential for improvement and expanded applications. One of the greatest human inventions of this century was the robot, a machine that can "see", "think", and "move". Since the sixties, engineers have known how to furnish machines with sight using computers and television cameras - the brain and the eye of the machine, respectively. Software tells the machine's brain how to manipulate and interpret the image formed by the machine's eye, and the machine can see what it is doing. But the earlier technology required high computing power, only available on expensive mainframe computers, for performing simple tasks. Only recently has it become possible for sophisticated tasks to be performed by inexpensive microcomputers. New applications are thereby available for machine vision in factories, in academia, and in research and development institutions. The various tasks performed by machine vision in agriculture are much the same as in other production environments such as inspection, location, measurement, or recognizing different kinds of objects.

The widespread application of digital image processing techniques for agricultural use is new. However, extensive research and development has taken place in recent years in the areas of com-

puter vision and pattern recognition in agricultural food processing. The promising results obtained by several researchers indicate that there are many more potential applications. Recent decreases in microcomputer costs and the development of specialized hardware and software open a new range of applications of this technology. As Naugle and Rehkugler (1987) stated recently, "...Digital imaging for agricultural field applications is a technology whose time has come. With the development of new computers which are faster and increasingly more powerful, using smaller and smaller components, the possibilities are endless...". The main goal of this study is to demonstrate whether oyster meats can be graded by size using inexpensive computer vision techniques.

Chapter II. Objectives

The overall goal of this study was the development of an inexpensive microcomputer based system for grading raw oyster meats. In this thesis, grading was defined as classifying the objects (i.e., oyster meats) into several categories without separation, and sorting was described as classifying and separating the objects into several categories. The specific objectives of this study were:

1. Determine the selected physical properties of the oyster meats.
2. Design and construct an electronic device for demonstrating a grading mechanism.
3. Determine the accuracy and speed of the electronic device.

Chapter III. Literature Review

3.1. General

By definition, digital image processing operates upon pictorial information in a digital form. A typical image processing system includes a camera, lighting equipment, image processor, host computer (minicomputer or microcomputer), image display monitor, programming terminal, and memory storage. Figure 1 shows the block diagram of a typical image processing system. An image from a television (TV) camera or solid-state sensor array is usually digitized to form a matrix of discrete points (pixels) of defined brightness which will be held in memory for further computer manipulation and interpretation.

A system can be purchased as a complete development package or can be build up from individual bus-based components thereby reducing the system cost (Kranzler, 1985). Usually the custom software development is supported by high-level languages. The cost and the speed of a system are influenced by the resolution of the imaging devices. Although the reliability and flexibility of a system are improved as the resolution increases, the speed of the system is reduced and the cost of the system increases due to additional hardware requirements. Typically, an imaging device has a

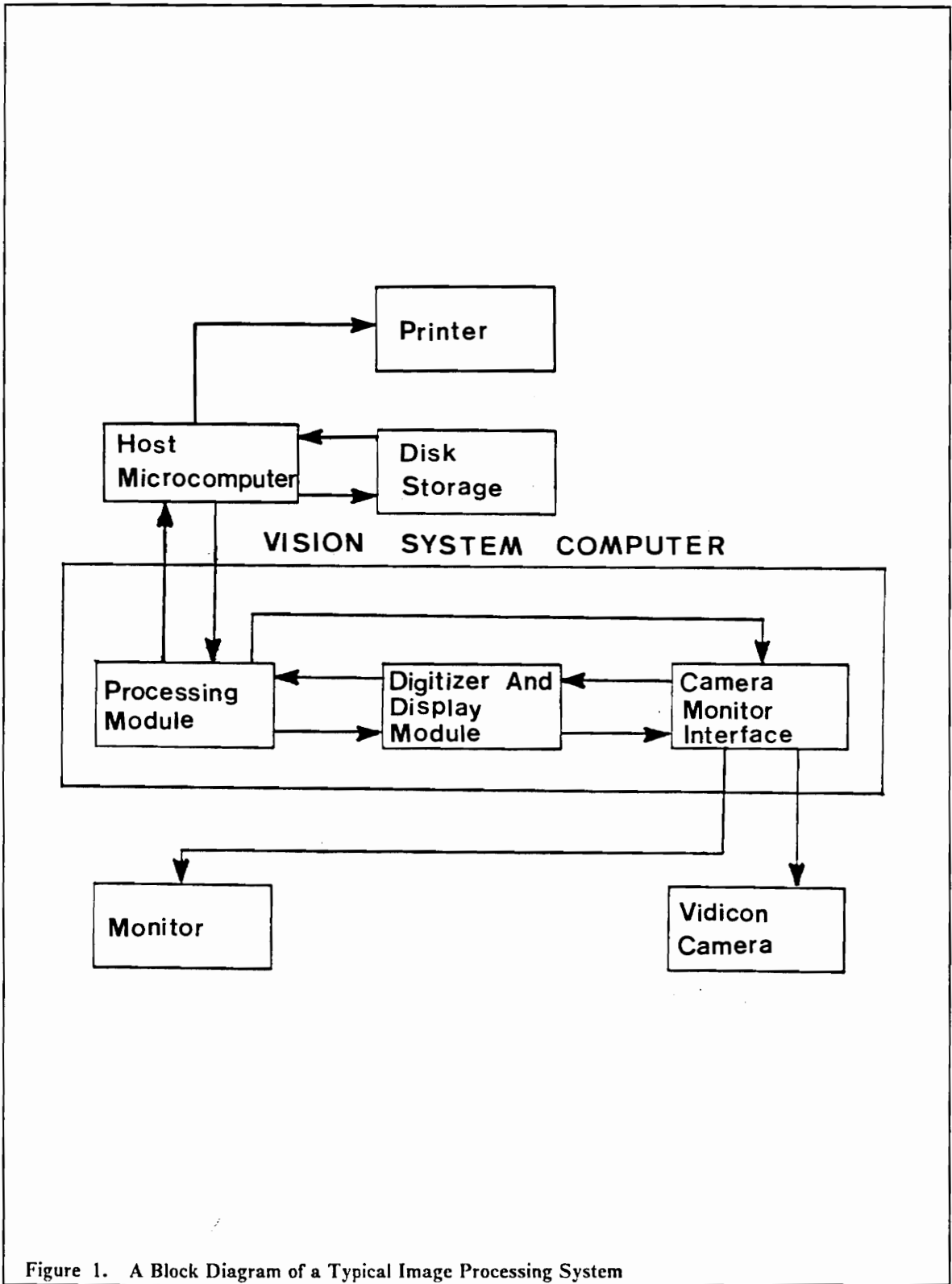


Figure 1. A Block Diagram of a Typical Image Processing System

resolution ranging from 64×64 to 512×512 pixels (or picture elements) and the resolution requirement is dependent on the application (Gonzalez and Safabakhsh, 1982).

The applications of digital image processing can be classified into three categories, as described by Kranzler (1985): 1. image analysis, 2. robotics vision, and 3. inspection. In image analysis, techniques are used to enhance information from the digitized image. Robotics vision refers to the use of camera-coupled image processing to provide real-time visual information. Machine vision inspection usually involves product identification, defect removal, and grading and sorting of raw and processed food products. It is the most frequent application of image processing in agriculture.

Several machine vision systems are now available commercially, and they are beginning to contribute significantly in the agricultural food processing industries. Many of the shape characteristics of the agricultural and biological products are not easily defined mathematically. Precise measurements of their physical characteristics are required before actual machine vision development is carried out.

3.2. Digital Imaging Methods

Whatever the application, machine vision always includes the following procedures which are used to extract, characterize, and interpret information obtained from the image (Gonzalez, 1983, Hollingum, 1984, and Kinnucan, 1983):

1. Image sensing - Acquiring a picture image of the object.
2. Image analysis - Processing the image in order to extract and quantify the important features of the image.

3. Image Interpretation - Identifying and classifying the necessary information based on certain characteristics.

3.2.1. Image Sensing

The basic element in obtaining an image is a light sensitive array which emits an electrical signal whose strength is proportional to the intensity of light falling on it. The image is broken into a matrix of pixels, or picture elements. Each pixel is converted to a number representing its relative lightness in a range of values called a gray scale. The number of gray scale levels which may be detected vary, depending on the image sensing device. Some devices only detect two levels, black and white. These are called binary systems. Others can detect a gray scale ranges from 64 to 256 levels. The image obtained for processing need not come from radiation in the visible range. Special infrared cameras are used for thermal imaging, and ultraviolet lights are used in crack detection. The image also can be derived from an x-ray or radar source. The digitized image is usually stored in computer memory for later processing.

3.2.2. Image Analysis

Image analysis begins with segmentation. Segmentation is the process of dividing an image into the regions of interest. The method of segmentation which is used depends on the actual image application. There are three basic segmentation techniques. Thresholding is the most commonly used approach because of its speed and ease of implementation. The basic idea of thresholding is to divide the image into separate areas by looking at the image intensity. In the simplest case, a pixel having intensity above a certain threshold value is treated as part of the object and a pixel with an intensity below the threshold value is considered as part of the background. With well-controlled illumination a single constant threshold value can usually isolate the object from the background.

A silhouette of the object is produced. For cases involving gray scale images, where the difference between the object and background is not clearly defined, several threshold values might be needed to separate the object from the background. In edge detection, the image is transferred to an outline drawing, usually by a mathematical technique called convolution. Convolution changes an image from a representation of variation of light intensity over a scene to a representation of rate of change of light intensities over a scene. This effectively reduces the image to a line drawing, since light values typically change most rapidly at object edges. Region-growing detection is applicable when thresholding or edge detection fails to differentiate the objects from others or from the background. In region-growing detection, the image is divided into batches of similar levels of gray scale. This method is seldom used because it requires intensive computation power. Many of the problems that would require region-growing detection can be handled by one of the previous two methods, through special illumination techniques or by other enhancement techniques.

3.2.3. Image Interpretation

Once an object is extracted from the background, the vision system must recognize and classify the object. Object recognition is the key to interpretation. Recognition is a labelling process, identifying each object and assigning a name or a label. The basic idea of recognition is to select a set of descriptive features from the extracted object and later use them to classify the object. The descriptive features include things such as area, perimeter, centroid, moment of inertia, Euler number, principal axis and other parameters. Image interpretation can be simple or complex depending on the application. Image interpretation ends with assigning a meaning to the labeled object, or decision making. The system will first go through "learning" sessions. This can be done by showing a number of "good" parts to the system. The system will then build up a numerical model of what constitute a "good" part. There are two basic forms of classification techniques: template matching and feature-matching. In template matching, the actual image of the object is stored. In feature matching, features of the object's image such as area and perimeter are stored. The input image is

matched or compared with the symbolic models stored and the classification is based on a pre-selected matching criteria or similarity measurements (e.g., correlation).

3.3. Illumination Techniques

Illumination is critical in designing an efficient computer vision system. Computer vision is very sensitive to lighting and reflection might be a problem. A well-designed illumination system will minimize the complexity of the resulting image and enhance information required for inspection and decision making. There are a number of illumination techniques developed to make detection, extraction, and interpretation of object features easier for recognition algorithms. Some of the illumination techniques and their applications in machine vision designs, as described by Gonzalez (1983) are:

1. Diffused front lighting - This technique can be used for objects characterized by smooth and regular surfaces.
2. Backlighting - Suitable for applications where object silhouettes are sufficient for recognition and other measurements.
3. Spatially modulated lighting - This method involves projecting points, stripes, or grids onto an object. The distortion of the light pattern is detected in the image and is used to determine the object curvature.
4. Directional lighting - This technique can be used particularly for the inspection of rough surfaces. Flaws on the surface can be detected with careful choice of projected light.
5. Laser sources - They are occasionally used for their brightness, coherence, and beam directionality.

Figure 2 shows the basic illumination techniques frequently used in vision system designs. Paulsen and McClure (1986) examined the effects of illumination on computer vision systems. They stated that diffused lighting is essential to enhance surface features, eliminate shadows, reflections, and to obtain well defined edges.

3.4. Agricultural Applications

With the present advancement of electronics technology, the use of artificial vision in agricultural applications is receiving increasing attention. There has been much research recently in using digital image techniques in product identification, quality inspection, grading and sorting, separation, and other functions.

A low resolution binary image processing system was described by Kaminaka, et al. (1982). The image processing system contained a Periphicon 5// camera and an Apple II microcomputer with a disk memory storage. The inexpensive system included algorithms for comparison of simple shapes and orientations. These images were compared with the images previously stored in the memory. This system could be used for measuring the size of simple objects.

In product identification and inspection, image processing has been used in a number of food processing applications. Nakahara, et al. (1979) used image processing on a large scale in the automation of a cucumber sorting line. The system consisted of a photo-diode line sensor, an image processor, a controller, an illumination source, and a multi-row tilting tray conveyor. Cucumbers were sorted into three shape categories and five size categories at rates up to 10 per second.

Sarkar and Wolfe (1985a) worked on digital image analysis and developed algorithms for orientation of fresh market tomatoes and for classifying them based on size, shape, color, and surface defects.

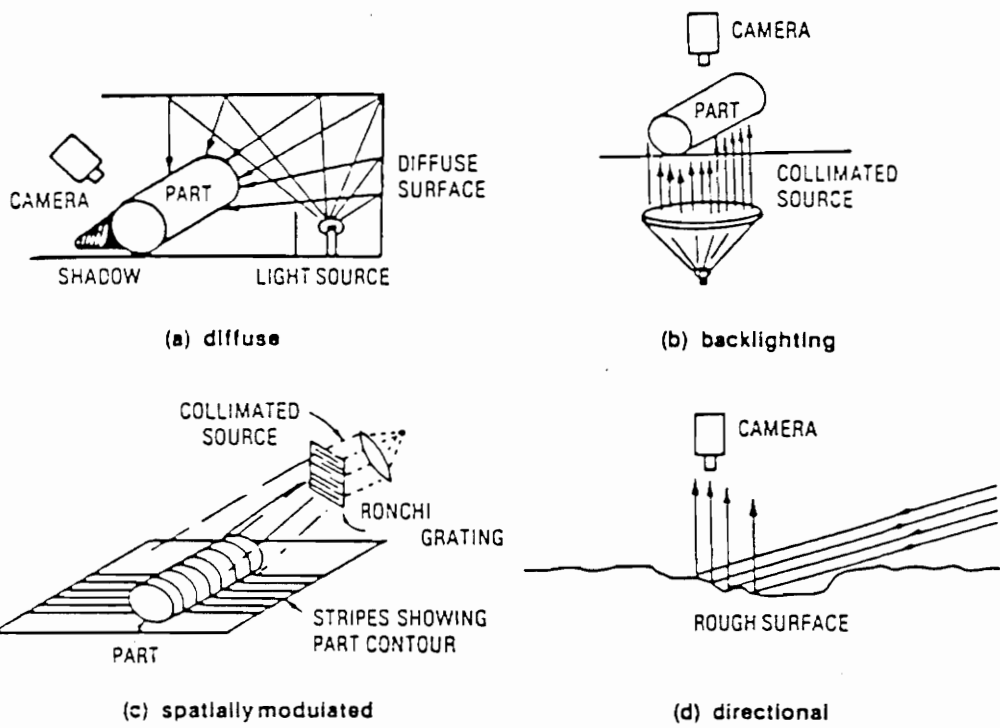


Figure 2. The Frequently Used Illumination Techniques (Gonzalez, 1983)

Results from their study demonstrated the feasibility of applying computer vision to inspecting tomatoes. Proper illumination was important in designing their computer vision system. In their later study (Sarkar and Wolfe, 1985b), they constructed an illumination chamber to minimize the reflections from the tomato surface. A flat white latex paint was used to paint the inside wall of a 52 cm diameter metal cylinder and a single layer of 1 mm thick translucent polyethylene sheeting was used to make the inner half cylinder. The illumination was provided by a 33 watt fluorescent tube. Tomatoes were transported through the illumination chamber by a belt conveyor. The complete tomato sorting system demonstrated a sorting error of 3.5%. However, the system was not suitable for commercial use because of the speed limitation, which was approximately 6 seconds per tomato.

Apple sorting with computer vision was investigated by Rehkugler and Throop (1986). They developed and tested an apple handling and sorting device for bruise detection and classification of apples into United State Department of Agriculture (USDA) grades. A rotating cone and wheel mechanism were built to rotate the fruit 360°, with the stem calyx axis in the vertical direction. Their vision system used a 64 pixel line scan camera. They developed a simplified image processing algorithm with a possible real time processing rate of 30 apples per minute. A correlation ranging from 0.63 to 0.84 was observed between the predicted and measured bruise areas. A strong correlation between bruise depth and measured bruise surface area was confirmed.

Sunkist, the well known citrus packer and distributor, developed unique sorting and packing equipment that performed functions not commercially available on other equipment (Jonhson, 1985). The citrus was sorted based on volume. The features of the machine included a singulator loader which loaded the cups on the sizing conveyor. The two electronic cameras above the cup took pictures of each fruit passing by. The computer determined the volume, the number of fruit in each size, and the total number of pieces handled. The sizer was modular, so lanes could be added at later date. The theoretical speed was 6 citrus per second per lane. However, the system was 90% efficient with a sorting rate of 5.4 citrus per second per lane considered as its maximum capacity.

Sistler, et al. (1983) worked on a video image analyzer which measured surface areas, volumes, and centroids of irregular shape objects. The object to be measured was rotated and several images were taken. They used a Data Cube *VG/20d* Video digitizer board to acquire and digitize the video image sent from a Cohu *4400* monochrome video camera with a 320 row \times 240 column pixel configuration. The camera had a 70-210 zoom lens with close-up rings. The computer system was an Intel *86/330A* and programs were written in FORTRAN *86* running under Intel's *iRMX 86* operating system. The object lighting was provided by a combination of incandescent and fluorescent light sources. Initial testing on sweet potatoes showed the volume error to be less than 5% for most samples and with a maximum of 13% for a very irregularly-shaped potato.

Recently, McClure and Morrow (1987) constructed a computer vision system for sorting white potatoes by size. They installed a Chorus Data Systems PC-EYE video capture system with a 320 row \times 200 column pixel resolution and with 4 bits grey level into an IBM PCTM. Two closed circuit video cameras were connected to the PC-EYE board for screening the side and top views of the potato. A light shielding box was constructed to keep extraneous light out. The object lighting was provided by four thirteen inch fluorescent lights. In addition, warm white fluorescent bulbs were used to give more surface definition. The software was written in MS-BASIC and machine language subroutines provided by the PC-EYE programmer reference software disc. The overall error for the major axis, intermediate axis, and minor axis were recorded to be -1%, 0%, and -2% respectively. Results also showed that weight can be predicted to within 5% for regularly shaped potatoes and the system might be usable for separation of misshapen potatoes. The root mean square value of the boundary directions was able to separate some misshapen potatoes.

The use of computer vision systems to recognize physical properties of small objects such as seed was investigated by several researchers. Berlage, et al. (1987) examined a computer vision system to classify diploid and tetraploid ryegrass seeds. Oriented seeds were sitting on a black rubber (2 cm \times 2 cm) background so that high seed/background contrast could be achieved. Backlighting provided through translucent stage and top lighting was provided by a Schott *KL 1500* fiber optic ring to eliminate shadowing. With this method, 85% of the seeds were correctly classified.

Rigney and Kranzler (1986) presented a real-time computer vision system for grading southern pine seedlings. Singulated seedlings were inspected on a moving non-reflective black conveyor belt. Illumination was provided by fluorescent room lighting and strobed Xenon flash. The classification criteria were based on stem caliper, shoot height, and projected root area. Seedlings were graded in approximately 0.25 seconds with an average classification error rate of 5.7%.

Image processing has not only been successfully used in recognizing small particles, but was also capable of detecting stress cracks in corn kernels as examined by Gunasekaran, et al. (1987). They used a Hitachi *KP-120* solid state video camera for image acquisition. The processing module consisted of an 8 MHz 8086 central processing unit and an 8087 numeric coprocessor. They also investigated different illumination schemes such as front lighting, back lighting, and side lighting. The sources of lighting were provided by the Schott *KL 1500* fiber optic light source. Their results indicated that white light in the back lighting mode with a black-coated background having a circular opening of 2.4 mm in diameter produced high contrast between the stress cracks and the rest of the kernel surface. The image processing algorithm was successful in detecting stress cracks in 90% of the kernels examined.

Image processing techniques were applied in the development of a system for measurement of the size and surface appearance of raw silk thread by Ohura, et al. (1987). The light source was a tungsten-type iodine lamp with a miller capacitor and a light guide, which was a bundle of quartz fibers each having a diameter of 16 micrometers. The light source emitted through the light guide, had a good illumination intensity, and was positioned in an appropriate angle so that the profile of both thread edges were distinctively illuminated. An image guide composed of optical fibers was used to detect and transfer the optical image of the thread to an ITV digital camera using a magnifying lens system. The data processing system included an image processor, a microcomputer with peripheral devices, and an electrical circuit to actuate mechanisms for size control. The system also contained a cathode ray tube (CRT) display, a printer, and floppy disk storage. It was confirmed that the image processing system could measure the size and width of the thread and display the thread image on the monitor screen.

3.5. Commercialized Machine Vision Systems

Several food processing applications have recently been successfully commercialized. These machines are sophisticated and capable of high speed operation. They have potential for improving quality control for the food processing industry. The price of these machines are considered expensive and ranged from \$10,000 to \$100,000; however, the payback periods were usually short, within two years or less (Swientek, 1987 and Wagner, 1983).

There are many food grader and sorter systems available in the market. Moore Brothers' Farms, a blueberry processor in North Carolina, reported that an automatic color sorter made by Clayton-Durand Manufacturing Company had reduced sorting costs 16% and had a sorting accuracy of 90% at a rate of 2400 lb/hr. Six hand sorting stations and blow sorting equipment were removed and the sorting rate rose by 33% (Wagner, 1983). Octek developed a system to classify fish by species, size, and weight (Swientek, 1987). Allen Machinery manufactured an electronic potato grader to sort potatoes according to their length and diameter. Their 8-lane grader handled about 48,000-50,000 lb of potatoes per hour. Accuracy of the grader was approximately 95% based on the length and diameter of the potatoes or a length or diameter difference of ± 0.1 inches (Swientek, 1987). *Opti-Sort* systems by Key Technology and Simco/Ramic was used to detect and segregate defective potato chips, peas, diced vegetables and sliced fruits and the Sortek 4000 bichromatic color sorter detected and rejected defective peach halves, potato chips, cereal flakes, and whole and peeled tomatoes at line speeds up to 25 tons per hour (Przybyla, 1986).

In August 1986, D & K Frozen tested an *Opti-Sort* automatic defect removal system manufactured by Key Technology for handling sliced carrots at 6000 lb/hr (the maximum sorting speed). Carrots fed from a dewatering vibratory shaker on a high-speed belt (500 ft/min). The carrot pieces were propelled from the end of the belt and were inspected on all sides by four cameras. The illumination source was standard fluorescent lamps enclosed in polycarbonate tubes. The machine re-

placed 13 manual inspectors and paid for itself in 2 years. The final product met all grade standards (Robe, 1988).

Vision systems have been developed to sort and pack citrus products, lemons were sorted into three grades (i.e., premium, table, and juice) based on skin blemishes, cucumbers were sorted into three grades according to shape and five sizes according to length, and several other vision grader and sorter systems are under development and investigation (Swientek, 1987). In 1983, several large companies were working on machine vision application in the food industry. Machine Intelligence Corp and its joint venture Yaskawa Electric Co. of Japan, the world largest robot builder, had the intention of entering food plants in the next few years. General Electric, the world largest intelligent systems manufacturer had few applications under development, and needed a few years before it become mature (Wagner, 1983).

3.6. Oyster Physical Properties and Grading Automation

There is very little literature or research done solely on physical properties of oyster meats, but there is some literature on physical properties of the oysters in the shell. In 1950, Newcombe (1950) analyzed certain dimensional relationships of the Virginia oyster. Length, width, total weight, total volume, shell weight, shell volume, wet weight, and dry weight of body tissue were measured. Volume was determined by the overflow displacement method. The values of correlation coefficient between all the measured parameters were found to be large enough to suggest an approximation to a straight line relationship. His results also showed that the dimension of inner volume and dry weight are regarded to be reliable in indicating size. Nascimento, et al. (1980) conducted a study to determine the optimum commercial size for the Mangrove oysters. Growth characteristics were studied by comparing the relationships between total live weight, volume of the shell cavity fluid and yield of meat, and dry body weight to size. The size was defined as the long axis

of the shell from the hinge to the opposite edge. A strong correlation was found between total live weight and size.

Riley and Smyth (1979) discussed the mechanization of handling and processing Maine's cultivated European oyster industry. Rotating tip-up weight graders for grading shellfishes such as oysters have been in use in Europe for many years. But these graders were huge and had a high-capacity and were therefore only feasible for large processing plants. A smaller version of these graders was investigated for use in Maine. In fact, Riley and Smyth (1979) built several experimental units consisting of 2 or 4 pans pivoted at the ends of 0.2 m rotating arms. The pans were designed to stop momentarily at every 90° of rotation and were driven by a geneva mechanism. A spring or counterweight mechanism was attached to the end of each pan. If the pan contents were above a set weight the pan tipped; if below it was carried to another discharge point. A fixed guide ring returned the pan to its horizontal position after tipping. In its most successful form, the machine graded up to 4000 oysters per hour, but hand feeding was still required. Some work was also conducted in conveying and singulating the oysters before they dropped into the grading pans.

Later, Riley and Smyth (1979) found that precise weight grading was not necessary, and it was possible to grade the oysters by size. Several statistical analysis were performed to examine the correlation between weight and size. The results showed that the best correlation was between weight and minimum diameter and the grading based on this criterion would be acceptable.

They also suggested several possible mechanical sorting mechanisms: vibrating tables, mechanical shanking sieves, and rotary drum sorters. Their study showed that the most successful method of grading oysters larger than 2.5 cm in diameter was the rotary drum sorter. The rotary drum sorter consisted of a drum perforated with desired diameter holes mounted at a slight pitch downward, a inlet hopper, and rollers with motor driven chain. The pitch angles were adjustable. The "standard" size sorter used an aluminum drum 91 cm long and 30.5 cm in diameter. They made several interchangeable drums perforated with holes of a diameter ranging from 1.25 cm to 9.5 cm, so that the oysters were separated into several size categories after passing through different drums. Several

tests were carried out with different pitch angles, feeding rates and drum speeds. Experimental results showed that the sorting efficiency was highest at slow drum speed, lower pitch angles, and slow feed rate. Since the goals of high sorting efficiency and high feed rate were conflicting, compromise settings for drum speed and pitch angle were selected. After studying several combinations, a pitch angle of 3.5° and a drum speed of 15.3 meter per minute at a feed rate of 120 oysters per minute (the maximum feed rate for these settings) was selected and gave a sorting accuracy of 95%.

The researchers in the department of Agricultural Engineering, University of Maryland looked into the potential use of a computer vision system in orientation and shucking oysters. Shays and Wheaton (1980) conducted a study on the biological properties of shellfish shells such as oysters. The internal and external shell dimensions were taken from machine photocopies of the oyster shell valves. A projected image of the valve was made by laying its internal side down on a piece of precision transparent grid material and the shell with the grid were placed on the copy machine. Their results show that if portions of the shell were more than 1.2 cm above the copier, edge distortions occurred. Indistinct edge definition was found on 84 out of 490 oysters measured on the photocopy machine. These oysters were measured again by using a ruler and calipers. In their later study, Wheaton, et al. (1985) used a computer vision technique. Their system consisted of a TV camera coupled through a digitizer to a digital computer and projected on a TV screen. Data were collected by projecting horizontal (side) and vertical (top) images of the oyster onto a flat surface containing a precision grid measurement paper. Length and width were measured from the vertical view and thickness was measured from the horizontal view. Data were measured manually by counting the number of grids and entered into the computer for further analysis. A total of 2430 oysters were measured. Linear regression analysis was used to develop empirical equations to relate the various parameter measurements.

After making the required measurements of the physical properties of the oysters, the researchers in University of Maryland carried out the actual computer vision machine development. A study on computer vision applied to oyster orientation was done by Tojeiro and Wheaton (1987). They felt that oysters must be first oriented before entering any shucking machines. A computer vision

system was set up to take a horizontal and vertical view of the oyster simultaneously. They mounted a mirror to an orientating plate which was driven by a stepping motor and a 35.5 cm × 35.5 cm plane mirror at 45° to the horizontal plane. Oysters were viewed by a Sony model *AVC-3200* black and white TV camera with a 1:18 zoom lens. The illumination was provided by two 100 watt soft white incandescent desk lamps. The image processing unit was a Video van Gough board incorporated with an IBM PC™ plus a 8087 coprocessor. The image was displayed on a Sony model *CUM 950* black and white monitor. The system correctly oriented 98.2% of the oysters. The software proved the capability of measuring oyster shell dimensions and efficiently identified the hinge from bill end of an oyster.

Chen and Wheaton (1987) developed a computer vision system to process oyster hinge-end images and extract oyster features. They used a Sony model *AVC-3200* TV camera with a focal length of 50 mm lens to view the trimmed hinge end and produce an analog video image. The oyster was placed on a white plate as background and was illuminated by a General Electric 22 watt, 20 cm diameter fluorescent light. A Video van Gough board digitizer incorporated with an IBM PC™ was used to convert analog image to a digital computer compatible form. The analog and digital images were stored on a video tape and floppy disk, respectively. The system was successfully applied to process oyster hinge-end image data and extract oyster features data. A sample size of 513 oysters was analyzed and the system had an average error rate of 3.2% in locating the oyster hinge-end. The ultimate goal of their study was to develop an automated shucking device.

Chapter IV. Measurement of Physical Properties

4.1. General

Physical characteristics of agricultural products are important in many engineering design and research applications. Knowledge of the volume, height, weight, and projected area of the oyster meats is essential in the development of grading devices. Oyster meats are soft, almost jelly like, and are easily pierced, cut, or torn. Because of the irregularity and variability encountered between individual oyster meats, the task of characterizing these physical parameters was not trivial.

The oyster meats used in this study were Eastern Shore oysters and were obtained from the Atlantic Ocean side of Virginia. Their weight, height, projected area, and volume were measured. The knowledge of the optical properties of the biological materials were also important in the development of a computer vision system. The measurement of the optical properties was not conducted, because it was previously reported by Wheaton, et al. (1985). Figure 3 shows the absorbance of oyster meat and oyster shell. The absolute intensity varied from oyster to oyster even when the same illumination conditions were used.

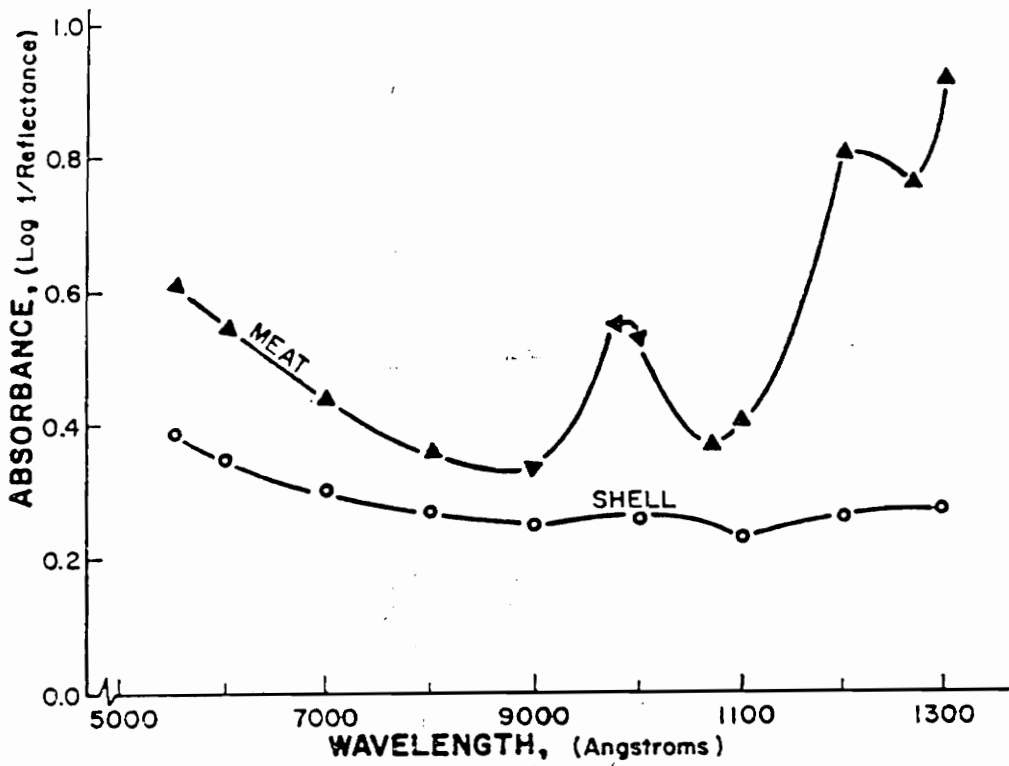


Figure 3. Absorbance of Oyster Shell and Meat as a Function of Wavelength (Wheaton, et al., 1985)

4.2. Methodology

Oyster meats were obtained from a packer on the Atlantic Ocean side of Virginia. A total of 250 oyster meats were analyzed. They were in two batches, 125 standards and 125 selects. Each oyster meat was placed on a glass plate in a manner that would imitate an oyster laying flat, but no special attempts were made to spread the gills. The following sequence of measurements were conducted: projected area, weight, height, and volume. The correlations between each pair of the measured physical properties were examined. An appropriate grade classification criterion was then established based on the results obtained from these correlation analyses.

4.2.1. Projected Area Measurement

The projected areas of the oyster meats were done by digital imaging technique. In order to determine the accuracy of this method, area measurement was also done independently by a photographic technique. Although error was expected in both methods due to the irregularities of the oyster meats, reasonable accuracy was assumed if no significant differences were observed.

In the photographic technique, a camera operating in an automatic exposure setting mode was fastened stationary on a tripod. A piece of grid paper was placed underneath the camera and the camera was then focused based on the grid paper. The same camera settings were used throughout the tests. The grid paper was to assist the area determination of the oyster meats. A oyster meat resting on a glass plate was positioned beneath the camera and a picture was then taken. The photographs were analyzed by a digital planimeter. The collected data were stored in the computer for future statistical analysis.

The digital camera used for this measurement consisted of an *IS32A* Optic RAM, and a 16 mm C-mount lens. The digital camera was connected to an IBM PCTM through a prefabricated circuit board. An excelerator 80286 turbo board (Everex Systems, Inc., 1986) was added to the IBM PCTM and software was developed in Turbo PASCAL version 3.1 with the intention of speeding up the process. Proper illumination was essential in designing the computer vision system. The illumination technique which was chosen was backlighting. A illumination box was built for the backlighting and the illumination was provided by four 15 watt cool white fluorescent tubes. Detailed descriptions of the development of the digital vision system and illumination technique used will be covered in the next two chapters.

Lens aperture affected the focus sharpness, the evenness of field illumination, and the amount of light transmitted; therefore, appropriate focal length and aperture were chosen. The camera lens was focused on an opaque target on translucent paper in the field of view of the camera. The target consisted of lettering and the camera was focused until the image of the letters appeared to be as clear as possible as shown in the monitor screen.

The camera was remarkably light sensitive. From preliminary work, it was observed that any change of the lighting conditions affected the number of pixels counted. This also meant that the area measurement varied significantly as the lighting conditions changed. In order to eliminate this lighting effect, a filter was constructed from three layers of Kodak Wratten gelatin filter N.D. 0.2 which allowed about 40% transmittance of light. The F-stop of the camera was then adjusted to give about 500 dark pixels. This was when approximately 2/3 of the image of the filter was dark pixels and the other 1/3 was bright. Oyster meats were partially translucent, with this lighting adjustment scheme a complete image of the oyster meat could be produced.

The field of view was proportionally related to the working distance. The working distance was defined as the distance from the object to the camera lens. The field of view must be big enough to cover a "large" oyster. Through several experiments, the field of view was found to be roughly

5 cm × 13 cm and the camera height was approximately 1 meter. The same working distance and lens setting were maintained throughout the tests.

Before the actual testing, the digital camera system had to be calibrated. Several metal targets of known area were used to find the area-pixel relationship. The area was determined by counting the number of pixels which appeared to be dark in the image. A linear regression with intercept was performed to determine the area-pixel relationship. It was natural to assume that an object of zero area will have no pixel counted. Through several observations, it was confirmed that this was not the case. For example, a thin wire did have area. But under the digital camera system no area was recorded (no pixel was counted). This was due to the lighting effect at the edge of the object. To further prove this issue, a statistical analysis was carried out. A significance test on dropping one parameter of the linear model (i.e., intercept) was conducted. The conclusion was that the model with an intercept was a better model in estimating the relationship between area and pixel and showed a much better scatter of the residuals. Table 1 shows the calibration statistics of the linear regression model with and without intercepts. Appendix A tabulates the raw calibration data.

The area-pixel least squares equation was found to be:

$$A = 15.3961 + 2.1726P \quad [1]$$

where : A = the area in mm², and

P = the number of pixels in the digital image

with an estimated measurement area of ± 52.38 mm² at 95% confidence level and R² value of 0.9989. The measurement error was determined based on the following principles. The sum of square error was the variability unexplained by the model and the mean square error was the sum of square error divided by the degrees of freedom. The mean square error could be viewed as the sample variance owing to the model error or experimental error. Therefore, root mean square error was the sample standard deviation due to the model error or experimental error (Myers, 1986). Statistically, 2 standard deviations were roughly equal to 95% confidence level which was also equal

Table 1. Results of the Linear Regression Model with/without Intercepts

	No Intercept	With Intercept
Sum of Square Error (SSE)	101784.88	94672.7561
Mean Square Error (MSE)	732.2653	686.03446
Degree of Freedom (DF)	139	138
Root Mean Square Error (RMSE)	27.0604	26.1923
Intercept	-	15.3961
Standard Error	-	4.7817
Slope	2.1902	2.1726
Standard Error	0.002948	0.006163
R²	0.9997	0.9989
Sum of Residuals	461.9418	1.1551E-09

Complete Model (c) : With Intercept

Supplement Model (s) : Without Intercept

Null Hypothesis : Intercept = 0

Alternative Hypothesis : Intercept \neq 0

Test Statistic : $SSE(drop) = SSE(s) - SSE(c)$
 $MSE(drop) = SSE(drop) / (DF(s) - DF(c)) = 7112.124$
 $F(obs) = MSE(drop) / MSE(c) = 10.367$

Rejection Region : $F(0.05,1,138) = 3.84$

Conclusion : Since $F(obs) > F(0.05,1,138)$, reject Null Hypothesis

to 2 root mean square errors. Therefore, a measurement error with a 95% confidence level could be estimated by taking 2 root mean square errors. This was a conservative way of estimating the error and it will be used throughout the text.

After calibration, the system could be used to measure projected areas based on the digital images of the oyster meats. An oyster meat on a glass plate was placed underneath the digital camera and then a digital image was taken and stored for further statistical analysis.

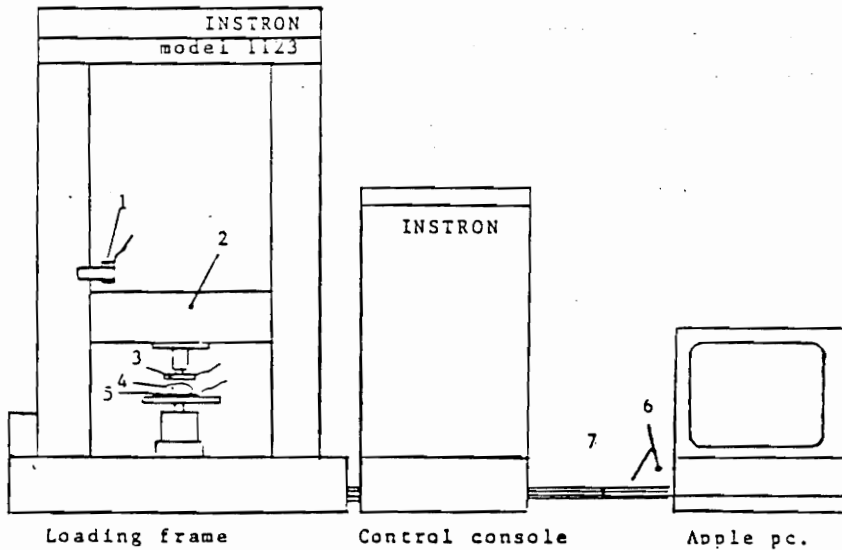
4.2.2. Weight Measurement

The weight was measured by a Sartorius Model *1712 MP8* (Brinkman Instruments Co., 1983) electronic analytical balance with a resolution of 0.0001 grams. The initial weight of the glass plate on which the oyster meat rested was measured and subtracted from the total weight in order to get the oyster weight.

4.2.3. Height Measurement

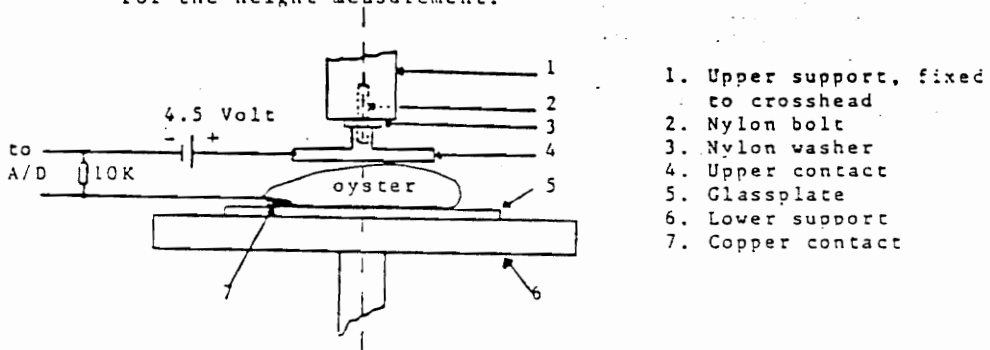
The height was measured by an Instron Model *1123* Universal Testing Instrument. This instrument was chosen due to its precision and movement controllability. Figure 4 is a diagram of the device used for height measurements. The height measurement was conducted with an LVDT (Schaevitz Engineering, 1987). With a 15 VDC excitation, this LVDT gave a voltage output linear to displacement of ± 10 volts over a ± 2.54 mm range.

A simple circuit was assembled using the electrical conductivity of the oyster meat. The circuit contained a 4.5 VDC source and a 10 K Ω resistor in series with the oyster meat. The circuit was isolated from the testing component by a glass plate (on which the oyster meat rested) and by a



1. LVDT
2. Crosshead
3. Upper-contact
4. Oyster
5. Glassplate
6. Cable that connects the A/D-converter to the LVDT and to the 'switch-circuit'.
7. Cable that connects the I/O-32 to the INSTRON

a) Schematic of the configuration as used for the height-measurement.



b) Schematic of the 'switch-circuit'.

Figure 4. Schematic of the Height Measurement Device

nylon bolt and nylon washer between the upper contact and the crosshead. The circuit was linked to an Apple II *plus* 48K microcomputer with a 12 bit A/D converter and an I/O-32 board (Applied Engineering, 1988). The microcomputer was used as a sampling, control, and data acquisition device and software was written in BASIC.

The operation principles were as follows. The crosshead was lowered at a rate of 5 mm per minute. At the moment the upper contact touched the oyster meat, the circuit was closed. Consequently, this caused the voltage across the resistor (which was zero when the circuit was opened) to leap to a higher value. When the voltage reached 300 mV, the control software stopped the crosshead and voltage from the LVDT was read and converted to height. The calibration was first done by zeroing the LVDT with a standard height. To prevent oysters from exceeding the range on the high side, the standard was chosen to be slightly higher than most oysters. Conversely, to adjust for oysters that might fall outside the lower region, calibrated fill plates were used to get those oysters within range.

From initial testing, this measurement method was verified to be accurate and consistent. A variation of ± 0.001 mm was observed when repetitive measurements were carried out on exactly the same point under the upper contact. The variation came from the crosshead movement between successive checks on whether contact was made. With zeroing at the center, repetitive measurements on different spots under the upper contact showed a maximum variation of ± 0.06 mm compared to measurements in the center. The variation was due to the upper contact not being completely paralleled to the plate on which the oyster meat rested.

During actual measurements, an oyster meat on a glass plate was positioned under the upper contact with its highest point as centered as possible. At the end of the negative junction of the wire, a piece of copper was soldered which was positioned under the oyster meat. A measurement was started when a key on the Apple's keyboard was pressed. The control software controlled the measurement and returned the crosshead to its initial position after the measurement was com-

pleted. When an oyster meat was too thin, a warning was given and the measurement was redone with a fill plate. The upper contact was cleaned before each successive measurement.

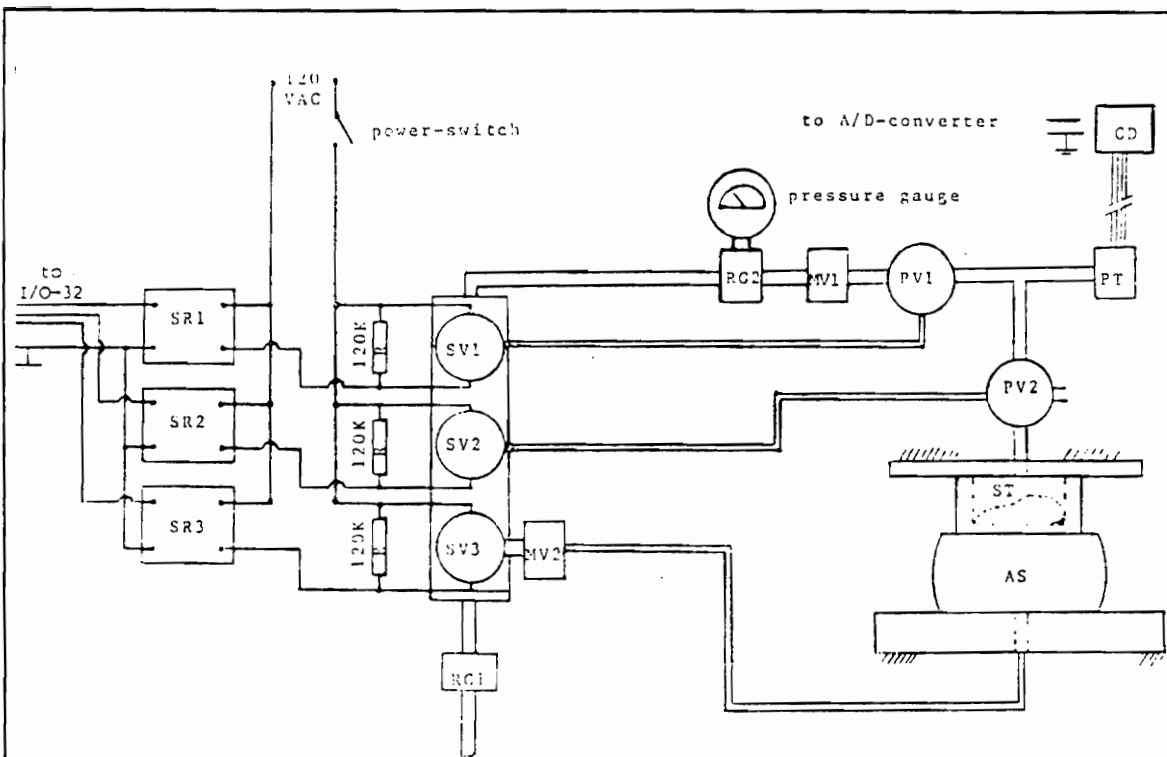
4.2.4. Volume Measurement

The volume was measured by an air-comparison pycnometer. The air-comparison pycnometer used air as the "immersion medium" and was initially designed to measure porosity of granular materials. An air-comparison pycnometer was modified and refined to measure volume of the oyster meats (Diehl, et al., 1988). Figure 5 shows a schematic of the air-comparison pycnometer.

A typical pycnometer consists of two chambers (sample and reference), a pressure valve connecting the two chambers, a differential pressure indicator, and two pistons which control the chamber movement. At the beginning, the differential pressure indicator is zeroed by balancing the pressure in both chamber. Inserting an object into the sample chamber would cause a pressure differential and would be recorded by the differential pressure indicator. The observed pressure differential is proportional to the volume being measured.

The pycnometer designed for this volume measurement used the same principles. The air pressure in the reference tank was allowed to rise when pneumatic valve 2 (PV2) was closed and pneumatic valve 1 (PV1) was opened. When the pressure in the reference tank reached 7 Kpa (1 psi), PV1 was closed. After waiting 20 seconds for equilibrium, the pressure in the reference tank was recorded. Subsequently, solenoid valve 3 (SV3) was opened, pressurizing the air spring which closed the sample tank. Then PV2 was opened and after the pressure reached a steady state, the pressure was recorded. The operation cycle was completed by closing PV2 and SV3. The air spring was depressurized by closing SV3. The sample volume can be determined by the following expression:

$$V_s = V_{2e} \left(\frac{P_i}{P_f} - 1 \right) V_1 \quad [2]$$



SR1, SR2, SR3	Solid state relais
SV1, SV2, SV3	Solenoid valve
PV1, PV2	Pneumatic valve
MV1, MV2	Metering valve
RC1, RC2	Regulator

PT	Pressure transducer
CD	Carrier demodulator
ST	Sample tank
AS	Airspring

Figure 5. Schematic of the Air-Comparison Pycnometer

where : V_s = sample volume,
 V_{2e} = empty sample volume,
 V_1 = reference tank volume,
 P_i = initial reference tank pressure, and
 P_f = final equilibrium pressure in both tanks.

All the volumes were measured in cm^3 and pressures were measured in Kpa. The pycnometer was calibrated by putting prescribed volumes of water and aluminum blocks of 9 different known volumes into the sample tank. Ten measurement were obtained from each volume. The R^2 was found to be 0.9993 with a measurement error of $\pm 0.57 \text{ cm}^3$ at the 95% confidence level.

The pycnometer was connected to an Apple II *plus* microcomputer and used the same hardware as described in height measurement. The control program was written in BASIC for recording the pressures and controlling the valves and solenoids.

4.3. Statistic Analysis

Several statistical analyses were performed on the collected data. All the statistical analyses were done by SAS (Statistical Analysis System Institute Inc., 1982) software, which was available on the mainframe computer. The collected data are listed in Appendix B. Pearson correlation coefficient analyses were conducted to examine the correlation between each pair of measured physical properties. The Pearson correlation coefficient is the measure of the strength of linear relationship between two variables on a sample of n paired measurements and is designated as R . Additionally, the R^2 is the measure of the total variability of the dependent variable that is accounted for by the independent variable in the linear model (Ott, 1984). Table 2 shows the results obtained from Pearson correlation coefficient analysis.

Table 2. Pearson Correlation Coefficient Analyses

	Volume	Height	Weight	Digital Area	Photo Area
Volume	-	0.6143	0.9805	0.9161	0.9053
Height	0.6143	-	0.5999	0.3944	0.3853
Weight	0.9805	0.5999	-	0.9312	0.9224
Digital Area	0.9161	0.3944	0.9312	-	0.9969
Photo Area	0.9053	0.3853	0.9224	0.9969	-

By examining the statistical results, the correlation of weight with volume or projected area with volume would form the grading algorithm since oyster meats are currently graded based on volume. The volume was highly correlated with the weight and the projected area with R values of 0.9850 and 0.9161, respectively. Figure 6, 7, and 8 show the plots of volume versus height, weight, and projected area, respectively. The R value for the volume and height was 0.6143 which was the lowest of those analyzed. The height was also poorly correlated to the weight and projected area with a R value of 0.5999 and 0.3944, respectively.

The weight was also strongly correlated with the projected area with a R value of 0.9312. Ultimately, the basis of grading criteria depended on the reliability of the grading unit. It would have been difficult to achieve the design operation speed with weight type sizers because too much time would be needed for the weighting instrument to be stabilized before an accurate weight measurement of the oyster meat could be recorded. Although the weight type sizers should accurately determine the volume, they would give no indication of the shape of the oysters, which could be detected by projected area measurements. Therefore, the one physical parameter chosen for this oyster meat grading machine was the projected area.

A high correlation was also observed between area obtained by digital imaging and photographic technique. The R value was found to be 0.9969. From this analysis the digital imaging technique was confirmed to be sufficiently reliable. Figure 9 shows a plot of area obtained from digital imaging technique versus area obtained from photographic technique.

Several nonlinear models were tried for modeling the volume-area relationship. None were found to fit the data and the linear least squares model was selected as the best model. The linear regression model chosen was without intercept, since an oyster of zero volume had no area. The volume-area least squares equation was:

$$V = 0.005426 * A \quad [3]$$

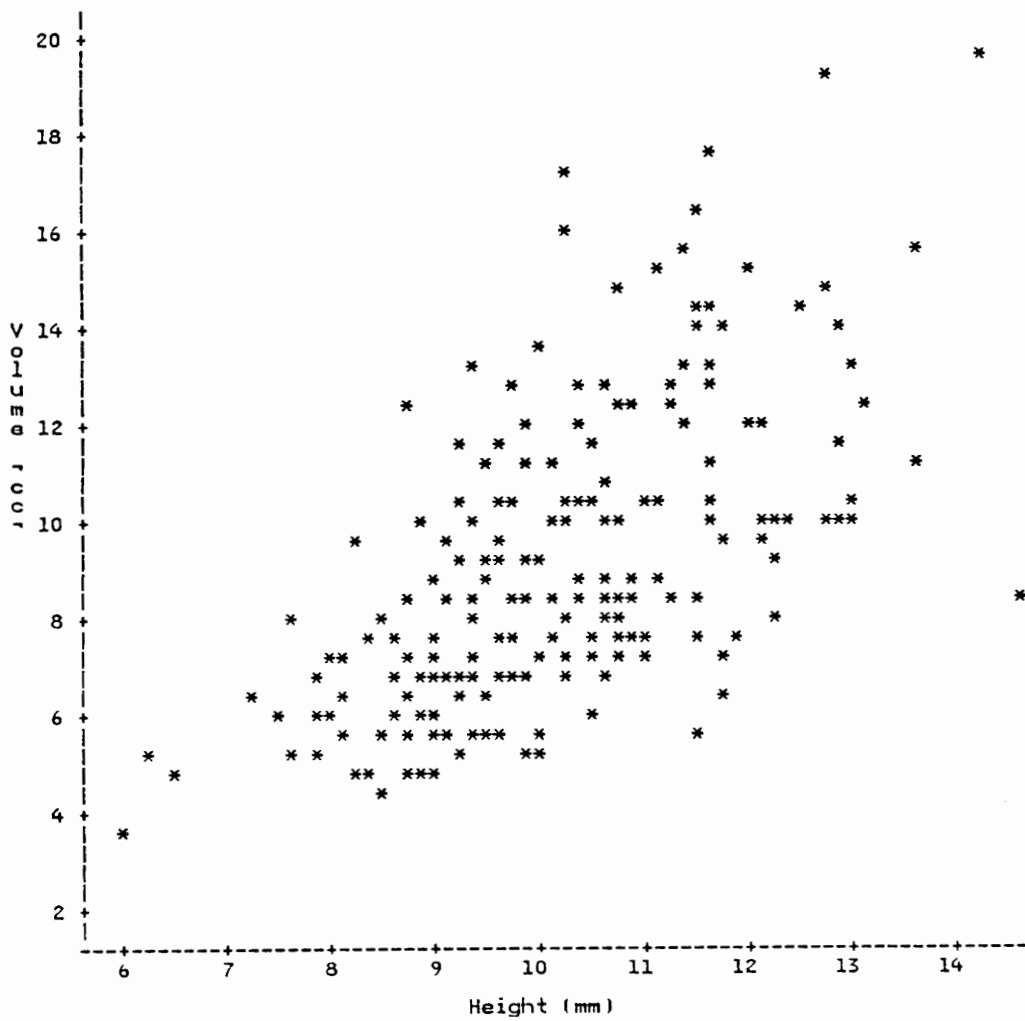


Figure 6. Plot of Volume versus Height

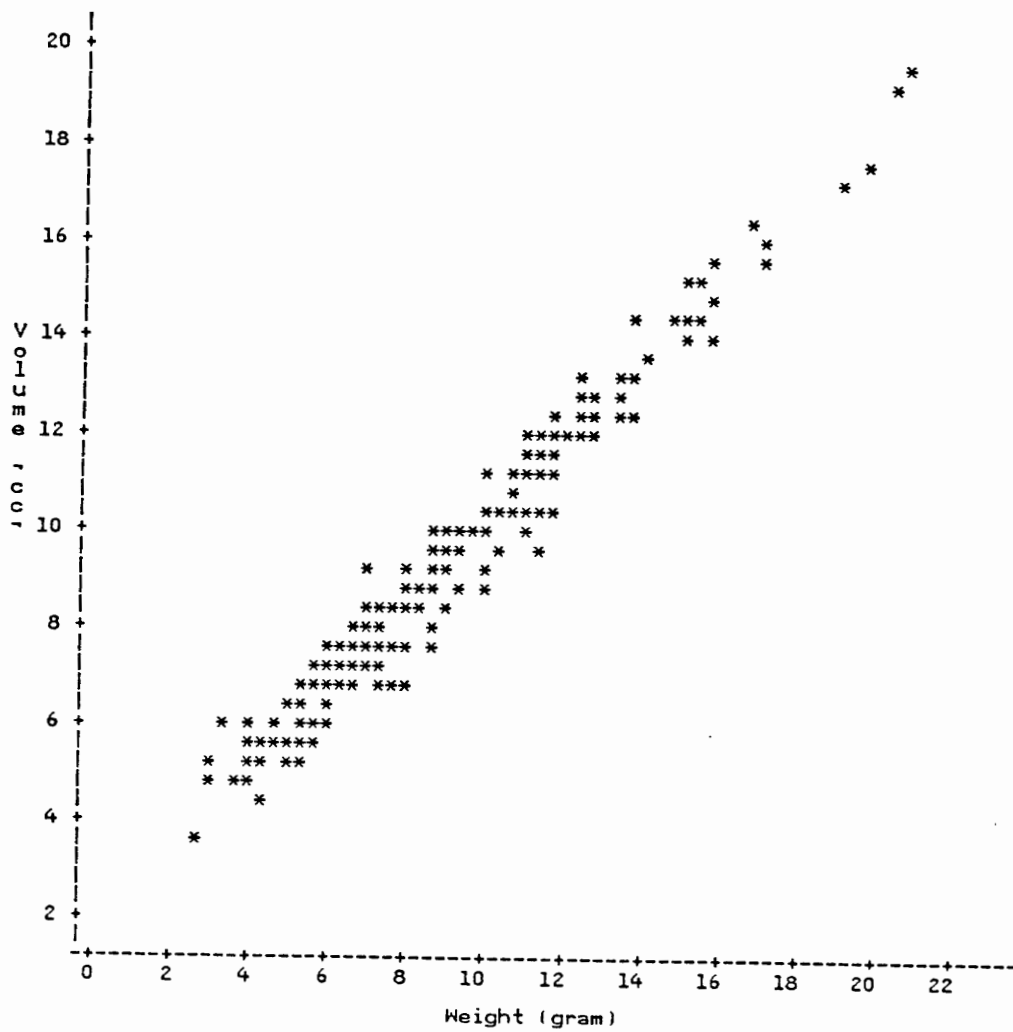


Figure 7. Plot of Volume versus Weight

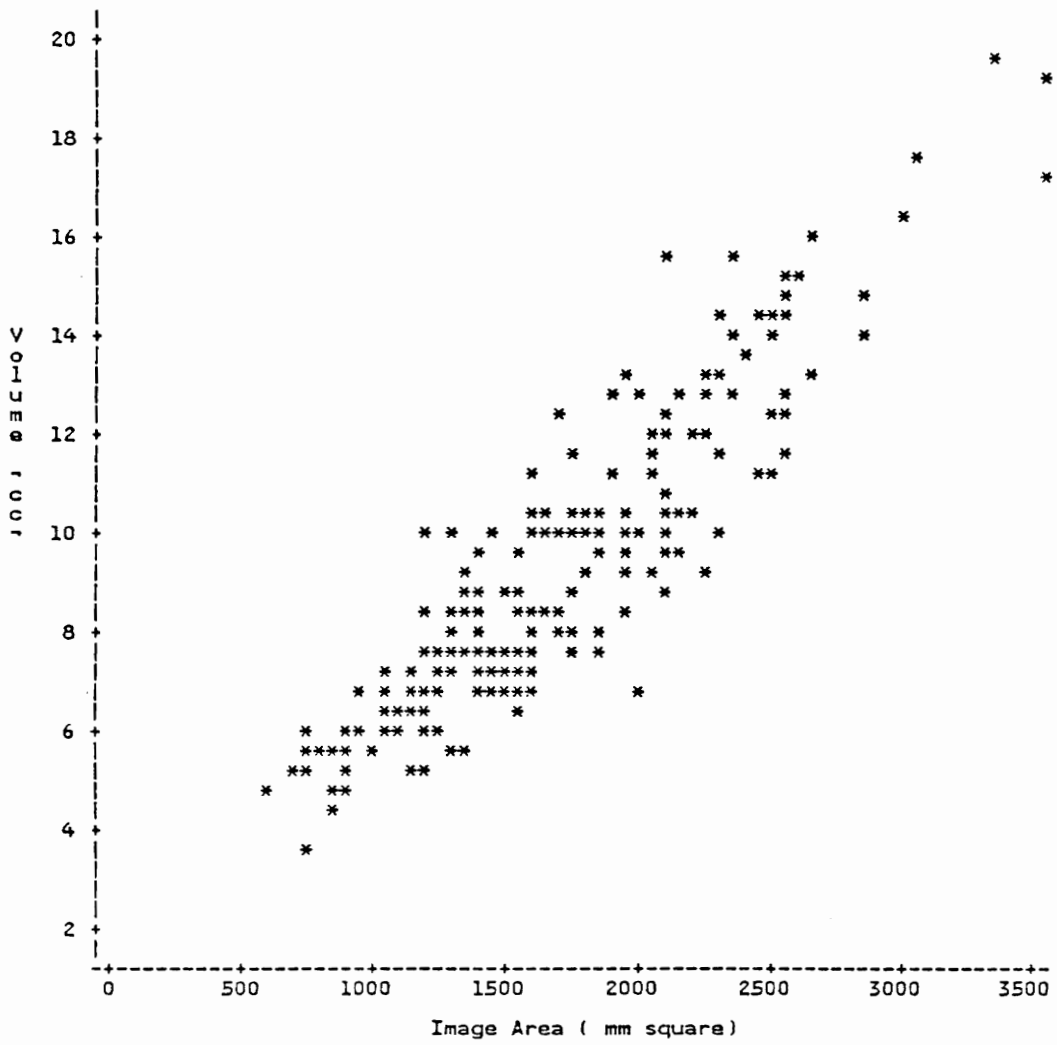


Figure 8. Plot of Volume versus Image Area

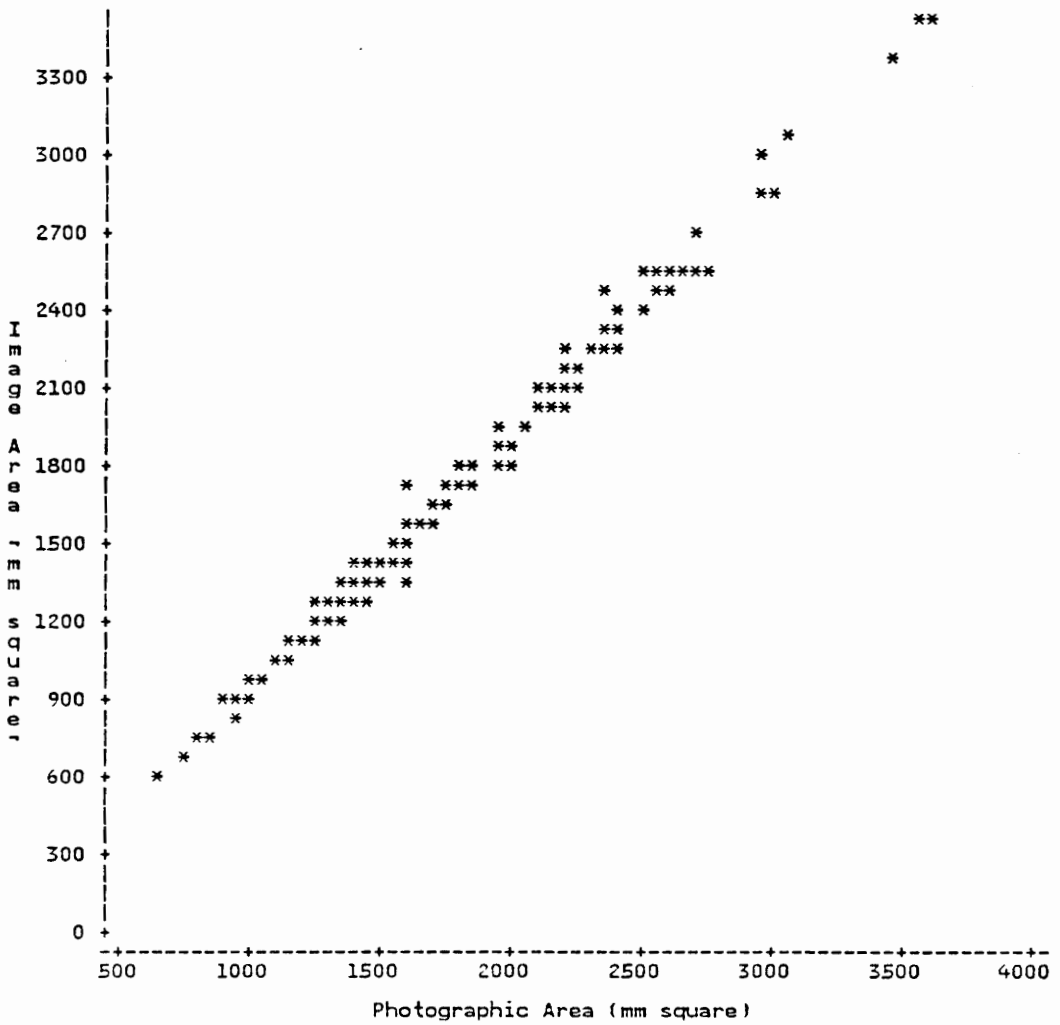


Figure 9. Plot of Image Area versus Photographic Area

where : V = the volume in cm^3 , and

A = the projected area in mm^2

with an estimated measurement error of $\pm 2.56 \text{ cm}^3$ at the 95% confidence level and R^2 value of 0.9823. A volume-pixel equation can be derived from from Equation 1 and 3 and as shown below:

$$\text{Volume} = 0.08354 + 0.01179 * \text{Pixels} \quad [4]$$

with an estimated measurement error of $\pm 2.84 \text{ cm}^3$ at the 95% confidence level. Since the conversion from area-pixel to volume-pixel was a linear transformation, the estimated measurement error could be determined by summing the measurement error due to the volume-area relationship with the measurement error due to the area-pixel relationship. Before the measurement error could be estimated, the measurement error due to the area-pixel relationship must be converted to volume by substituting the measurement error into the volume-area equation. This method was used throughout the text for determining the transformed measurement error. This accuracy was adequate for grading oyster meats into several categories based on the volume of the oyster meats.

A linear regression analysis was also done to predict the weights from the areas. The resulting least squares equation was:

$$W = 0.00534 * A \quad [5]$$

where : W = the weight of the oyster meats in grams, and

A = the projected area in mm^2

with an estimated measurement error of ± 2.74 grams at the 95% confidence level and R^2 value of 0.979. The weight-pixel equation was:

$$\text{Weight} = 0.08222 + 0.0116 * \text{Pixels} \quad [6]$$

with an estimated measurement error of ± 3.02 grams at the 95% confidence level. The accuracy obtained from the weight-pixel relationship also suggested that the oyster meats could be graded into several categories corresponding to the weight of the oyster meats using a digital image technique. Figure 10 shows a plot of weight versus projected area. Table 3 shows the statistics of the linear regression of the volume-area and weight-area models.

4.4. Conclusion

From the measurement and analysis of physical properties of oyster meats, it was concluded that the volume was highly correlated with the weight and the projected area. The height was found to be unimportant for grading purposes because it exhibited a low correlation with the volume, weight, and projected area. The image area was proved to predict the oyster volume and weight satisfactorily. As a result, the projected area was chosen as the grading criterion.

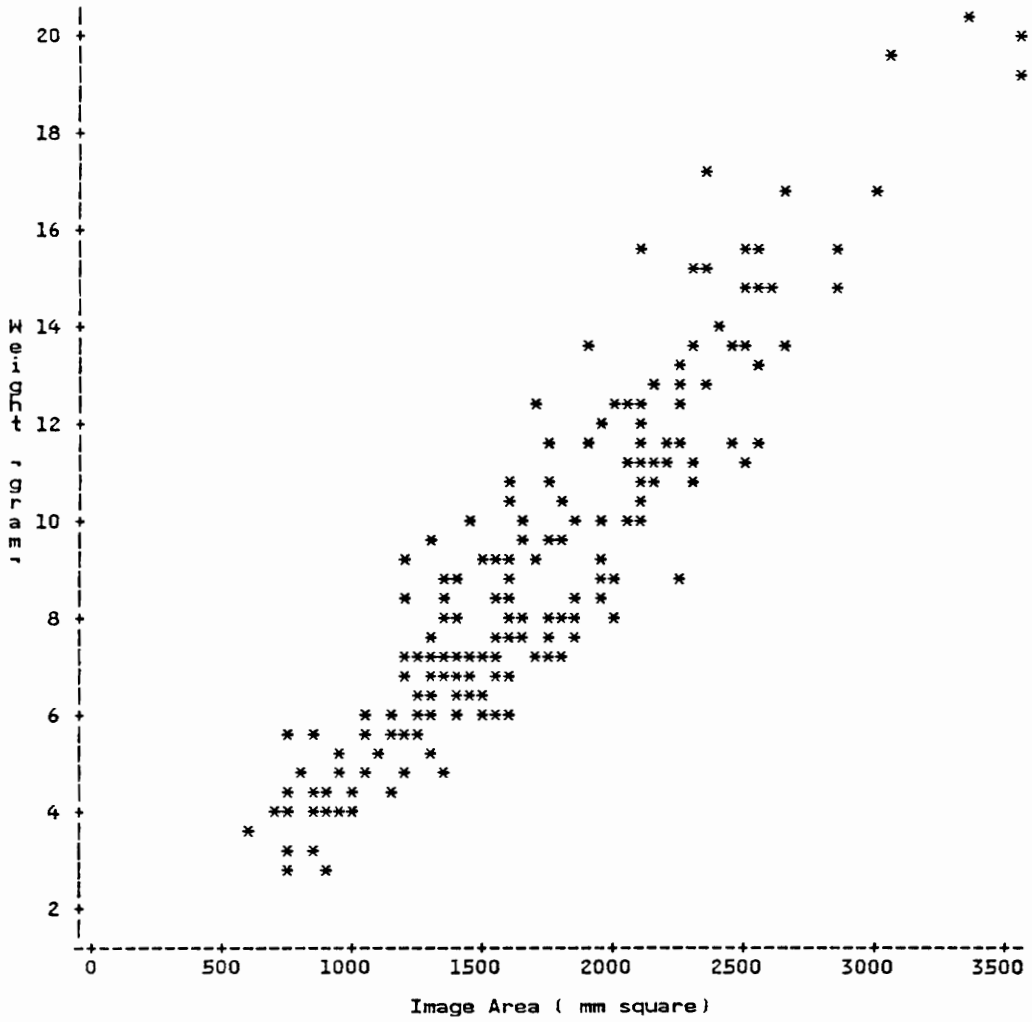


Figure 10. Plot of Weight versus Image Area

Table 3. The Linear Regression for Volume-Area and Weight-Area Models

	Volume-Area (cm³)	Weight-Area (grams)
Sum of Square Error (SSE)	334.7857	385.3800
Mean Square Error (MSE)	1.63310	1.8799
Degree of Freedom (DF)	205	205
Root Mean Square Error (RMSE)	1.2779	1.3711
Slope	0.005426	0.005340
Standard Error	0.00005	0.00005
R²	0.9823	0.9790
Sum of Residuals	20.5726	-22.8491

Chapter V. Digital Camera System Testing

5.1. General

Some fluctuation in the number of pixels counted was observed with the object in the same position under the same illumination conditions. This was because not all the pixels change state at the same condition, nor did a single pixel always change state at exactly the same condition, as stated in the manufacturer's specification sheet (Personal Computing Tools, Inc., 1988). This explained why the confidence bands were found to be larger than preferred. But, these results were still considered to be tolerable for a material with wide biological variability. Two independent tests were done to investigate the seriousness of these fluctuations. The tests were the lighting readjustment and oyster replacement tests.

5.2. Lighting Readjustment Test

A test was conducted to determine how repeatable the lighting conditions were. The original seven metal targets which had been used for calibration were used in this test. The number of pixels for each target was recorded, and then the light adjustment was changed. The filter was used to readjust the light settings and the number of pixels was again recorded. The test was repeated four times.

This test can be analyzed as a randomized block design with the different lighting adjustments as the treatments and the metal targets as the block effects. By using this design, the variability due to the use of different metal targets was filtered out and a precise comparison among the treatment (i.e., lighting adjustment) means could be made. The test statistic used to test the equality of the treatment means was an F-test. The F-statistic was expressed as a ratio between variance explained by the model divided by variance due to model error or experimental error (Myers, 1986). Based on the F-test it was concluded that the differences observed in each lighting readjustment were not significant at both 0.05 and 0.01 levels. To further verify the results, the collected data were analyzed with Duncan's multiple range test (Ott, 1984). Duncan's multiple range test was developed to obtain all pairwise comparisons among treatment means. It was a powerful test in that there was a high probability of declaring a difference when there was actually a difference between the population means. The procedure was as followed: 1) Rank the treatment means, and 2) Two treatment means were declared significantly different if the absolute value of their sample differences exceeded

$$W_r = q_{\alpha}(r, v) \sqrt{\frac{MSE}{n}} \quad [7]$$

where : n = the number of observation in each treatment means,

MSE = mean square error obtained from the analysis of variance table,

ν = the number of degree of freedom for MSE,

r = the number of mean steps apart, and

$q_{\alpha}(r,\nu)$ = the critical value.

Based on this test, it was concluded that the differences observed in each treatment mean were not significantly different at 0.05 level. Table 4 summarizes the statistical results of the lighting readjustment test.

The lighting readjustment test was repeated with 6 oyster meats and analyzed with the same statistical methods. The identical conclusions were drawn that there were no differences due to lighting. These statistics are tabulated in Table 5.

The results of these tests showed that the lighting can be adjusted by the filter technique. This was important so that the device can continue testing without recalibration of the area-pixel relationship.

5.3. Replacement Test

It was observed that by placing the oyster in different areas in the camera's field of view the number of pixels counted was different. Therefore, a test consisting of removing and replacing the oyster meats in the field of view was conducted. The purpose of this test was to examine the variation of the estimated area caused by placement in the camera's field of view, and to provide an estimate of the repeatability of the oyster area measurements. The test was done by replacing the oyster meat twice with an attempt of slightly shifting the oyster meat to the left and to the right from its

initial position (less than 1 cm). The reason for doing this was to arbitrarily create three treatments (i.e., left, center, and right) so that the randomized block design could be used for analyzing the collected data. A total of 7 oyster meats were tested. Based on the F-test it was concluded that the differences observed in each treatment were not significant at both 0.05 and 0.01 levels and the Duncan test confirmed that the differences observed in each treatment were not significantly different at 0.05 level. The test results were summarized in Table 6. This test suggested that placement of the oyster meat in the field of view has minimum effect.

5.4. Conclusion

The results from the readjustment test indicated that the lighting can be adjusted by the filter technique, and can be readjusted between tests so that testing can continue with no recalibration of the device. The results from the replacement test showed that the exact placement of the oyster meats in the field of view was not important. These test results were important because it would be impossible to maintain unchanging lighting conditions in a working environment and it would be also impossible to assure identical placement of the oyster meats in the field of view.

Table 5. Lighting Readjustment Test Results with Oyster Meats

a) F-statistic

Null Hypothesis, H_0 :	$\mu_1 = \mu_2 = \mu_3 = \mu_4 = \mu_5$
Alternative Hypothesis, H_1 :	At least one of the means are not equal
Test Statistic, T.S. :	$F(\text{obs}) = 0.8205$
Rejection Region, R.R. :	$F(\text{obs}) > F(\text{critical})$
Conclusion : Since $F(\text{obs}) < F(4,5) = 5.19$ at 0.05 level, Accept H_0	
Since $F(\text{obs}) < F(4,5) = 11.39$ at 0.01 level, Accept H_0	

b) Duncan's Multiple Range Test

Oyster No.	Lighting Readjustment (pixels)				
	496	503	508	486	502
1	1100	1101	1098	1096	1086
2	902	897	896	896	889
3	1006	999	996	986	988
4	912	927	925	936	921
5	1295	1307	1317	1329	1339
6	719	725	734	732	735
mean	989.000	992.667	994.333	995.833	993.000
Treatment	1	2	3	4	5

Alpha Level, α = 0.05
 Degrees of Freedom, DF = 20
 Mean Square Error, MSE = 102.367

Number of mean steps apart, r : 2 3 4 5
 Critical value : 12.1687 12.7791 13.2011 13.448
 Ranked Mean : 995.833 994.333 993.000 992.667 989.000
 Treatment : 4 3 5 2 1
 Grouping : AA

Means with the same letter were not significantly different.

Table 6. Replacement Test Results with Oyster Meats.

a) F-statistic

Null Hypothesis, H_0 :	$\mu_1 = \mu_2 = \mu_3$
Alternative Hypothesis, H_1 :	At least one of the means are not equal
Test Statistic, T.S. :	$F(\text{obs}) = 0.6384$
Rejection Region, R.R. :	$F(\text{obs}) > F(\text{critical})$
Conclusion : Since $F(\text{obs}) < F(2,6) = 5.14$ at 0.05 level, Accept H_0	
Since $F(\text{obs}) < F(2,6) = 10.92$ at 0.01 level, Accept H_0	

b) Duncan's Multiple Range Test

Oyster No.	Replacement Position		
	Left	Center	Right
1	471	474	479
2	567	562	563
3	419	415	421
4	784	788	791
5	722	719	720
6	392	387	388
7	855	854	847
mean	601.429	599.857	601.286
Treatment	1	2	3

Alpha Level, α = 0.05
 Degrees of Freedom, DF = 12
 Mean Square Error, MSE = 11.3413

Number of mean steps apart, r :	2	3	
Critical value :	3.91459	4.10067	
Ranked Mean :	601.429	601.286	599.857
Treatment :	1	3	2
Grouping :	AAAAAAAAAAAAAAAAAAAAAAAAAAAA		

Means with the same letter were not significantly different.

Chapter VI. Oyster Meat Grading System

Development

6.1. General

One of the constraints in developing a grading device is that it must be as simple and as inexpensive as possible. In addition, the overall cost of developing the necessary hardware and software must be below the current system costs. The accuracy and speed of grading were two additional important factors and were analyzed carefully.

The testing system consisted of a rotating disc, a grading section, and a host microcomputer. A motor driven translucent disc was used to move the oyster meats or the metal targets one at a time into the grading sensing area. The grader consisted of a low cost (approximately \$250) 2-dimensional direct-output digital analyzer connected to a microcomputer. A suitable illumination scheme was tested to give a maximum contrast between the oyster meat and the background. Spreading of the oyster meats due to gravitational force provided the profile for the camera to take a good picture. After "visualizing" an oyster meat in the camera's field of view, the image processing

unit converted the optical information into a digital image. The digital image was then transmitted to the host microcomputer. In this case, the required shape parameter was the projected area of the oyster meat as concluded in Chapter 4. Finally, the computer software analyzed the image and a category was assigned to the oyster meat. Figure 11 is the schematic of the completely assembled system.

6.2. System Components

The system hardware can be separated into three sections, the digital camera system, the illumination equipment, and the conveying device.

6.2.1. Digital Camera

The same digital camera used in physical properties measurements was used. The Digital camera (Micromint, Inc., 1984, Ciarcia, 1983a, and Ciarcia, 1983b) contained a 16 mm C-mount and an *IS32A* Optic random access read/write memory (RAM) chip. The 16 mm C-mount lens had a variable aperture and a focus adjustment. The lens was designed for viewing objects from a distance of at least 45 cm. The Optic RAM was made up of two 128×256 arrays of pixels. The arrays were separated from each other by a "dead zone" about 25 pixels in width. The arrays consisted of light-sensitive capacitors which were arranged in a "honeycomb" configuration. Alternate capacitors from even rows from one array were used (Figure 12). The arrays were exposed to light through a glass lid. Table 7 shows the array dimensions of the Optic RAM.

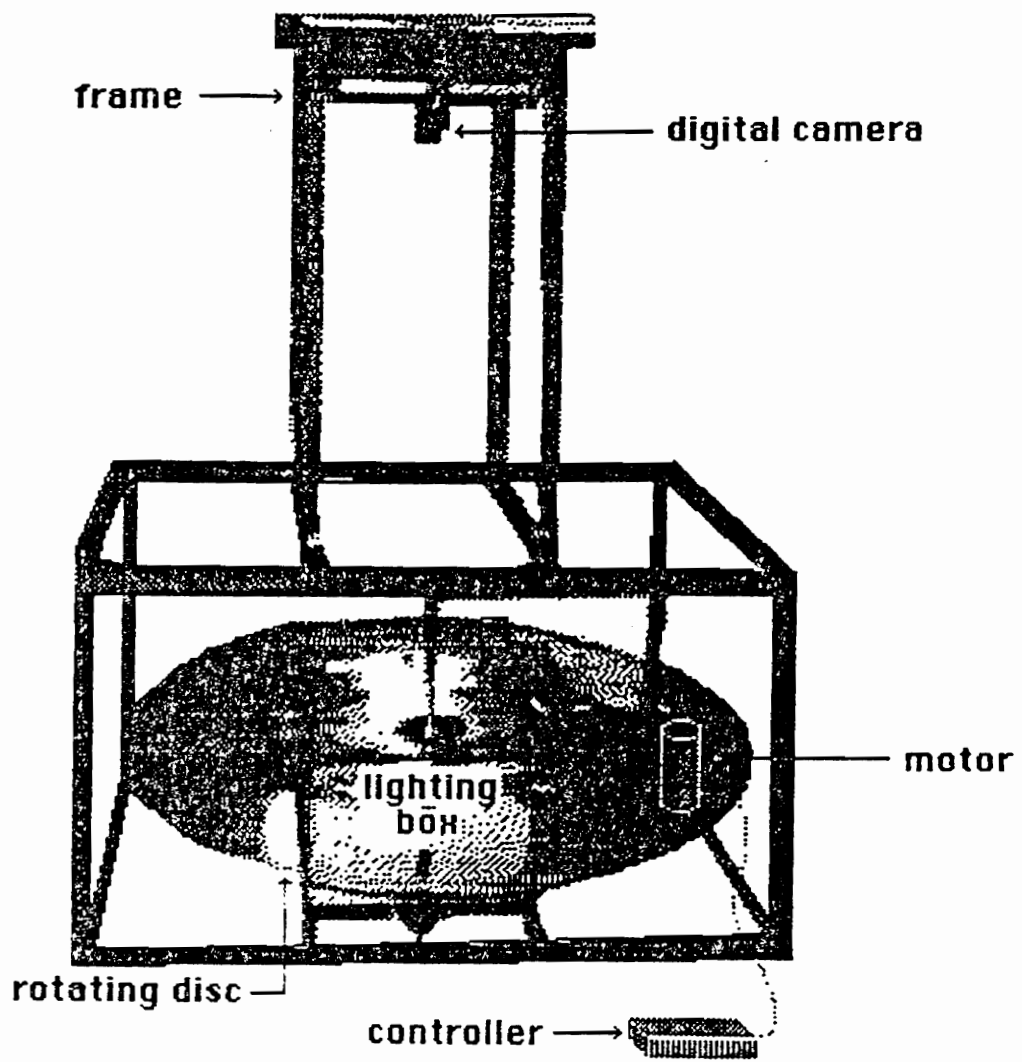


Figure 11. Schematic of the Completed System

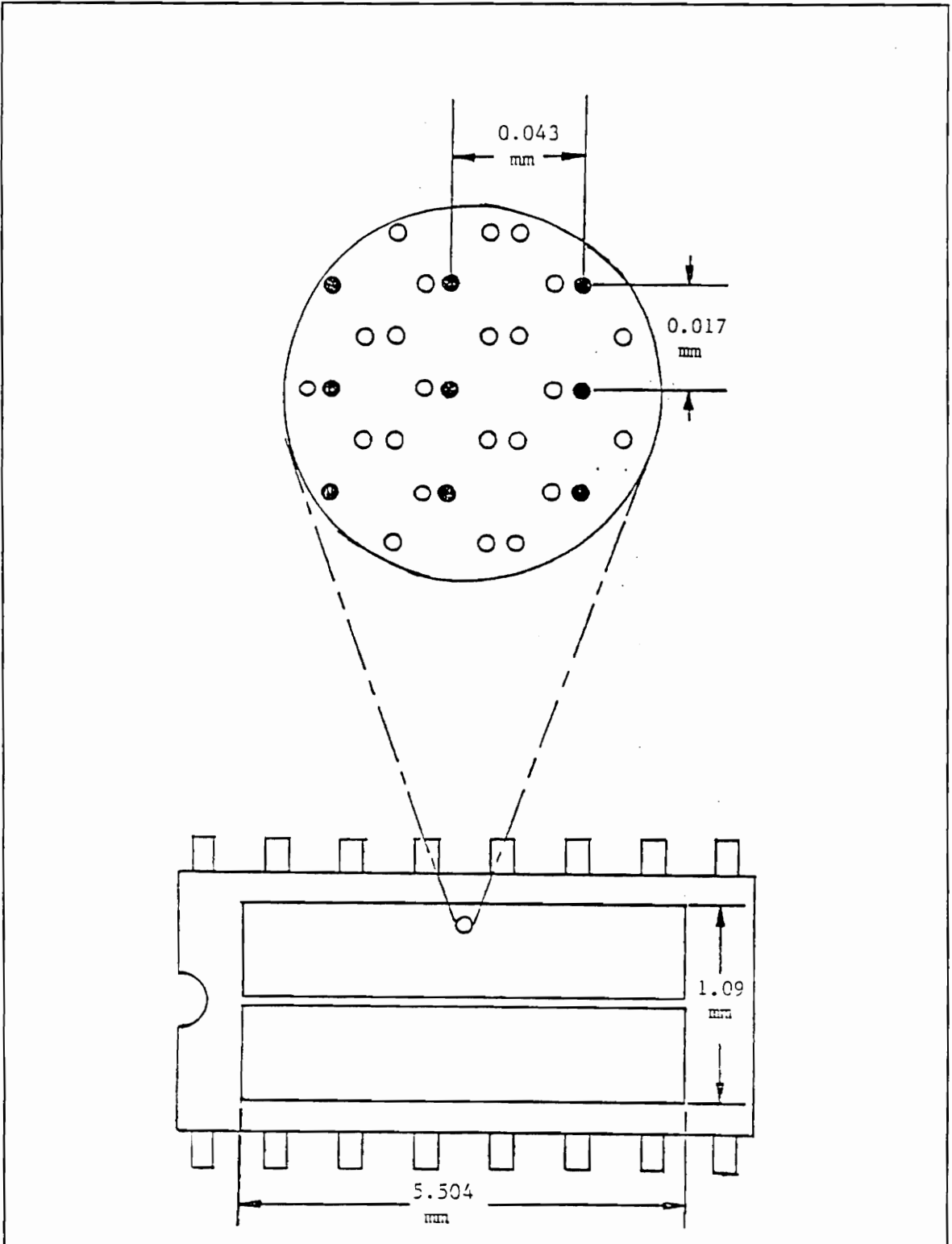


Figure 12. The 256 x 256 Optic RAM and The "Honeycomb" Pixel Arrangement

Table 7. Optic RAM Dimension

Element	Dimension (mm)
128 × 256 ARRAY	5.504 × 1.088
Pixel	0.008 × 0.009
Horizontal Spacing	0.0085
Vertical Spacing (Center to Center)	0.0215
Alternate Pixel Spacing	0.043
Dead Zone Spacing	0.15

6.2.1.1. Principle of Operation

A digital image was formed on the Optic RAM when light from the viewed object passed through a lens, and was focused (optically) onto the Optic RAM surface. The individual light sensitive capacitors, initially charged to 5 volts, began to discharge when exposed to light photons. The rate of discharge was proportional to the light intensity throughout the duration of the exposure. There were only two gray-scale levels, black and white. The light sensitive capacitor was accessed as a memory cell and the capacitor's voltage was read. This voltage was then compared to a fixed threshold voltage. If the potential was above a threshold voltage of +2.1 volts it was considered a black surface (logic 1), and if the potential was below the threshold value it was a white surface (logic 0). The camera aperture (size of opening) which passed the light to the Optic RAM surface was mechanically controlled and measured in F-stops. The exposure time (shutter speed) was controlled electronically through software by a "SOAK" command which "opened" the shutter and kept it open for a specified exposure. The "REFRESH" command "closed" the shutter and "froze" the memory cells. Then the control circuitry activated the interrupt stage and the value of each cell was fetched and transmitted to the host microcomputer. After transmitting all the values the cells were returned to their nominal voltage (logic 1), and the image sensing cycle was restarted.

The time (in milliseconds) required to transfer an image from the digital camera to the microcomputer was shown in Table 8 and can be calculated from the following equation.

$$TIME = \frac{\text{Rows} \times \text{Bytes-per-row} \times 10000}{\text{Baud rate}} \quad [8]$$

The digital data was transferred from the camera to the microcomputer for display and manipulation at a baud rate of 153600 bits per second (bps), which was the maximum allowable speed. The baud rate controlled the operating speed of the digital camera and different baud rates could be obtained by setting the appropriate baud rate jumpers. The minimum time required for transmitting an image with this speed was 67 milliseconds.

Table 8. Picture Transmission Time (in Milliseconds).

Rows	Bytes-per-row	Baud Rate			
		9600	19200	76800	153600
64	16	1067	533	133	67
64	19	1267	633	158	79
64	32	2133	1067	267	133
64	37	2467	1233	308	154
128	16	2133	1067	267	133
128	19	2533	1267	317	158
128	32	4255	2133	533	267
128	37	4933	2467	617	308
128	64	8533	4267	1067	533
128	73	9733	4867	1217	617
256	32	8533	4267	1067	533
256	37	9867	4933	1233	617
256	64	17066	8533	2133	1066
256	73	19466	9733	2433	1217

6.2.1.2. Control Hardware

A prefabricated TTL (Transistor-Transistor Logic) serial control board was used to interface the camera with the host microcomputer. The board contained two sections with five wires between the computer and camera, carrying the transmit, receive, clock, + 5 volt power, and ground signals.

The first section of the image interface controlled the camera operation and received data from the optical image. It consisted of a timing-generator, a command-receiver, an address register, address descramble and array soak circuitry, a transmitter and interrupt generator, and adder and end-of-frame circuits. The timing-generator circuit was used to generate timing signals for the operation of the Micro D-Cam. The commands sent from the computer to the camera were carried by a serial command line. The data entered the command-receiver circuit a bit at a time according to the following protocol. The start bit was the first bit to arrive, followed by 8 data bits and then a stop bit. The address registers circuit latched the row-address, column-address, and refresh pointers for the Optic RAM addressing. The address-descramble circuit unscrambled the data from the address registers into a new address, which the Optic Ram decoded to access the desired pixel. The purpose of the SOAK circuit was to prevent the refresh addresses from reaching the Optic RAM during the exposure cycles. The transmitter and interrupt-generator circuit was used to transmit the pixel data serially to the host microcomputer by inserting start and stop bits where appropriate, and to generate interrupt signals for fetching the pixel formation from the Optic RAM. The adder and the end-of-frame section was used to add the proper increments to the row, column, and refresh registers and to generate signals indicating end-of-frame (EOF) in the Optic RAM.

The second section contained a general-purpose type 6850 asynchronous communication interface adapter (ACIA) which manipulated and transferred the picture data to the host computer. The ACIA comprised a data register and a status register. The ACIA was first initialized to the appropriate configuration before the host computer could access the camera. This was done by writing two bytes, a 03 Hex followed by a 14 Hex, into the status register. The first byte was used to reset

by dark spots. The figure also indicated that everything lines up better in ALTBIT than NOALTBIT mode. NOALTBIT mode was used exclusively.

The WIDEPIX mode double transmitted each pixel in the array. Since each image sensing element was rectangular in shape, a proper ratio between the height and the width of the picture could be maintained by double transmitting the pixels. The WIDEPIX mode was used.

The 7BIT mode was compatible with APPLE's high resolution format and 8BIT mode was used by all other computers. The 8BIT mode caused the camera to transmit in normal bit map format, where all 8 bits in the byte contained image data and it was used in this study.

The 1ARRAY mode used only one of the two 128×256 pixel arrays and it was selected for this study. If 2ARRAY mode was selected, the data from both arrays were transmitted and caused a split-screen effect due to the spacing between the two arrays in the Optic RAM chip.

In order to develop a properly formed image, capacitors must receive a sufficient amount of light. Too much light will overexposed the image, and too little will underexposed the image. The exposure time was determined by how long the control program allowed the Optic RAM to be exposed to light without its capacitors being refreshed. In the REFRESH mode, the capacitors were charged up to 5 volts while the camera was transmitting an image. When capacitors were not refreshing, they were said to be in the SOAK mode. The SOAK mode allowed the capacitor charges to leak away at a rate proportional to the intensity of the light focused on them. The SOAK mode was invoked automatically when the camera ended the transmission of an image and was retained until another command was received.

The SEND mode was invoked by setting bit 0 of command byte to 0 which initiated the transmission of an image. If the SEND mode was set to 1, the camera did not transmit any image and the refreshing or soaking depended on the status of the second bit (i.e., bit 1) of the command byte.

It was also necessary to set bit 4 to 1 in order to prevent a 1-bit-offset of the next picture image if the NO SEND mode was selected.

The operating modes chosen for this study were : SEND, SOAK, 1ARRAY, 8BIT, WIDEPix, and ALTBIT. With these operating modes, the setting for the command byte was 5B Hex.

6.2.2. Illumination Technique

The illumination must be uniform and controllable. The development of a good illumination system was a matter of experimentation. From earlier investigation, backlighting was known to be an excellent way of obtaining a high contrast image of the oyster meats. The oyster meats appeared to be black on a white background and accurate measurement of the projected area could be achieved without interference from its irregular surface. The oyster meats were transported across a translucent surface with illumination from the bottom. With this translucent surface, the incident light energy was scattered from its original direction of travel and provided a more distributed illumination scheme.

Normal human eyes respond to light from the range of 350 to 700 nm (violet to red) with a peak response at 550 nm (yellow-green) under completely illuminated light conditions. A typical photodiode sensor responds in a spectral range of 200 to 1100 nm with a peak response at 750 nm with about one-half of the detector sensitivity outside the human visible regions (Paulsen and McClure, 1986). In order to fully use the sensitivity of the photodiode, the light source must have a peak response at a wavelength near 750 nm. Incandescent light sources emitted light predominantly outside the visible region and in the infrared (IR) region with a peak response at 850 nm (Kaufman, 1968). Figure 13 shows a typical spectral response of photodiodes and an incandescent light source at 3000° K. The photodiode sensor intercepted with the incandescent light source at a wavelength of 825 nm with a relative response of 0.95. For this particular Optic RAM, the peak

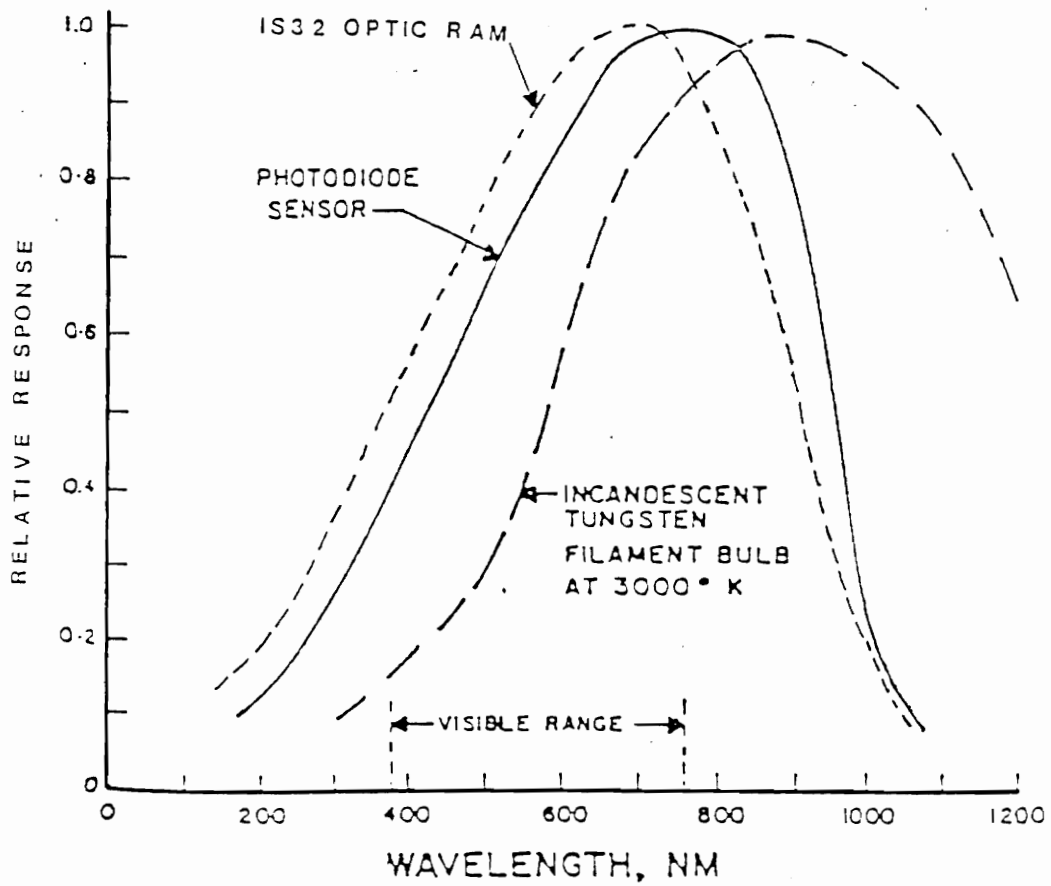


Figure 13. Spectral Response of Photodiodes and an Incandescent light Source

response was at 700 nm (Personal Computing Tools, Inc., 1988). Figure 14 shows the reciprocal fluence versus wavelength for IS32 Optic RAM. Reciprocal fluence is a measurement of sensitivity. The response curve of this IS32 Optic RAM was shifted slightly to the left of the typical photodiode response curve. As a result, the combination of this IS32 Optic RAM with an incandescent light source produced a relative response of 0.9 at a wavelength of 750 nm. In other words a 90% sensitivity could be maintained by using this IS32 Optic RAM with incandescent light sources. At the wavelength of peak source-detector response, the absorbance of the oyster meat was approximately 0.40 (Figure 3). This was the reason why part of the oyster meats were translucent when illuminated. Although, fluorescent lamps could reduce the high amount of infrared light produced by incandescent lights they could not solve the problem of missing features owing to the photodiode response and the fluorescent lamp's low production of 700 nm light.

After learning the Optic RAM had a peak sensitivity to illumination near the infrared region the four 15 watt cool white fluorescent tubes were replaced with twelve 60 watt incandescent light bulbs. A piece of diffusing paper was placed over the window in the light box in order to provide more uniform illumination. The dimensions of the window were 10.5 cm × 17 cm, larger than the field of view of the camera which was 5 cm × 13 cm. A small ventilation fan was added to the box to remove the heat produced by the light bulbs.

6.2.3. Conveying Mechanism

After designing the digital camera system and the illumination equipment, the next step was to design a transportation mechanism for conveying the oyster meats through the field of view of the camera. For experimental purposes, a rotating disc was used instead of a conveyor belt. The rotating disc was easier to construct and was able to produce the same results as a conveyor belt. Therefore, a translucent disc driven by a gearmotor controlled by an adjustable speed motor controller was used.

Reciprocal Fluence
($10^5 \text{ cm}^2/\text{J}$)

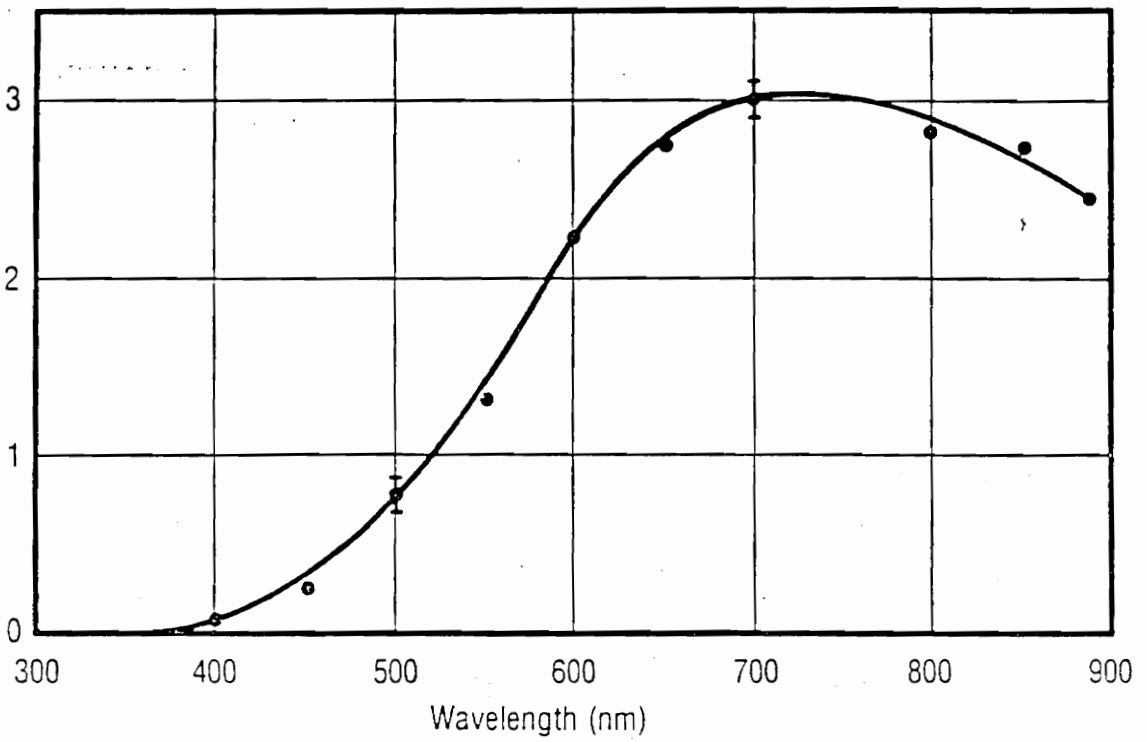


Figure 14. Reciprocal Fluence versus Wavelength for IS32 Optic RAM

6.2.3.1. Gearmotor

The gearmotor was a Dayton model 4Z382 gearmotor, was constructed from high strength aluminum die cast alloy, and was rated for continuous duty (10 hour/day) with a 1.0 service factor (Dayton Electric MFG. CO., 1988a). The gearmotor was a permanent magnet motor with an input horsepower of 1/8 and a gear ratio of 28 to 1. The motor was operated under a 90 VDC source with an average current of 1.5 amperes. The full load RPM of this motor was 64 and the full load torque was 113 in-lbs. The motor could be operated under a maximum ambient temperature of 40°C with class B insulation. Figure 15 shows a diagram of the gearmotor.

6.2.3.2. Speed Controller

The speed controller was a Dayton SCR model 4Z829 motor controller (Dayton MFG. CO., 1988b). The Dayton SCR controller was an adjustable speed controller designed for applications requiring constant (or diminishing) torque such as conveyors, fans, and blowers. The speed controller was designed for use with DC permanent magnet and DC shunt wound motors rated from 1/8 to 1 horsepower. The controller can be operated in the FORWARD, REVERSE and BRAKE modes. There was an internal dynamic braking circuit for stopping the motor smoothly in the BRAKE mode with no appreciable external inertia. As a precaution, the braking mode was not used more than five times a minute. There was a built-in "soft start" circuit in the controller. Therefore, it took 1 to 3 seconds for the motor to accelerate from a stop to a set speed. The speed controller was suitable for controlling the gearmotor mentioned above. Figure 16 shows a diagram of the speed controller.

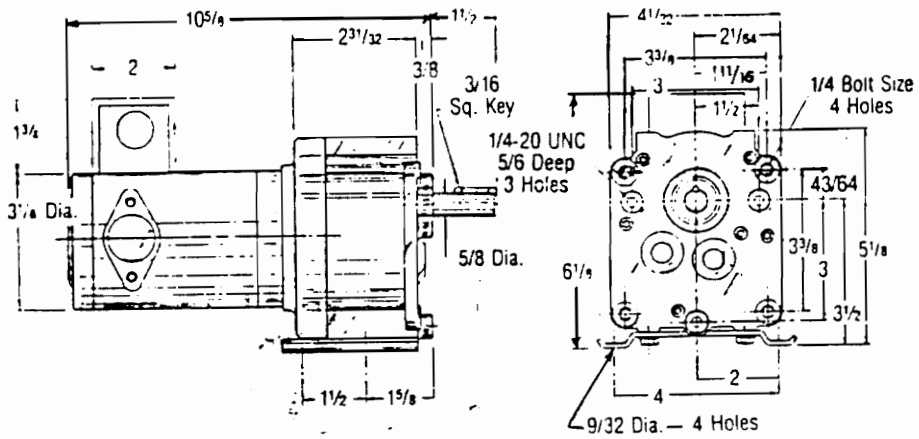
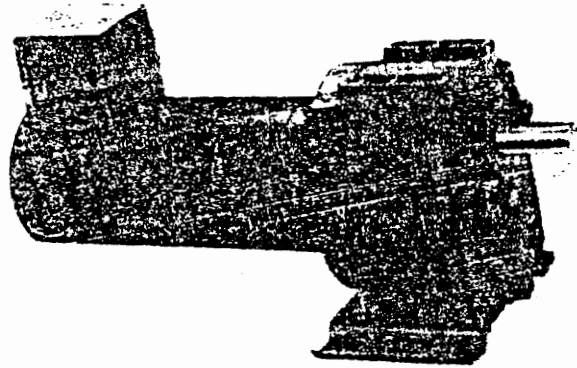
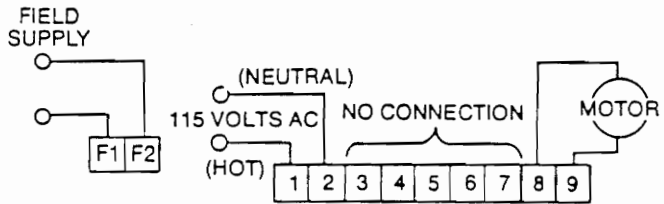


Figure 15. Diagram of the Gearmotor



Controller Terminal Strips

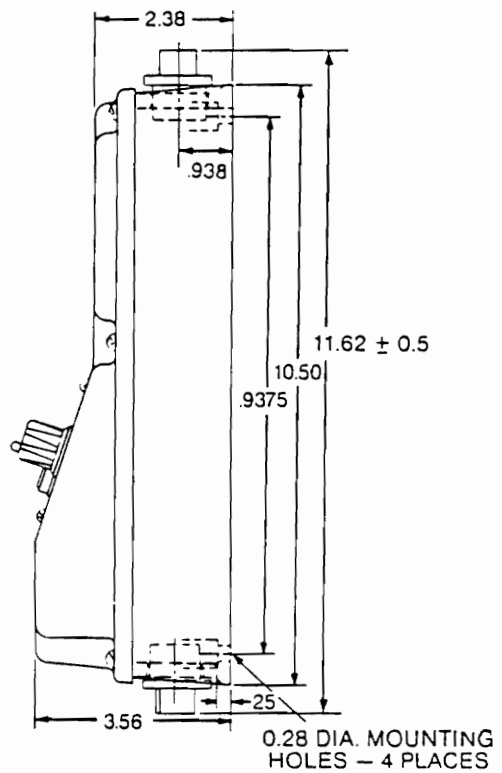
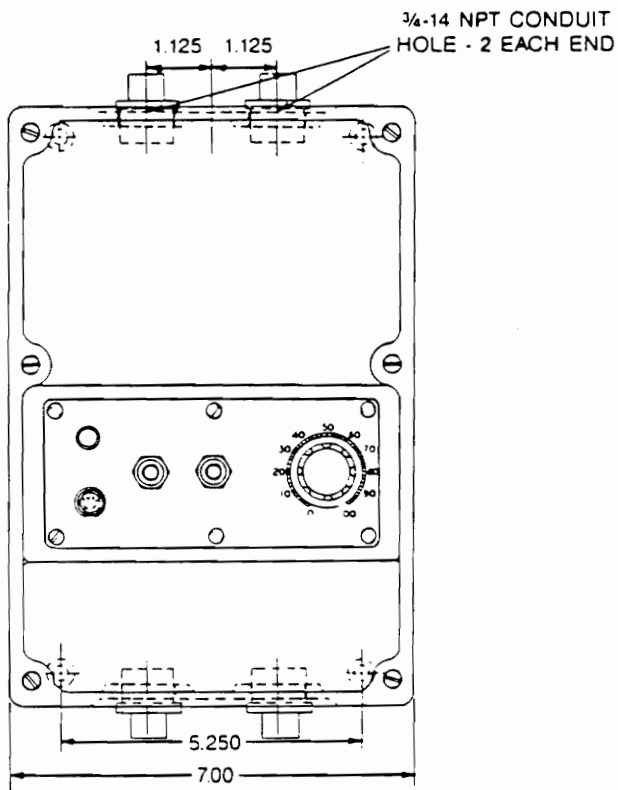


Figure 16. Diagram of the Speed Controller

6.2.3.3. Rotating Disc

The translucent disc was made from a piece of plexiglas. The disc was 1 meter in diameter, which was slightly larger than the maximum design size. The reason for having an oversized disc was to allow for redesigning if needed. Figure 17 shows the detail of the rotating disc, including the physical dimensions of the disc and the location of the oyster meats. With this arrangement, the disc could accommodate 20 oyster meats. The oyster meats were 18° apart center to center so that no overlapping of the images occurred. Excessive speed of the motor would cause the oyster meats on the rotating disc to be propelled due to centrifugal force. As a result, detailed studies on the centrifugal force of the rotating disc, and the coefficient of friction between the oyster meats and the rotating disc were conducted.

Centrifugal force is the force that directed a rotating object away from the rotating axis. This force can be calculated by one of these equivalent expressions (Cook, 1960):

$$CF = M\omega^2 r = \frac{M\pi^2 \mathcal{R}^2 r}{900} = \frac{MV^2}{r} \quad [9]$$

where : CF = centrifugal force in Newtons,

M = mass in grams,

ω = angular velocity in radians per second,

\mathcal{R} = angular velocity in revolutions per minute,

r = radius in meters, and

V = linear velocity in meters per second.

Friction is defined as the resistance to relative motion between two bodies in contact. In this case, the two contacting bodies were the oyster meat and the rotating disc. The Coulomb's Law of friction stated that under certain limiting conditions for unlubricated surfaces, the frictional force was proportional to the normal force,

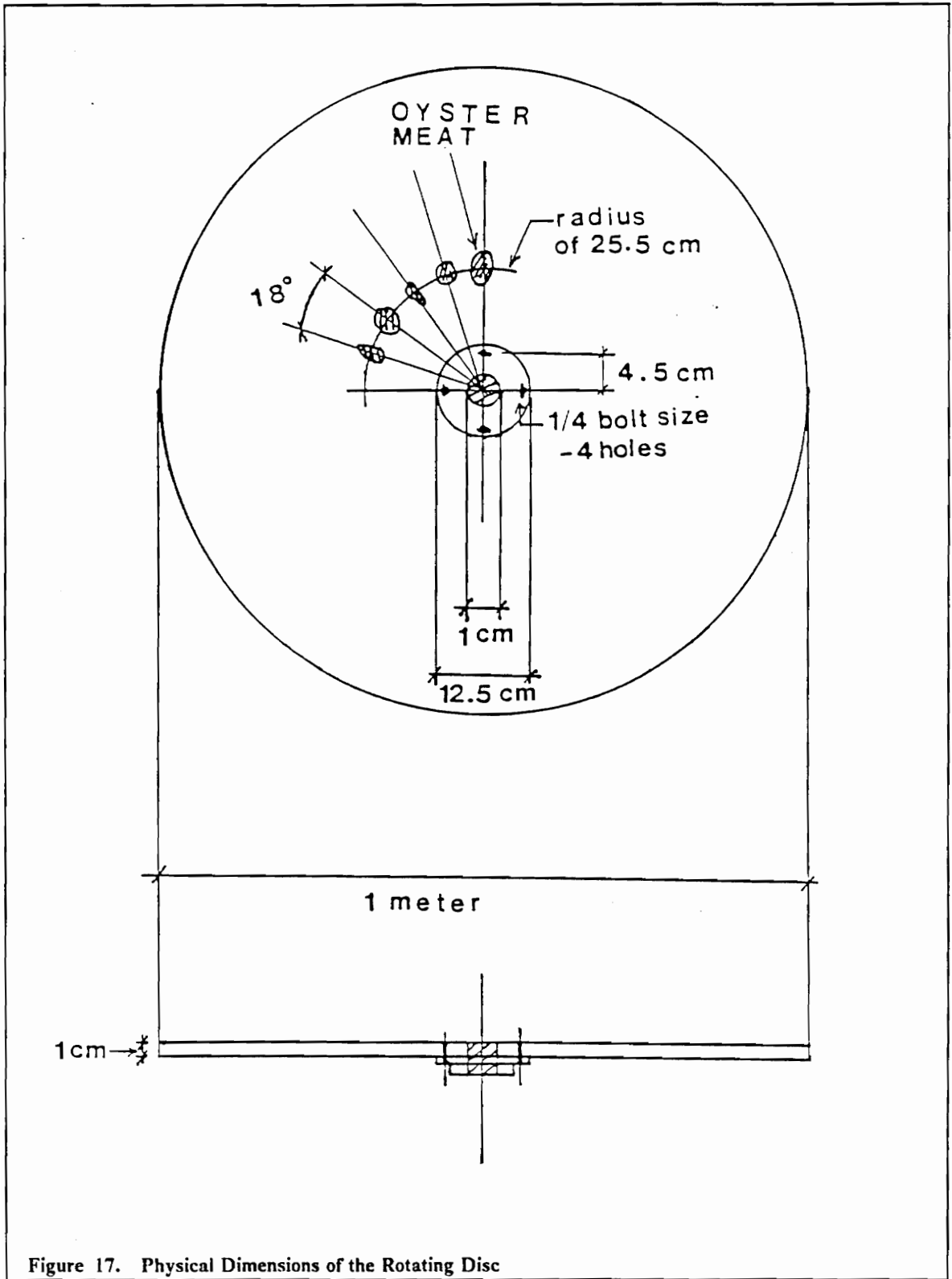


Figure 17. Physical Dimensions of the Rotating Disc

$$\mu = \frac{F}{N} \quad [10]$$

where the dimensionless ratio μ was the coefficient of friction (Cook, 1960). Since there was no published value for the coefficient of friction between plexiglas and oyster meat, an experiment was conducted to determine the coefficient of friction between these materials. The procedures of the experiment were as follows. An oyster meat was laid flat on a piece of plexiglas with no intention of flattening its gills and then the plexiglas was inclined very slowly until the oyster meat began to slide. This scheme has been used to determine the coefficient of friction of many materials (Cook, 1960). The operating principle behind this was that by increasing the angle, a limiting angle at which sliding was impending could be determined. This angle was named angle of repose, θ , where:

$$\mu = \tan \theta \quad [11]$$

The sliding was due to the weight of the object (i.e., oyster meat) on the incline. The normal force was the reaction force due to the weight of the object. Therefore, Equation 5 can be expressed as

$$F = \mu Mg \quad [12]$$

where : F = limiting force in Newtons,

μ = coefficient of friction,

M = mass of the oyster meat in grams, and

g = gravitational force which is 9.81 m²/s.

By equating Equation 9 and 12, the following expression was obtained.

$$\frac{M\pi^2 R^2 r}{900} = \mu Mg \quad [13]$$

The maximum allowable angular velocity in revolutions per minute (RPM) can be obtained by rewriting Equation 13,

$$\mathcal{R} = \frac{30}{\pi} \sqrt{\frac{\mu g}{r}} \quad [14]$$

The only two unknowns in this equation were the angular velocity in RPM and the radius of the rotating disc. From Equation 14, it was clear that the maximum allowable angular velocity only depended on the radius of the disc and was independent of the weight of the oyster meats. The same result was observed in the coefficient of friction determination. The coefficient of friction of the oyster meats was found to be 0.087 with an estimated measurement error of $\pm 8.7\text{E-}03$, as shown in Table 9. The desired location for the oyster meats on the disc was 0.255 meter away from the rotation axis. Therefore, the maximum allowable angular velocity in RPM, with this radius specification, was calculated to be approximately 17 RPM. With one oyster each 18° the maximum grading rate was about 5.7 oysters per second.

6.3. System Software

The image obtained from each oyster was analyzed and the decision of the oyster size category was made based on the image. The control program was written in Turbo PASCAL (i.e., a high level language) so that the software development tasks were significantly simplified and easier to understand compared to machine language. Three dimensional information could be achieved by using more than one camera, but the tasks of interconnecting the information obtained from several cameras were difficult and time consuming (in terms of processing time). Timings were critical in designing computer vision grading devices. The software must be as simple as possible in order to reduce the image processing time. It was concluded that height measurements were not necessary since they were not well correlated to volume. Therefore for this study, 2-dimensional planar images were considered sufficient to provide the necessary information regarding the shape of the oyster meat and complicated feature extraction algorithms were not needed.

Table 9. Friction Coefficient of the Oyster Meats

Oyster No.	Weight (grams)	Angle of Repose (Degree)
1	7.6325	5° ± 0.5°
2	7.0265	5° ± 0.5°
3	11.3305	5° ± 0.5°
4	6.0535	5° ± 0.5°
5	10.1755	5° ± 0.5°
6	12.5565	5° ± 0.5°
7	11.1225	5° ± 0.5°
8	8.2155	5° ± 0.5°
9	5.8535	5° ± 0.5°
10	8.5765	5° ± 0.5°

$$\begin{aligned}
 \text{Coefficient of Friction, } \mu &= \text{Tan } \theta \\
 &= \text{Tan } 5^\circ (\pm \text{Tan } 0.5^\circ) \\
 &= 0.08749 \pm 8.7269\text{E-}03
 \end{aligned}$$

The initial software was developed under Turbo PASCAL version 3.1. The software was capable of displaying the digital image on the monitor screen, counting the number of dark pixels representing the image, and storing the image area in term of pixels on a floppy diskette. The graphics were done using Turbo PASCAL's TOOL BOX procedures.

The initial software was slow and was rewritten in Turbo PASCAL version 4.0. Turbo PASCAL version 4.0 had more features and a faster compiler. Since displaying the image was not necessary for real time operation, the image display software was not converted to run under version 4.0. The source code for the image display software is listed in Appendix C.

The system software can be broken into four major sections. They were image receiver- to acquire images from the digital camera, image detector - to detect and capture good images, pixel counter - to count the dark pixels made up the image areas, and image classifier - to classify the images into several groups by size. Appendix D is the listing of the source code for the system software. The software development was based on two conditions : 1) the oyster meats must be in the field of view, and 2) the oyster meats must be separated, i.e. no overlapping images were allowed. The second condition was accomplished by locating the oyster meats 18° apart on the rotating disc. But the first condition was more difficult to achieve. The degree of difficulty was increased because the oyster meats must be moved through the field of view of the camera. The software algorithm had to be intelligent enough to tell when there was a oyster meat in the camera's field of view.

The image receiver algorithm used the preselected modes as specified in section 6.2.1.3. Command Functions. An intelligent detecting algorithm was developed to signal when a good image was captured by the camera. A good captured image also implied that there was an oyster meat in the view of the camera. By examining the moving images displayed by the display software, the characteristics of the moving images were understood. The actual size of the image frame was 64 × 128 pixels (the image frame was not 128 × 256, because only alternate capacitors from even rows from one array were used). To cut down the processing time, only the center part of the image frame

was used. The size of the image frame which was analyzed was therefore reduced to 64×64 pixels (or $5 \text{ cm} \times 13 \text{ cm}$).

The general approach of capturing a good image was as follows. The image detector was written to examine the first row and the last row of the image frame. If there were any dark pixels encountered in one of these rows, the only logical explanation was that the image was at one of the edges. As a result, the image was discarded and the detector algorithm continued with the next available image. Alternatively, if there were no dark pixels encountered in the first and last rows, the detector algorithm then checked the center row, which was row 32. If there were any dark pixels encountered in this row, it was a good image and this image was analyzed further. If there were no dark pixel encountered in the center row, the detector algorithm then checked rows 16 and 48. If there were any dark pixels encountered in these rows, it was a good image and this image was analyzed further. This algorithm ensured that any image over 14 rows (or 1 cm oyster width) was detected. Figure 18 is a system flow chart with special attention to the image detecting scheme. From examining the displayed images it was noted that the oyster meats were placed far enough from each other that the image of two oyster could not be captured on one image frame at anytime. A good image may be discarded by the algorithm if the previous or next image lies on the edge as shown in Figure 19a. This was prevented by maintaining a center spacing between oyster meats greater than 64 rows. This still permitted partial images to appear on the edges of the image frame simultaneously as shown in Figure 19b.

After detecting the existence of a good image, the next step was to count the number of dark pixels which made up the image. The final and most important algorithm was the grading algorithm. There were no official oyster standards set up by USDA. Therefore, the category standards were based on military grading standards for Eastern Shore oysters. The standards were based on count per gallon and the approximate volume for each oyster in each category was defined as shown in Table 10. The Eastern Shore oysters were used in all the testing in order to be consistent with the standards. Since the relationship between the volume and the area was known and the relationship between area and number of pixels was also known, the relationship between the volume and the

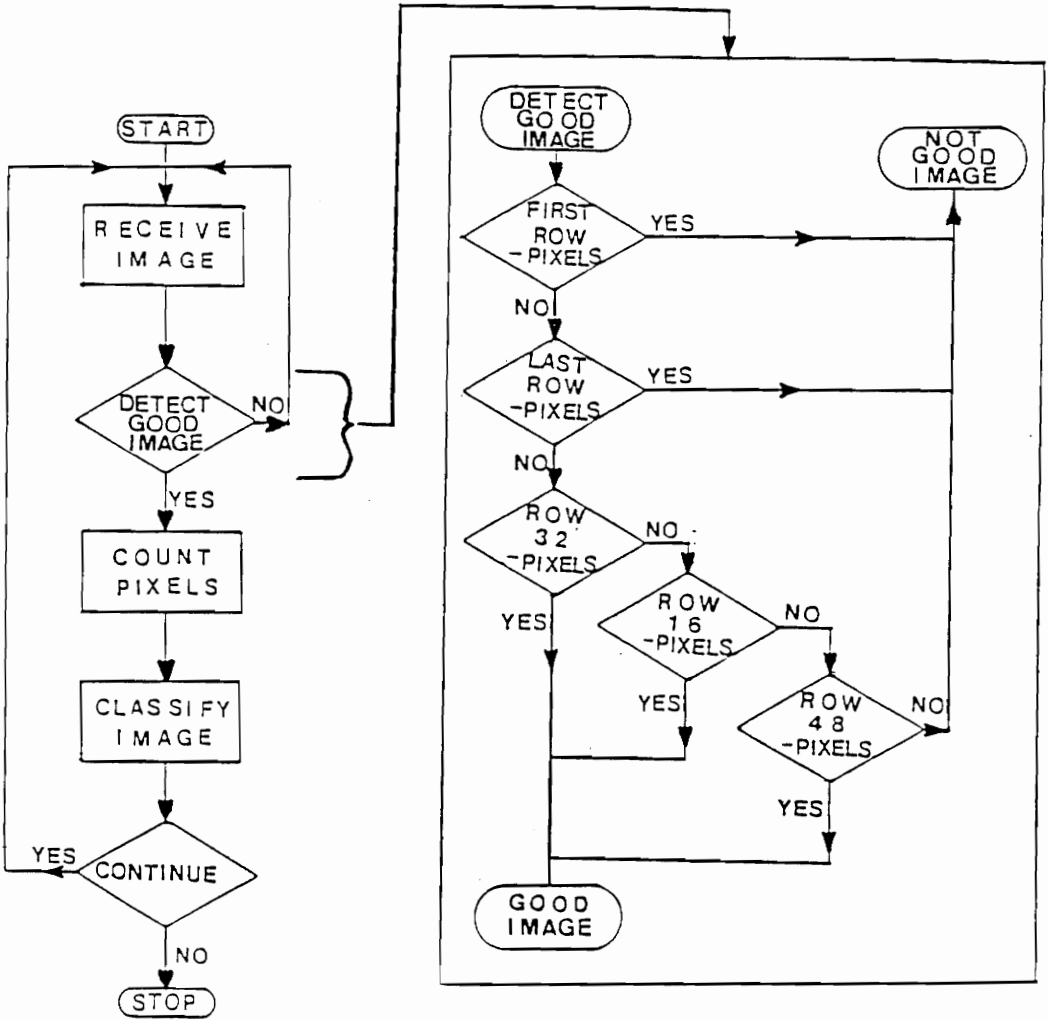


Figure 18. System Flow Chart

(A)

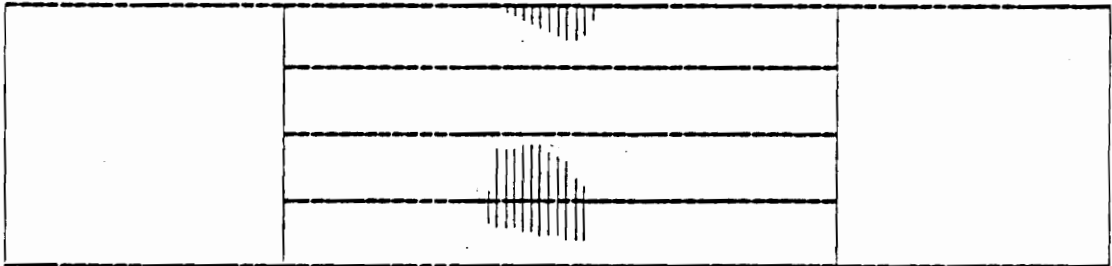
To Continue

Press Any Key !

Number of Pictures = 63

Number of Pixels = 281

Area = 0 MM SQUARE



(B)

To Continue

Press Any Key !

Number of Pictures = 5

Number of Pixels = 130

Area = 0 MM SQUARE

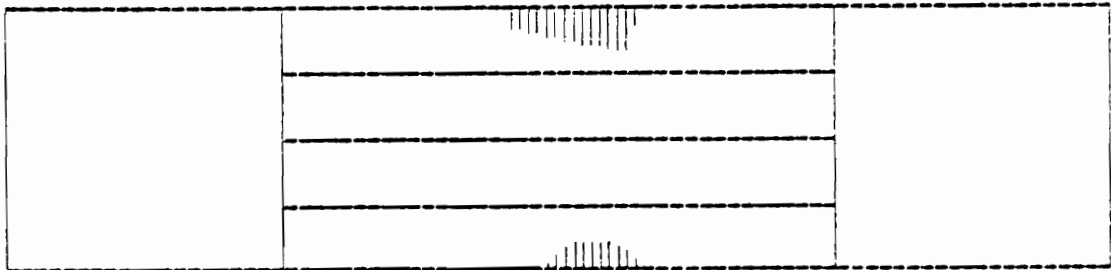


Figure 19. Overlapping images

image area in terms of pixels could be determined. After converting volumes into number of pixels, the information was then inserted into the system software.

Table 10. Industry Sorting Standards For Eastern Shore Oysters

Category	Count per gallon	Approximate Volume (<i>cm</i>³)
Very Small	> 500	< 7.57
Standard	301 - 500	7.57 - 12.6
Select	211 - 300	12.6 - 18.0
Extra Select	160 - 210	18.0 - 23.7
Extra Large	< 160	> 23.7

Chapter VII. System Testing and Evaluation

7.1. General

The two limiting factors in designing this computer vision system were the timing and lighting conditions. The later was previously discussed (see 6.2.2. Illumination Technique). There were several time factors involved in the system, the exposure time needed to obtain an image, the time required to transmit an image from the digital camera to the host microcomputer, the time needed to interpret the image, which was influenced by the processing time of the microcomputer, and the time required to convey an oyster meat through the camera's field of view. The exposure time was closely associated with the image transmission time. The synchronization of the system was important especially synchronization of the time required to convey an oyster through the camera field of view and the time needed for the camera to take a picture. Therefore, the system was tested with both moving and multiple targets.

7.2. Processing Time

The processing time could be improved by utilizing a faster and more powerful microcomputer. The IBM PCTM was replaced by a Jameco model *JE1017* microcomputer (Jameco Electronics, 1988) which used the 16 bit 80286 microprocessor and has processing speeds of 6 MHz, 8 MHz, 10 MHz, or 12 MHz. A test was conducted to examine the effect of processing speed on the rate of acquiring images from the digital camera. A simple program was written to receive images without interpreting them. The test software continuously received 100 images and the required time was recorded with a stop watch. Since the time was recorded manually, five readings were obtained and the average time was calculated. From this test a rough estimate of the image acquisition rate was determined. The test was repeated four times under the four different processing speeds. The test was also conducted with version 3.1, so that the speeds of these two versions could be compared. The test results were tabulated in Table 11. When examining the results, the differences were observed to be small, less than a second. But in computing time these time differences were considered significant. The observed rates were less than the theoretical rate which was 14.93 images per second (the transmission time was 67 milliseconds per image). This test also proved that software which ran under version 4.0 was faster than the software which ran under version 3.1. The rate of image acquisition increased with the speed of processing. The time needed to interpret an image was dependant on the structure of the software (see 6.3. System Software).

7.3. Area Calibration at Different Target Velocities

Several rotating speeds were tested which were 7.5 RPM, 10 RPM, 15 RPM, and 20 RPM. Although 20 RPM exceeded the maximum allowable angular velocity of 17 RPM, it was included to examine the behavior of the system with respect to different speeds. The system was recalibrated

Table 11. Results of the Processing Speed Analysis

a) Time in Seconds per 100 Images With Turbo PASCAL version 3.1

Processors Clock Speed:	6 MHz	8 MHz	10 MHz	12 MHz
	7.30	7.26	7.13	7.12
	7.26	7.18	7.09	7.12
	7.28	7.18	7.13	7.08
	7.31	7.21	7.15	7.10
	7.32	7.20	7.16	7.10
Average	7.294	7.206	7.132	7.104
Images per Second	13.71	13.88	14.02	14.08

b) Time in Seconds per 100 Images With Turbo PASCAL version 4.0

Processors Clock Speed:	6 MHz	8 MHz	10 MHz	12 MHz
	7.27	7.16	7.11	7.07
	7.30	7.14	7.12	7.07
	7.31	7.21	7.13	7.02
	7.23	7.14	7.09	7.06
	7.28	7.19	7.06	7.08
Average	7.287	7.168	7.106	7.06
Images per Second	13.74	13.95	14.07	14.16

with stationary metal targets and with the metal targets moving at the different speeds. Linear regressions with intercepts were used to analyze the area-pixel relationship for each of the cases. Table 12 shows the least squares statistics at stationary position and at the different speeds. Appendix E shows the raw calibration data of this new system at stationary position and at different speeds. As speeds increased, the root mean square errors increased. This also meant that the measurement errors increased and the R^2 values decreased.

As speeds increased, the size of the images decreased. Figure 20 and 21 show sample images obtained at each different speed. The percent decrease in image sizes was studied at a motor speed of 15 RPM and were tabulated in Table 13. It was interesting to notice that the size decreased more in the horizontal directions (from the top to bottom rows) than in the vertical directions (columns). This was expected and was due to the lag time where the digital camera failed to record the first few rows and the last few rows of a image. As the speed increased, the lag time increased and the digital camera missed more rows. The results also showed that metal targets had a lower percentage decrease in apparent area as compared to oyster meats. This was because the metal targets had well defined edges. The percent of decrease in the image size for the oyster meats were scattered and depended on the shape of the oyster meats.

7.4. Grading Rate

With motor speeds of 7.5 RPM, 10 RPM and 15 RPM, the grading rates were 2.5, 3.33, and 5.0 oysters per second, respectively. As mentioned before, a motor speed of 20 RPM exceeded the maximum allowable rotating speed for oysters so the system was not evaluated at that speed. From this point onward, the system was evaluated at 15 RPM with a theoretical grading rate of 5 oysters per second. Table 14 shows the grading rates for the different motor speeds. The calibrated area-pixel least squares equation was:

Table 12. The Linear Statistics at the Different Speeds

	Motor Speed (Revolutions per Minute)				
	Stationary	7.5	10	15	20
SSE	12635.77	26821.65	58221.29	124634.86	156488.28
MSE	200.57	425.74	924.15	1978.33	2483.94
DF	63	63	63	63	63
RMSE	14.16	20.63	30.40	44.48	49.84
Intercept	207.7567	203.4747	220.4811	306.7860	468.2210
Standard Error	6.4293	9.3985	13.7147	19.0023	18.9877
Slope	2.02616	2.5876	2.8395	3.4556	3.8397
Standard Error	0.008688	0.01618	0.02619	0.04678	0.05833
R²	0.9988	0.9975	0.9947	0.9886	0.9857
Sum of Residuals	1.08E-10	1.05E-10	1.09E-10	1.08E-10	1.00E-10

SSE = Sum of Square Error

MSE = Mean Square Error

DF = Degree of Freedom

RMSE = Root Mean Square Error

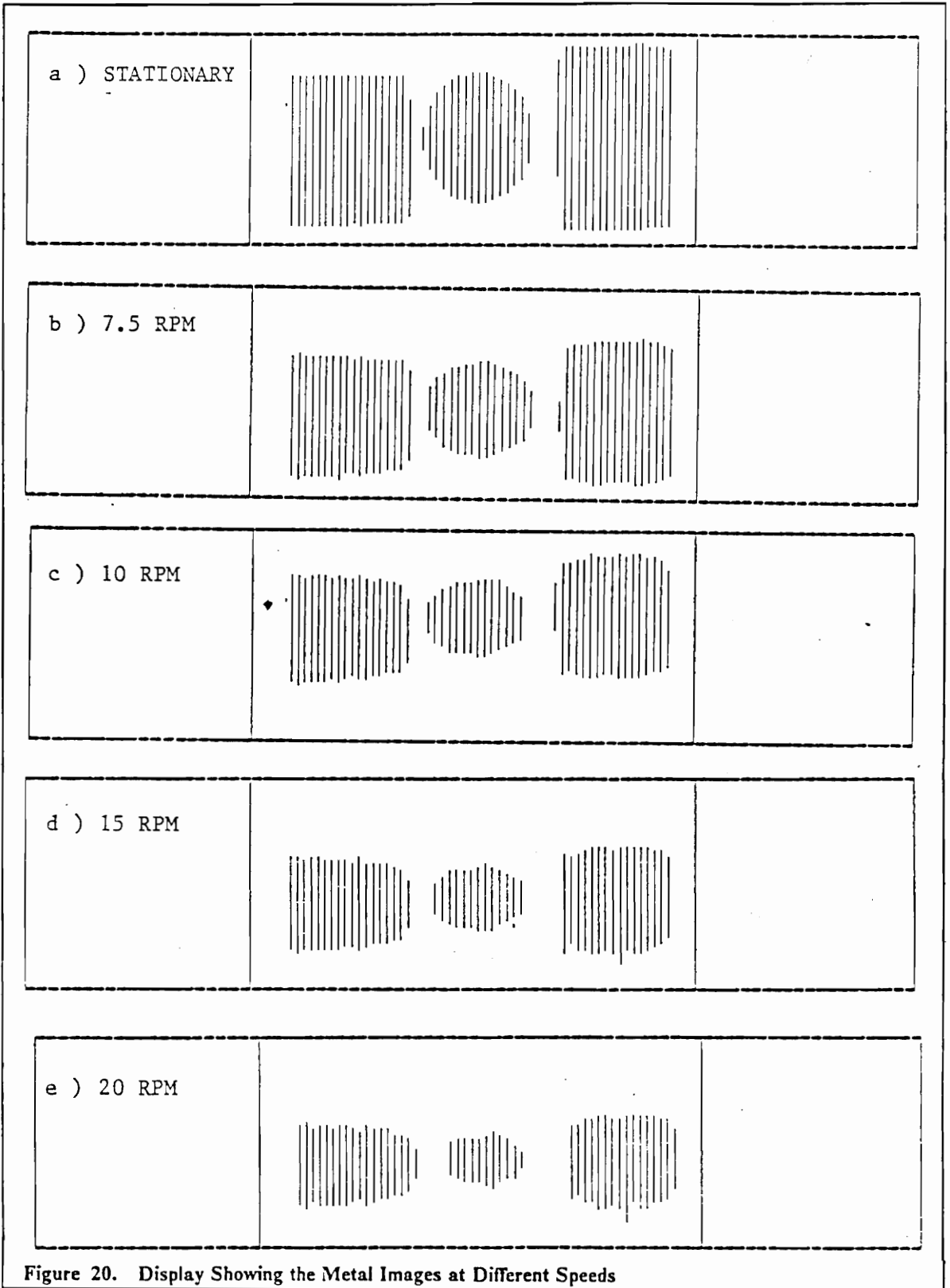
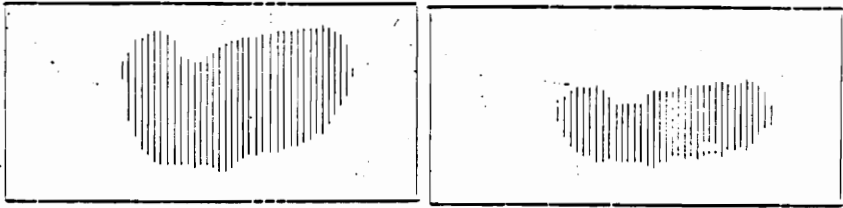


Figure 20. Display Showing the Metal Images at Different Speeds

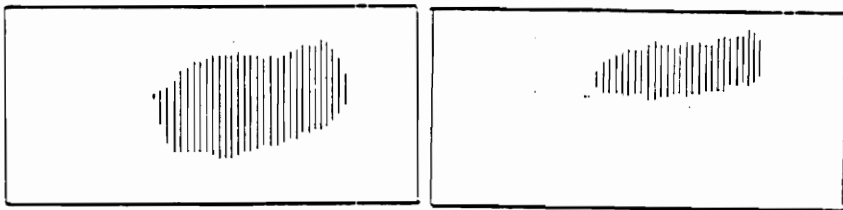
STATIONARY

(1)

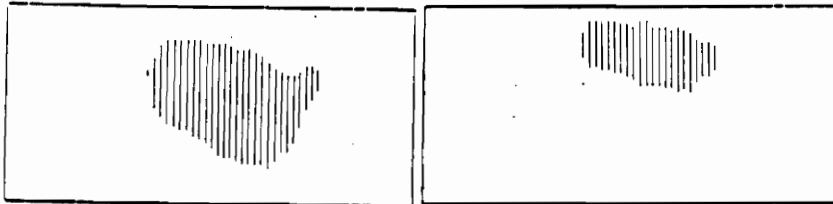
15 RPM



(2)



(3)



(4)

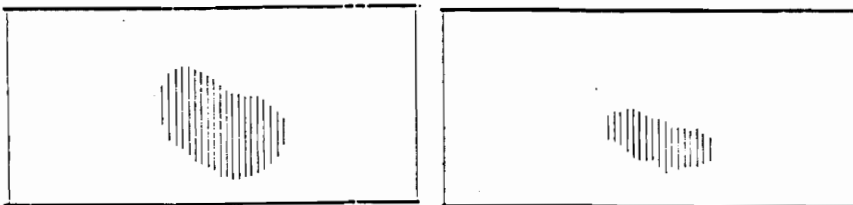


Figure 21. Display Showing the Oyster Images Stationary and at 15 RPM

Table 13. Percent of Image Size Decreases at 15 RPM Compared to Stationary

Object	Vertical (Width)			Horizontal (Length)		
	Actual (cm)	Reduced (cm)	Percent of Decrease	Actual (cm)	Reduced (cm)	Percent of Decrease
1. Metal Target	3.8	2.5	34.21%	3.2	3.0	6.25%
2. Metal Target	3.3	2.3	30.30%	2.6	2.1	19.23%
3. Metal Target	4.6	3.0	34.78%	2.8	2.6	7.14%
4. Oyster Meat	3.0	1.8	40.00%	3.4	3.0	11.76%
5. Oyster Meat	3.4	2.0	41.18%	4.8	3.7	22.92%
6. Oyster Meat	3.2	2.0	37.50%	5.3	4.5	15.09%
7. Oyster Meat	3.9	2.3	41.03%	6.3	5.9	6.35%

Actual = The measured area of the stationary image

Reduced = The reduced size of the image at motor speed of 15 RPM

$$Area = 306.7860 + 3.4556 * Pixels \quad [15]$$

with an estimated measurement error of $\pm 88.96 \text{ mm}^2$ at the 95% confidence level and R^2 value of 0.9886. A volume-pixel equation can be derived from this area-pixel equation for the motor speed of 15 RPM and the volume-area relationship (Equation 1) developed previously as shown below:

$$Volume = 1.6645 + 0.01875 * Pixel \quad [16]$$

with an estimated measurement error of $\pm 3.04 \text{ cm}^3$ at the 95% confidence level. This was a slight increase over the measurement error obtained at stationary position which was 2.84 cm^3

Since the image acquisition rate was approximately 14 images per second excluding the image interpretation time, the system should be able to grade 5 oysters per second. By doing a rough estimation, there were 2.8 images for every oyster at the rate of 5 oysters per second. Including the image interpretation time, the actual images per oyster was less.

Through preliminary testing the system software worked well at a processing speed of 8 MHz and oyster meats could be graded at the rate 5 per second. It took substantial time for the computer to display the grading results on the monitor screen and in real time operation display was not required. Therefore, the system software was modified to grade 5 oysters at once and then display the results. Figure 22 shows a monitor display format of the graded oyster meats. The display indicated the category of each oyster and the total number of oyster graded.

Table 14. Grading Rates at Different Motor Speeds.

	Motor Speed (Revolutions per Minute)			
	7.5	10	15	20
Seconds per Revolution	8	6	4	3
Oysters per Revolution	20	20	20	20
Oysters per Second	2.5	3.33	5	6.67
Oysters per Minute	150	200	300	400

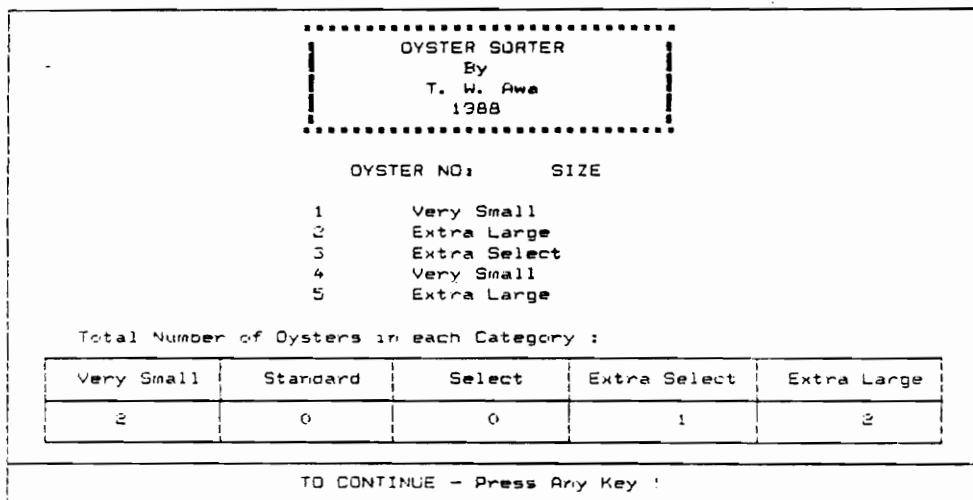


Figure 22. A Monitor Display Showing the Sorted Oyster Meats' Category

7.5. System Testing

A small routine was inserted to the system software for examining how many images were required for each oyster including the image interpretation, classification, and displaying times. It was found that there were on average one good image out of two received images at the rate of 5 oysters per second or roughly 10 images per second. A simple test was also implemented to study whether the system missed any target (i.e., oyster meat) at any time. Five of the original metal targets were placed on the rotating disc and viewed at the rate of 5 per second. The system analyzed 100 good images and the number of target missed was recorded. The test was repeated four times with five different targets and at different positions. The system successfully analyzed all the targets for all the five tests.

A cross validation was conducted to determine the performance of Equation 15, the calibrated area-pixel least squares equation. The validation data were obtained by placing five metal targets at one time on the disc rotating at 15 RPM and ten measurements were recorded for each of the five targets. The collected data were then substituted into the area-pixel least squares equation to get the predicted area. A sample correlation coefficient, ρ , was determined between the area predicted and the actual area, and then a hypothesis test on ρ was conducted, as shown in Table 15 (Myers, 1986). This hypothesis test was based on the principle that if the calibrated equation could accurately predict the area of the oyster meats then the sample correlation coefficient between the actual area and the predicted area should be high and positively correlated. The test result confirmed that the calibrated area-pixel least squares equation was successful in predicting the actual area at a 99% confidence level. Appendix F shows the collected data including the actual and predicted areas.

Table 15. Cross Validation for Determination of Model Performance

Null Hypothesis, H₀ :	$\rho(\text{Actual area, Predicted area}) = 0$
Alternative Hypothesis, H₁ :	$\rho(\text{Actual area, Predicted area}) > 0$
Test Statistic, T.S. :	$T(\text{obs}) = r \sqrt{\frac{n-2}{1-r^2}}$ <p>where sample size, n = 50 and r = 0.9916 T(obs) = 75.27</p>
Rejection Region, R.R. :	$T(\text{obs}) > T(n-2, 0.99) = 2.423$
Conclusion :	Since $T(\text{obs}) > T(48, 99\%)$, reject Null Hypothesis.

Table 16. Oyster's Category Standards in Term of Area and Pixels at 15 RPM

Category	Volume (cm³)	Area (mm²)	Pixels at 15 RPM
Very Small	< 7.57	< 1370.48	< 309
Standard	7.75 - 12.6	1370.48 - 2281.12	309 - 568
Select	12.6 - 18.0	2281.12 - 3258.75	569 - 848
Extra Select	18.0 - 23.7	3258.75 - 4290.68	849 - 1143
Extra Large	> 23.7	> 4290.68	> 1144

7.6. System Evaluation

After size-volume standards were established from the commercial grading standards, the system was tested with oyster meats. Table 16 shows the approximate volume, area, and pixels of each category at the motor speed of 15 RPM. The grading rate of the system was 5 oysters per second and five oyster meats were placed on the rotating disc and five measurements of the set of 5 oysters were recorded. A total of 25 manually graded oyster meats (10 of category select and 15 of category standard) were tested with results shown in Table 17. The vision based system measured the oyster meats size as smaller than the commercial category. Out of the 10 select oysters, the system graded them as 4 selects and 6 standards. The 15 standard oysters were graded as 1 select, 4 standards, and 10 very smalls. For each of the five trials the results were consistent. The observed fluctuation in the number of pixels counted for each oyster was also consistent (as it was proven that these fluctuations were not significant).

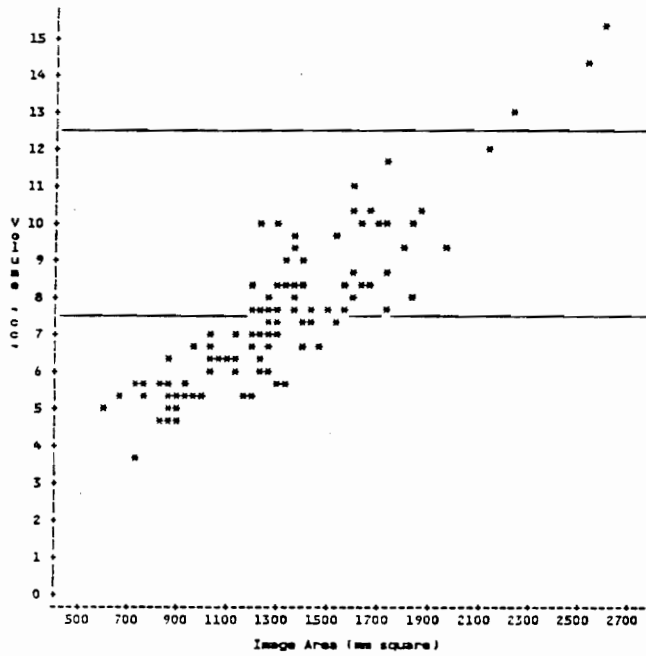
When measuring oysters which were not moving, the system also undergraded the oyster meats. This was observed during the physical properties measurements. Figure 23 shows two plots of the volume versus the area for the select and the standard oysters. Overlapping between the graded oyster sizes could be seen from these plots. For these observations, it was believed that there was a significant error in manual grading, and the discrepancy was due to the commercial grader and was not due to the developed system.

Table 17. Data Collected and Analyzed for the 25 Oyster Meats

Oyster No.	Trial 1	Trial 2	Trial 3	Trial 4	Trial 5
1. Select - 1	673 Se	671 Se	654 Se	649 Se	652 Se
2. Select - 2	843 Se	824 Se	805 Se	797 Se	805 Se
3. Select - 3	483 St	469 St	460 St	457 St	469 St
4. Select - 4	456 St	443 St	444 St	438 St	438 St
5. Select - 5	671 Se	648 Se	657 Se	654 Se	650 Se
6. Select - 6	351 St	352 St	350 St	348 St	346 St
7. Select - 7	642 Se	625 Se	637 Se	655 Se	637 Se
8. Select - 8	492 St	484 St	489 St	487 St	486 St
9. Select - 9	474 St	476 St	475 St	464 St	462 St
10. Select - 10	477 St	475 St	467 St	472 St	455 St
11. Standard - 1	536 St	533 St	532 St	529 St	522 St
12. Standard - 2	619 Se	612 Se	613 Se	616 Se	611 Se
13. Standard - 3	483 St	479 St	495 St	486 St	473 St
14. Standard - 4	226 Vs	219 Vs	219 Vs	228 Vs	223 Vs
15. Standard - 5	270 Vs	264 Vs	265 Vs	269 Vs	264 Vs
16. Standard - 6	284 Vs	279 Vs	279 Vs	277 Vs	270 Vs
17. Standard - 7	354 St	364 St	361 St	356 St	347 St
18. Standard - 8	460 St	460 St	460 St	473 St	443 St
19. Standard - 9	258 Vs	255 Vs	257 Vs	261 Vs	249 Vs
20. Standard - 10	165 Vs	154 Vs	153 Vs	158 Vs	157 Vs
21. Standard - 11	277 Vs	266 Vs	276 Vs	278 Vs	262 Vs
22. Standard - 12	284 Vs	284 Vs	302 Vs	281 Vs	280 Vs
23. Standard - 13	161 Vs	165 Vs	143 Vs	138 Vs	163 Vs
24. Standard - 14	143 Vs	143 Vs	155 Vs	136 Vs	139 Vs
25. Standard - 15	223 Vs	229 Vs	255 Vs	217 Vs	224 Vs

Se = Select
 St = Standard
 Vs = Very Small

a) STANDARDS (The two lines indicate the boundary for Category Standard)



b) SELECTS (The two lines indicate the boundary for Category Select)

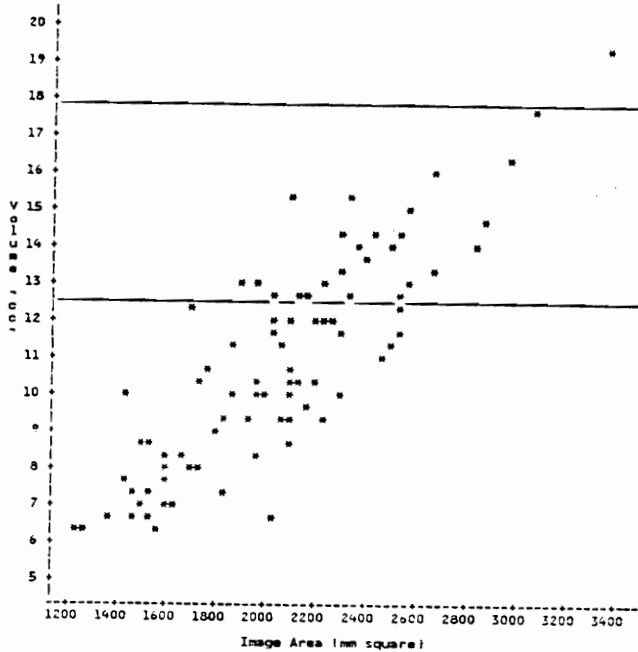


Figure 23. Plots of Volume versus Area for Both the Select and Standard Oysters

Chapter VIII. System Improvement

8.1. General

The design of a computer vision system was not an actual science. It was more like a trial and error experimental science. After knowing that the system worked accordingly to the desired conditions, two separate investigations were carried out hoping to further improve the system. The first problem was to find a way to reduce the camera-object distance and the second was to examine a way to increase the grading rate.

8.2. New Camera Design

The field of view of the camera was dependant on the distance from the lens to the Optic RAM and the working distance. As previously defined, the working distance was the distance between the lens and the object. The distance between the lens and Optic RAM was fixed. In order to

increase the field of view, it was necessary to increase the working distance, or increase the lens magnification. For a field of view of approximately 5 cm × 13 cm, the working distance was 1 meter with a 16 mm lens. With a wider angle lens, a shorter working distance would produce the same size field of view. Therefore, the 16 mm C-mount lens was replaced with a 6.5 mm C-mount lens. With this new camera lens the working distance was reduced to 45 cm and the field of view was roughly 5.5 cm × 12 cm. This new camera lens system was then calibrated with metal targets and analyzed with linear regression with an intercept and results were tabulated in Table 18. Appendix G shows the raw calibration data for this new 6.5 mm lens. The area-pixel least squares equation was:

$$Area = 136.1332 + 2.0894 * Pixels \quad [17]$$

with an estimated measurement error of $\pm 59.14 \text{ mm}^2$ at the 95% confidence level and R^2 value of 0.9986. The data were collected with stationary targets. The statistics for this new 6.5 mm lens seem very acceptable as compared with the previous statistics. This investigation showed that it was possible to reduce the working distance by employing a wider angle lens (in this case 6.5 mm) and very acceptable regression statistics could still be obtained. The problem encountered with this new lens was that it had only an aperture adjustment and no fine focusing adjustment, which made it difficult to use in experiments. After demonstrating the capability of reducing the working distance with wider angle lens and learning the difficulty of focusing the new lens, no further work was carried on with this new lens.

8.3. Three Images per Exposure

A investigation was performed to more fully use the whole array. Previously the system software only used the middle parts of the array (see 6.3. System Software). The total dimension of the field of view was approximately 5 cm × 26 cm (or the image frame was 64 × 128 pixels). The objective

Table 18. Linear Regression Results for the 6.5 mm C-mount Lens

Sum of Square Error (SSE)	10287.3747
Mean Square Error (MSE)	874.4415
Degree of Freedom (DF)	17
Root Mean Square Error (RMSE)	29.5710
Intercept	136.1332
Standard Error	13.0219
Slope	2.0894
Standard Error	0.01926
R²	0.9986
Sum of Residuals	9.0949E-13

of this investigation was to take three images per exposure instead of one image per exposure. This can be done by dividing the total field of view into three equal sections of roughly 5 cm × 9 cm each. This also meant that the initial rate of 5 oysters per second could potentially be improved three times (i.e., 15 oysters per second) with one line of grading in each of the three sections. Figure 24 shows some graphics of three images per field of view. The 12 light bulbs did not provide enough illumination to cover the whole area. Therefore, the light bulbs were replaced by eight 15 watt fluorescent tubes. The length of each fluorescent tube was 41 cm and was large enough to illuminate the whole field of view.

The system was then calibrated with the metal targets. Seven metal targets were placed at each section (i.e, left, center, and right) one at a time and the number of pixels counted for each section and each metal target was recorded. Three separate linear regressions with intercepts were performed and the results were tabulated in Table 19.

The least squares equation for the left region was:

$$Area = 7.03414 + 2.4631 * Pixels \quad [18]$$

with an estimated measurement error of $\pm 25.57 \text{ mm}^2$ at the 95% confidence level and R^2 value of 0.9993. The least squares equation for the center region was:

$$Area = 10.8467 + 2.4722 * Pixels \quad [19]$$

with an estimated measurement error of $\pm 11.95 \text{ mm}^2$ at the 95% confidence level and R^2 value of 0.9998. The least squares equation for the right region was:

$$Area = 15.9875 + 2.4401 * Pixels \quad [20]$$

with an estimated measurement error of $\pm 17.00 \text{ mm}^2$ at the 95% confidence level and R^2 value of 0.9997. By studying these equations, the center region seemed to have a lower error than the other two regions. This was expected since the light was more intense and uniform at the center of the camera than in the end regions. This can be further verified by examining the number of

To Continue
Press Any Key !

Number of Pictures =

1

Number of Pixels =

2282

Area =

4998

mm square

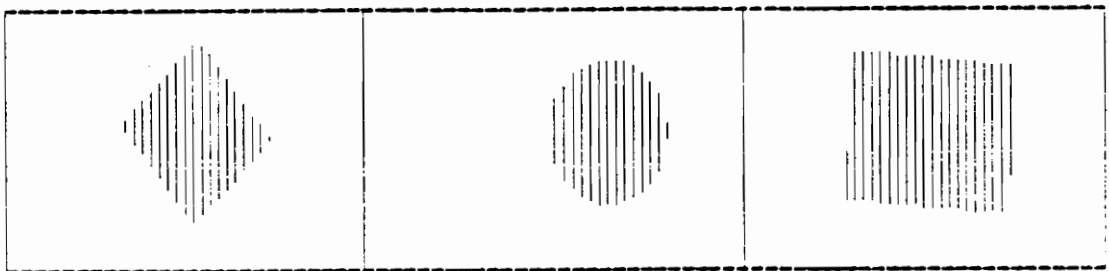
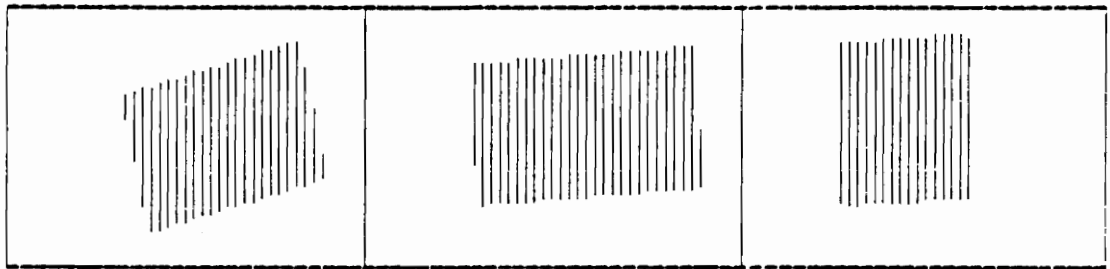


Figure 24. Three Images per Exposure Displays

Table 19. Linear Regression Results for Three Images per Exposure

	Left	Center	Right
Sum of Square Error	1961.2670	428.1377	868.9244
Mean Square Error	163.4389	35.6781	72.4104
Degree of Freedom	12	12	12
Root Mean Square Error	12.7843	5.9732	8.5004
Intercept	7.0341	10.8467	15.9875
Standard Error	12.9832	6.0509	8.5950
Slope	2.4631	2.4722	2.4401
Standard Error	0.01937	0.0091	0.0128
R²	0.9993	0.9998	0.9997
Sum of Residuals	1.8758E-12	3.0695E-12	2.2737E-12

pixels counted at the center which was less than both ends because at the center its received more light (see Table 20). The number of pixels counted were different from each section. Two statistical tests were performed to see whether these differences were significant. The same statistical methods applied in light readjustment and replacement tests were used. The F-Test and Duncan test statistics were tabulated in Table 20. The F-statistic indicated that the differences observed in each region were not significant at both 0.05 and 0.01 levels. But the Duncan test, which was a more powerful test, showed that the center region was significantly different from the end regions at 0.05 level (see 5.2. Lighting Readjustment Test). The left and right ends were statistically similar which was suspected since the ends received equal amount of light intensity. The results from this experiment showed that it would be possible to grade three oysters per exposure with better lighting development. The software development tasks would be more difficult. The oyster meats must be separated and the software should be able to identify three different oyster images and analyze them separately. Three least squares equations might be required for three regions if the differences observed were still significant after a better lighting development. The experiment was conducted on stationary targets, not at motor speed of 15 RPM because the tangential velocity at the left section (i.e., outer radius) was greater than the right section (i.e., inner radius). As a result the differences observed in each section would be more pronounced. This problem could be eliminated if the rotating disc was replaced by a linear conveyor belt.

Table 20. F-test and Duncan test Statistics for Three Images per Exposure

a) F-statistic

Null Hypothesis, H_0 :	$\mu_1 = \mu_2 = \mu_3$
Alternative Hypothesis, H_1 :	At least one of the means are not equal
Test Statistic, T.S. :	$F(\text{obs}) = 0.0010$
Rejection Region, R.R. :	$F(\text{obs}) > F(\text{critical})$
Conclusion :	Since $F(\text{obs}) < F(2,13) = 3.81$ at 0.05 level, Accept H_0 Since $F(\text{obs}) < F(2,13) = 6.70$ at 0.01 level, Accept H_0

b) Duncan's Multiple Range Test

Oyster No.	Replacement Position		
	Left	Center	Right
1	766	752	763
2	758	754	762
3	750	760	766
4	762	756	768
5	409	405	414
6	407	411	415
7	628	623	626
8	628	623	627
9	686	681	689
10	685	680	689
11	899	896	906
12	905	898	901
13	385	378	378
14	385	381	379
mean	646.643	642.714	648.786
Treatment	1	2	3

Alpha Level, α = 0.05
 Degrees of Freedom, DF = 26
 Mean Square Error, MSE = 14.5842

Number of mean steps apart, r :	2	3	
Critical value :	2.96453	3.11506	
Ranked Mean :	648.786	646.643	642.714
Treatment :	3	1	2
Grouping :	AAAAAAAAAAAAAAAAAAAA		BBBBBBBB

Means with the same letter were not significantly different.

Chapter IX. Summary and Conclusion

The overall goal of this study was to develop an inexpensive automation system for grading raw oyster meats.

Knowledge of the physical properties of the oyster meats was essential. Since there was no published literature on the physical properties of oyster meats, a study on the physical properties of the oyster meats was carried out. The measured parameters included the projected area, weight, height, and volume of the oyster meats. The projected area was measured by digital imaging and photographic techniques. The correlations between each pair of the measured parameters were calculated. The statistical results indicated that the digital area could predict the volume and weight competently and therefore could be used as a grading criterion. A strong correlation was found between the digital and the photographic areas. This suggested that the area measurements were accurate. In this grading application, complicated feature extraction algorithms were not required because simple silhouettes were accurate enough in predicting the volume. This also meant that the software development was simplified and the image processing time was reduced significantly.

A calibrated volume-pixel least squares equation was obtained and could be used to measure the volume of the oyster meats with an estimated measurement error of $\pm 2.84 \text{ cm}^3$ at a 95% confidence level. During the measurements of physical properties, some fluctuation in the number of

pixels was seen. Two tests were conducted to study the effect of these fluctuations and the results showed that the fluctuations were not important.

After completing the physical properties measurements of the oyster meats the next stage was to design and construct the grading system. The system consisted of a rotating disc, a grading section, and a microcomputer. The rotating disc was translucent and was used to convey oysters into the grading section. The disc was driven by a motor which was controlled by an adjustable speed controller. The grader was a digital camera connected to and controlled by a microcomputer.

The computer software was written in Turbo PASCAL. Two version of Turbo PASCAL were utilized. Version 3.1 was used to display the image on the screen and the actual grading algorithms were developed with version 4.0, which was faster. Basically, the system software consisted of four main sections. They were the image receiver, the image detector, the image analyzer, and the image classifier. Since there were no official USDA standards for the oyster meat categories, standards were established from the commercial grading standards for Eastern Shore oysters.

Illumination and timing were the two most important factors in designing the computer vision system. The illumination technique chosen for this study was backlighting. Several lighting schemes were tested before a suitable scheme was selected. There were several timing factors involved. The aperture opening of the camera was dependant on the lighting condition. Different motor speeds and processor speeds were tried. Since timing was crucial, the system software must be as simple as possible but "intelligent". It must have the ability of detecting good images and analyzing them to determine appropriate categories. Through several experiments, the system successfully graded 5 oysters per second with a motor speed of 15 RPM and computer processing speed of 8 MHz.

The volume-pixel least squares equation was verified with a cross validation test and the system was proved to be reliable at the rate of 5 oysters per second with an estimated measurement error of $\pm 3.04 \text{ cm}^3$ at a 95% confidence level.

Some initial work was also conducted in attempt to improve the system and its grading rate. A new camera was tested and the results indicated that there was a potential of using a wider angle lens to reduce the working distance. Preliminary tests on obtaining three images per exposure were successful but showed the need for more attention to better lighting. Since it took the same amount of time to acquire one image or three images per exposure from the digital camera, using three images per exposure could potentially improve the grading rate from 5 to 15 oysters per second with well written software. The software development tasks would be slightly more complicated but still manageable.

Chapter X. Recommendations

The following are some of the recommendations suggested for machine designers, the oyster industry, and further improvement of the developed digital imaging system for grading oyster meats:

1. The knowledge of the variation found in the physical properties would be an asset to the system designers. With this knowledge, the designers could determine whether it was more economical to discard a few very large oysters, instead of building machines for accommodating the maximum sized oysters, which might be only one out of a hundred. More measurements of the physical properties should be conducted so that the degree of variation of these parameters could be known.
2. There was much overlapping between the graded oyster categories which implied that there existed a great deal of error in the manual grading process. This type of error was due to the shuckers' biases. The shuckers were paid more for grading larger sizes; therefore, there was a tendency for them to overgrade the oyster meats. The computer vision grading device could be used to reduce the observed discrepancy and the graded sizes would be more consistent.
3. Digital imaging technique could not only be used as a grading scheme but also could be further implemented to check for quality. For example, additional features could be extracted from the images of the oyster meats by developing more advance algorithms. Any abnormality found in an

image would indicate a defect in the oyster meat and would lead to a rejection before going through the grading scheme. There will be a trade off, the grading rate will be decreased since processing time would be required for extracting more features.

4. The image transmission time was 67 milliseconds or 14.93 images per second and assuming that it required on average two images per oyster, it would be possible to increase the grading rate to 7 oysters per second. If three images per exposure can be implemented the possible grading rate would be 21 oysters per second or 1260 oysters per minute. There are many possible ways of achieving this grading rate. Well developed illumination equipment will certainly help. One other way would be to increase the computer processing time, from 8 MHz to 12 MHz, but this time must be synchronized with the transmission time in order to provide sufficient time for the camera to take a picture. The software execution time could be improved by using an independent processor for executing different algorithms or special purpose dedicated image processing software. The processing time could be cut by implementing parallel image processing architectures. In its final form, the computer vision system will probably need some of these techniques or improvements in order to achieve real-time speeds required for a cost effective commercial application.

5. The only limitation which could be visualized at this stage was the problem of conveying the oyster meats into the camera sensing area. The conveying system must move the oysters fast enough into and out of the sensing area. Synchronization was the most tedious task in developing a computer vision system. Since the computer and the motor were independently operated at different speeds, the task of synchronization was tougher. Currently, the synchronization was depended on the system software and it worked well at a processing speed of 8 MHz and a motor speed of 15 RPM. No further effort was made to synchronize the system because this was a demonstration device. In the future, when the rotating disc is replaced by a linear conveyor belt, a better way of synchronizing the system will be highly recommended. This can be accomplished with an external sensing device or by developing better software. An external sensing device could signal the camera to take a picture when an oyster is in the field of view of the camera. In this case, the

camera only needs to take one picture per oyster instead of continuously taking pictures. The other possibility is to develop better software by using a faster and more powerful software packages.

Bibliography

- Applied Engineering. 1988. *User Manual*. P.O. Box 798, Carrollton, TX 75006.
- Berlage, A. G., T. M. Cooper and J. F. Aristazabal. 1987. *Machine Vision Identification of Diploid and Tetraploid Ryegrass Seed*. ASAE Paper No. 87-6052, St. Joseph, Michigan.
- Brinkmann Instruments CO., Div. of Sybron. 1983. *Startorius : Electronic Analytical Balances*. Westburg, NY 11590.
- Chen, S. S. and F. W. Wheaton. 1987. *Oyster Hinge Line Detection Using Image Processing*. ASAE Paper No. 87-3047, St. Joseph, Michigan.
- Ciarcia, S. A. 1983a. *Build the Micro D-Cam Solid-State Video Camera - Part 1: The IS32 Optic RAM and the Micro D-Cam Hardware*. Byte, 8(9):21-31.
- Ciarcia, S. A. 1983b. *Build the Micro D-Cam Solid-State Video Camera - Part 2: Computer Interfaces and Control Software*. Byte, 8(10):67-86.
- Cook, D. I. 1960. *Engineering Mechanics Statics*. International Textbook Company, Scranton, Pennsylvania.
- Dayton Electric Manufacturing Co. 1988a. *Installation Instructions and Parts Manual for SCR MOTOR CONTROLLER*. Chicago, IL 60648.
- Dayton Electric Manufacturing Co. 1988b. *Operating Instructions and Parts Manual for GEARMOTORS*. Chicago, IL 60648.
- Diehl, K. C., V. A. Garwood, and C. G. Haugh. 1988. *Volume Measurement Using the Air Comparison Pycnometer*. TRANSACTIONS of the ASAE 31(1):284-287.
- Everex Systems, Inc. 1986. *Excelerator 80286 Turbo Board for the IBM PC and XT (Version 2.0)*. 48431 Milmont Drive, Fremont, Ca 94538.
- Gonzalez, R. C. and R. Safabakhsh. 1982. *Computer Vision Techniques for Industrial Applications and Robot Control*. Computer, 15(12):17-32.

- Gonzalez, R. C. 1983. *How Vision Systems See*. Machine Design, 55(10):91-96.
- Gunasekaran, S., T. M. Cooper, A. G. Berlage and P. Krishnan. 1987. *Image Processing for Stress Cracks in Corn Kernels*. TRANSACTIONS of the ASAE 30(1):266-271.
- Hollingum, J. 1984. *Machine Vision; the Eyes of Automation*. IFS(Publications) Ltd, Bedford, United Kingdom.
- Jameco Electronics, 1988. *User Manual for Jameco Model JE1017 Microcomputer*. 1355 Shoreway Road, Belmont, CA 94002.
- Johnson, M. 1985. *Automation in Citrus Sorting and Packing*. Proceedings of Agri-Mation I Conference and Exposition, Chicago, IL. pp 63-68.
- Kaminaka, M. S., S. Zahner, D. Slaughter and T. Fortis. 1982. *Low Cost Digital Image Processing with Short Algorithms and Sparse Data*. ASAE Paper No. 82-6012, St. Joseph, Michigan.
- Kaufman, J. E. 1968. *IES Lighting Handbook*. Illumination Engineering Society. New York, New York. 4th. ed.
- Kinnucan, P. 1983. *Machines That See*. High Technology, April, 1983. pp 30-36.
- Kranzler, G. A. 1985. *Applying Digital Image Processing in Agriculture*. Agricultural Engineering, 66(3):11-13.
- McClure, J. E. and C. T. Morrow. 1987. *Computer Vision Sorting of Potatoes*. ASAE Paper No. 87-6501, St. Joseph, Michigan.
- Micromint, Inc. 1984. *Micro D-Cam IBM PC Version, Users Manual*. 561 Willow Avenue, Cedarhurst, NY 11516.
- Myers, R. H. 1986. *Classical and Modern Regression with Application*. PWS Publishers, Duxbury Press, Boston, Massachusetts.
- Nakahara, S., A. Maeda, and Y. Nomura. 1979. *Automatic Cucumber Sorting Using Pattern Recognition Techniques*. IEEE, Tokyo Proc., Tokyo. No. 18:46-48.
- Nascimento, I. A., S. A. Pereira and R. C. Souza. 1980. *Determination of the Optimum Commercial Size for the Mangrove Oyster (Crassostrea Rhizophorae) in Todds Os Santos Bay, Brazil*. Aquaculture, 20:1-8.
- Naugle, J. and G. E. Rehkugler. 1987. *Grapevine Cordon Following Using Digital Image Processing*. ASAE Paper No. 87-3045, St. Joseph, Michigan.
- Newcombe, C. L. 1950. *An Analysis of Certain Dimensional Relationships of the Virginia Oyster (Crassostrea Virginica, Gmelin)*. American Nature, 84(816):203-214.
- Ohura, M., T. Nishide and Y. Toshima. 1987. *Size Detection of Raw Silk Thread by Means of Image Processing*. ASAE Paper No. 87-3044, St. Joseph, Michigan.
- Ott, L. 1984. *An Introduction to Statistical Methods and Data Analysis*. PWS Publishers, 20 Park Plaza, Boston, MA 02116.
- Paulsen, M. R. and W. F. McClure. 1986. *Illumination for Computer Vision Systems*. TRANSACTION of the ASAE 29(5):1398-1404.

- Personal Computing Tools, Inc. 1988. *IS32 Optic RAM Spectral Data Applications*. The Catalog of Personal Computing Tools for Scientists and Engineers. 101 Church Street Unit 12, Los Gatos, CA 95032-6927.
- Przybyla, A. E. 1986. *Tomorrow's Technology, Part I*. Food Engineering, 58(4):45-59.
- Rehkugler, G. E. and J. A. Throop. 1986. *Apple Sorting with Machine Vision*. TRANSACTIONS of the ASAE 29(5):1388-1397.
- Rigney, M. P. and G. A. Kranzler. 1986. *Machine Vision for Grading Southern Pine Seedlings*. ASAE Paper No. 86-1597, St. Joseph, Michigan.
- Riley, J. G. and D. A. Smyth. 1979. *The Mechanization of Cultivated European Oyster Processing*. ASAE Paper No. 79-5037, St. Joseph, Michigan.
- Robe, K. 1988. *Optical Scanner inspects and rejects vegetables at 6000 lb/hr*. Food Processing, Chicago, IL. pp 122-124.
- Sarkar, N. and R. R. Wolfe. 1985a. *Feature Extraction Techniques for Sorting Tomatoes by Computer Vision*. TRANSACTIONS of the ASAE 28(3):970-974.
- Sarkar, N. and R. R. Wolfe. 1985b. *Computer Vision Based System for Quality Separation of Fresh Market Tomatoes*. TRANSACTIONS of the ASAE 28(5):1714-1718.
- Schaevitz Engineering. 1987. *LVDT Type 100 HR, Users Manual*. Pennsauken, New Jersey.
- Shays, D. R. and F. W. Wheaton. 1980. *Biological Properties of Shellfish Shells*. ASAE Paper No. 80-5048, St. Joseph, Michigan.
- Statistical Analysis System Institute Inc. 1982. *SAS User's Guide: Statistics*. Box 8000, Cary, NC 27511.
- Sistler, F. E., M. E. Wright and R. M. Watson. 1983. *Measurement of Physical Properties of Biological Products with a Video Analyzer*. Agricultural Electronics - 1983 and Beyond : Volume II, Proceeding of the National Conference on Agricultural Electronics Applications, ASAE Publication 9-84:646-651.
- Swientek, R. J. 1987. *Machine Vision Systems*. Food Processing, April, 1987. pp 68-80.
- Tojeiro, P. and F. W. Wheaton. 1987. *Computer Vision Applied to Oyster Orientation*. ASAE Paper No. 87-3046, St. Joseph, Michigan.
- Wagner, J. N. 1983. *Inspecting the 'Impossible'*. Food Engineering, 55(6):79-92.
- Wheaton, F. W., J. W. Grid and G. E. Kaiser. 1985. *Use of Biological Properties in Food Processing Automation*. Proceedings of Agri-Mation I Conference and Exposition, February 25-28, 1985. pp. 38-52.

Appendix A. Digital Camera Calibration Data

The following is the data collected for digital camera calibration. Since some fluctuation of the number of pixels counted were observed for each object under experimental conditions, ten pictures were taken for each metal target.

Obs	Actual Area (mm ²)	Pixels
1	3825.36	1758
2	3825.36	1758
3	3825.36	1758
4	3825.36	1758
5	3825.36	1758
6	3825.36	1758
7	3825.36	1758
8	3825.36	1758
9	3825.36	1758
10	3825.36	1758
11	1881.65	850
12	1881.65	850
13	1881.65	850
14	1881.65	849
15	1881.65	849

16	1881.65	849
17	1881.65	849
18	1881.65	850
19	1881.65	849
20	1881.65	850
21	1881.65	855
22	1881.65	856
23	1881.65	856
24	1881.65	855
25	1881.65	855
26	1881.65	855
27	1881.65	855
28	1881.65	856
29	1881.65	856
30	1881.65	855
31	1881.65	859
32	1881.65	859
33	1881.65	859
34	1881.65	859
35	1881.65	859
36	1881.65	859
37	1881.65	859
38	1881.65	859
39	1881.65	859
40	1881.65	859
41	1010.75	433
42	1010.75	433
43	1010.75	433
44	1010.75	433
45	1010.75	433
46	1010.75	433
47	1010.75	433
48	1010.75	433
49	1010.75	433
50	1010.75	433
51	1010.75	462
52	1010.75	462

53	1010.75	462
54	1010.75	462
55	1010.75	462
56	1010.75	462
57	1010.75	462
58	1010.75	462
59	1010.75	462
60	1010.75	462
61	1096.41	513
62	1096.41	513
63	1096.41	513
64	1096.41	513
65	1096.41	513
66	1096.41	513
67	1096.41	513
68	1096.41	513
69	1096.41	513
70	1096.41	513
71	1096.41	498
72	1096.41	497
73	1096.41	498
74	1096.41	498
75	1096.41	498
76	1096.41	498
77	1096.41	497
78	1096.41	498
79	1096.41	497
80	1096.41	498
81	1096.41	520
82	1096.41	520
83	1096.41	520
84	1096.41	520
85	1096.41	520
86	1096.41	520
87	1096.41	520
88	1096.41	520
89	1096.41	520

90	1096.41	520
91	1704.08	760
92	1704.08	760
93	1704.08	760
94	1704.08	760
95	1704.08	760
96	1704.08	760
97	1704.08	760
98	1704.08	760
99	1704.08	760
100	1704.08	760
101	1704.08	772
102	1704.08	772
103	1704.08	772
104	1704.08	772
105	1704.08	772
106	1704.08	772
107	1704.08	773
108	1704.08	772
109	1704.08	772
110	1704.08	772
111	1704.08	790
112	1704.08	791
113	1704.08	790
114	1704.08	790
115	1704.08	788
116	1704.08	790
117	1704.08	790
118	1704.08	790
119	1704.08	789
120	1704.08	790
121	782.83	352
122	782.83	352
123	782.83	352
124	782.83	352
125	782.83	352
126	782.83	352

127	782.83	352
128	782.83	352
129	782.83	352
130	782.83	352
131	458.06	207
132	458.06	207
133	458.06	207
134	458.06	207
135	458.06	207
136	458.06	207
137	458.06	207
138	458.06	207
139	458.06	207
140	458.06	207

Appendix B. Physical Properties Data

The following is the collected data (including both standard and select) of physical properties of oyster meats from the initial sample of 250 oysters (Some readings were discarded due to error).

Obs	Volume (cm ³)	Height (mm)	Weight (grams)	Digital Area (mm ²)	Photo Area (mm ²)	Pixels
a) Select						
1	17.72	11.67	19.52	3052.66	3059.20	1398
2	12.90	9.81	13.18	2561.65	2611.20	1172
3	9.25	9.94	10.04	2059.79	2206.72	941
4	8.67	8.98	9.88	2101.07	2245.12	960
5	6.78	9.05	7.35	1549.23	1658.88	706
6	12.52	10.90	13.69	2524.72	2634.24	1155
7	7.45	8.41	8.08	1831.67	1927.68	836
8	9.48	8.28	10.41	2111.93	2229.76	965
9	9.58	9.09	11.20	2161.90	2224.64	988
10	15.49	11.41	17.11	2327.01	2414.08	1064
11	10.54	9.69	11.51	1762.14	1802.24	804
12	10.60	10.64	10.63	2088.03	2176.00	954
13	6.85	9.21	7.50	1623.10	1692.16	740

14	14.43	11.64	15.38	2300.94	2332.16	1052
15	11.12	9.56	11.63	2474.75	2588.16	1132
16	14.09	11.71	15.10	2370.47	2419.20	1084
17	8.40	9.82	9.04	1677.41	1712.64	765
18	10.38	9.61	11.71	2083.68	2117.12	952
19	7.97	12.21	8.55	1597.03	1710.08	728
20	9.90	10.08	10.94	2285.74	2421.76	1045
21	14.11	12.90	15.71	2496.47	2567.68	1142
22	7.04	8.06	6.17	1586.17	1669.12	723
23	6.82	9.33	8.05	2018.51	2163.20	922
24	17.32	10.31	19.03	3528.45	3612.16	1617
25	10.24	11.06	11.33	2216.21	2339.84	1013
26	15.41	13.65	15.78	2114.11	2142.72	966
27	7.48	8.96	6.66	1531.85	1576.96	698
28	12.36	8.76	13.24	2533.41	2588.16	1159
29	10.14	10.23	10.03	1853.40	1930.24	846
30	11.89	9.92	11.11	2111.93	2211.84	965
31	10.54	11.17	10.58	1779.52	1868.80	812
32	11.98	11.40	12.63	2255.32	2296.32	1031
33	8.70	10.38	9.20	1507.95	1592.32	687
34	8.23	9.12	8.40	1586.17	1692.16	723
35	10.36	10.48	10.71	1749.11	1807.36	798
36	19.44	14.26	20.58	3361.16	3440.64	1540
37	16.04	10.31	16.90	2668.11	2721.28	1221
38	10.30	10.19	10.91	2148.86	2219.52	982
39	9.87	12.76	9.80	1436.26	1523.20	654
40	12.28	11.21	11.57	2539.93	2693.12	1162
41	12.97	11.64	13.41	1892.50	1937.92	864
42	8.68	9.50	8.48	1531.85	1566.72	698
43	7.73	9.73	8.63	1616.58	1728.00	737
44	14.34	12.44	14.88	2526.89	2544.64	1156
45	9.19	9.29	8.86	2231.42	2306.56	1020
46	12.60	10.67	12.70	2344.39	2337.28	1072
47	11.69	9.66	11.67	2546.45	2488.32	1165
48	6.73	9.00	6.48	1464.50	1528.32	667
49	6.44	8.13	6.03	1564.45	1602.56	713
50	11.32	9.92	10.01	2051.10	2173.44	937

51	12.45	13.10	12.40	1714.35	1832.96	782
52	11.92	11.37	12.45	2035.89	2091.52	930
53	15.13	12.03	15.45	2566.00	2652.16	1174
54	13.02	11.33	13.26	2233.60	2339.84	1021
55	11.92	11.99	11.47	2242.29	2393.60	1025
56	19.14	12.69	20.17	3541.48	3548.16	1623
57	7.11	9.37	6.52	1505.78	1617.92	686
58	6.17	8.99	5.88	1264.62	1372.16	575
59	13.39	11.59	13.72	2292.25	2373.12	1048
60	13.13	13.02	12.18	1955.50	2048.00	893
61	7.95	7.67	7.10	1703.49	1786.88	777
62	9.99	11.60	10.15	1962.02	2068.48	896
63	13.70	9.94	14.06	2385.68	2488.32	1091
64	9.44	9.68	8.97	1933.78	2027.52	883
65	11.62	10.51	11.36	2046.75	2181.12	935
66	6.82	9.13	6.29	1379.77	1484.80	628
67	6.94	7.84	6.78	1601.38	1687.04	730
68	14.02	11.51	14.85	2831.05	2987.52	1296
69	11.31	11.59	11.40	1879.47	1971.20	858
70	9.96	9.34	8.80	1996.79	2140.16	912
71	7.31	8.10	6.39	1457.99	1597.44	664
72	13.34	9.36	13.52	2663.77	2693.12	1219
73	14.88	12.81	15.53	2568.17	2672.64	1175
74	11.84	10.37	11.75	2185.80	2237.44	999
75	12.83	11.23	12.64	2157.55	2242.56	986
76	12.52	10.79	12.52	2122.80	2176.00	970
77	9.45	9.10	8.57	1827.32	1927.68	834
78	16.43	11.48	16.74	2976.61	2964.48	1363
79	12.85	10.59	12.82	2227.07	2280.96	1018
80	9.07	9.55	7.05	1801.25	1781.76	822
81	10.09	8.88	9.92	2105.42	2137.60	962
82	11.32	10.15	11.16	2489.95	2552.32	1139
83	8.37	8.71	8.46	1951.15	1937.92	891
84	11.54	9.25	11.23	2305.29	2408.96	1054
85	6.28	9.27	4.92	1223.35	1282.56	556
86	7.77	8.36	6.84	1444.95	1507.84	658
87	12.62	10.40	12.57	2009.82	2076.16	918

88	14.77	10.79	15.70	2854.95	2956.80	1307
89	8.11	8.46	7.39	1744.77	1758.72	796
90	14.34	11.60	13.61	2448.68	2370.56	1120
91	10.32	9.21	9.95	1953.33	2035.20	892

b) Standard

92	6.07	7.86	5.50	1255.93	1354.24	571
93	8.43	10.86	7.05	1405.84	1479.68	640
94	7.54	8.41	6.22	1488.40	1553.92	678
95	10.30	11.60	10.03	1653.51	1738.24	754
96	6.44	8.16	5.46	1062.58	1118.72	482
97	8.21	8.76	7.51	1564.45	1669.12	713
98	7.56	9.64	6.31	1229.86	1295.36	559
99	5.91	7.98	4.66	1040.85	1146.88	472
100	8.27	10.68	8.07	1410.18	1464.32	642
101	8.00	10.23	6.82	1381.94	1448.96	629
102	6.60	9.37	5.31	962.64	1031.68	436
103	6.79	9.72	6.05	1392.81	1423.36	634
104	8.30	10.07	7.60	1303.74	1338.88	593
105	8.50	9.76	8.08	1590.51	1702.40	725
106	6.94	10.61	5.93	1136.44	1216.00	516
107	6.74	8.90	5.90	1479.71	1623.04	674
108	6.19	9.01	3.88	877.90	906.24	397
109	5.23	9.27	3.95	682.38	732.16	307
110	5.93	9.03	5.62	1219.00	1326.08	554
111	12.85	10.58	12.34	2244.46	2219.52	1026
112	6.39	7.31	5.00	1101.68	1149.44	500
113	8.28	8.77	7.51	1633.96	1751.04	745
114	8.74	10.83	7.99	1736.08	1774.08	792
115	3.54	5.98	2.65	749.72	808.96	338
116	9.31	12.20	8.83	1351.53	1367.04	615
117	14.20	11.47	4.70	2522.55	2736.64	1154
118	5.17	9.89	5.40	769.28	814.08	347
119	5.68	9.62	4.90	777.97	847.36	351
120	4.86	8.75	3.52	595.47	660.48	267
121	9.91	12.39	9.64	1638.31	1753.60	747

122	6.90	9.82	6.76	1184.24	1251.84	538
123	10.46	13.00	10.41	1601.38	1671.68	730
124	8.44	10.39	7.97	1412.36	1497.60	643
125	5.83	8.92	4.81	932.22	1013.76	422
126	7.77	11.89	7.25	1219.00	1272.32	554
127	5.69	11.50	5.59	871.39	919.04	394
128	7.09	11.02	5.54	1027.82	1105.92	466
129	7.12	8.75	6.26	1247.24	1262.08	567
130	11.58	12.92	10.91	1746.94	1576.96	797
131	4.66	8.89	3.12	843.14	939.52	381
132	4.58	8.47	4.32	873.56	936.96	395
133	7.53	9.72	7.30	1507.95	1576.96	687
134	11.11	13.62	10.80	1599.20	1699.84	729
135	6.79	10.28	6.10	1049.54	1093.12	476
136	8.47	11.46	7.94	1381.94	1415.68	629
137	5.97	10.54	5.34	1119.06	1169.92	508
138	6.24	9.49	5.45	1029.99	1111.04	467
139	5.41	9.39	4.01	867.04	875.52	392
140	8.32	10.74	7.23	1373.25	1405.44	625
141	10.02	12.95	9.52	1288.52	1344.00	586
142	7.70	8.98	7.69	1736.08	1827.84	792
143	8.91	10.60	8.34	1338.49	1400.32	609
144	5.38	9.31	3.97	771.46	814.08	348
145	6.43	8.77	4.99	1221.17	1274.88	555
146	7.41	10.08	6.56	1438.44	1472.00	655
147	4.61	8.96	4.05	882.25	936.96	399
148	4.88	8.25	3.95	858.35	931.84	388
149	7.29	8.98	6.61	1403.67	1489.92	639
150	7.57	9.61	6.74	1421.05	1489.92	647
151	8.40	14.61	8.41	1212.48	1236.48	551
152	7.13	10.47	7.18	1258.11	1300.48	572
153	6.74	9.59	6.15	1255.93	1326.08	571
154	8.38	11.29	8.09	1329.81	1390.08	605
155	5.23	10.01	4.39	919.19	983.04	416
156	8.00	10.62	7.23	1277.66	1379.84	581
157	7.24	9.43	7.14	1408.01	1489.92	641
158	9.87	12.19	9.00	1223.35	1287.68	556

159	7.59	10.80	6.58	1264.62	1300.48	575
160	5.52	9.07	4.46	749.72	783.36	338
161	7.42	10.85	6.88	1405.84	1482.24	640
162	8.42	9.41	8.08	1657.86	1763.84	756
163	7.12	10.72	6.49	1308.08	1408.00	595
164	7.63	11.56	6.79	1208.14	1269.76	549
165	5.22	6.21	4.32	1166.86	1249.28	530
166	9.25	9.83	8.02	1809.94	1930.24	826
167	7.39	10.79	6.76	1527.50	1589.76	696
168	7.74	8.58	6.15	1379.77	1482.24	628
169	9.99	10.69	9.06	1620.93	1720.32	739
170	9.63	12.16	8.96	1381.94	1441.28	629
171	7.03	11.71	6.09	1125.58	1213.44	511
172	5.27	7.87	4.93	1190.76	1246.72	541
173	5.48	9.60	4.54	975.67	1018.88	442
174	6.47	11.70	5.85	1149.47	1269.76	522
175	7.62	10.97	7.09	1440.61	1548.80	656
176	7.19	10.22	6.76	1303.74	1425.92	593
177	5.53	9.00	5.29	1297.22	1364.48	590
178	8.98	11.13	8.60	1392.81	1428.48	634
179	5.46	10.05	4.33	899.64	952.32	407
180	7.24	19.94	6.35	1271.14	1344.00	578
181	7.54	10.81	6.84	1364.56	1461.76	621
182	9.50	11.75	9.35	1527.50	1615.36	696
183	5.46	8.52	4.19	993.05	1044.48	450
184	5.83	8.67	4.04	940.91	1031.68	426
185	5.62	9.54	4.46	849.66	926.72	384
186	9.87	10.66	9.66	1818.63	2009.60	830
187	7.56	10.48	7.37	1368.91	1477.12	623
188	10.31	10.37	9.84	1868.60	2022.40	853
189	6.73	8.58	5.48	1199.45	1246.72	545
190	10.04	12.14	9.26	1710.01	1792.00	780
191	7.62	10.14	6.90	1560.09	1597.44	711
192	8.07	10.75	6.65	1614.41	1702.40	736
193	15.31	11.15	14.91	2583.38	2629.12	1182
194	6.90	9.14	5.58	1125.58	1187.84	511
195	9.89	12.82	9.58	1731.73	1845.76	790

196	7.03	9.34	5.86	1260.28	1351.68	573
197	11.96	12.07	11.99	2120.62	2181.12	969
198	7.55	10.48	6.06	1299.39	1402.88	591
199	5.43	8.72	4.37	884.42	977.92	400
200	4.96	8.34	4.01	914.84	972.80	414
201	8.11	9.41	7.42	1831.67	1958.40	836
202	5.00	7.67	2.89	875.73	942.08	396
203	5.81	7.54	3.20	751.89	821.76	339
204	4.78	6.49	3.97	884.42	972.80	400
205	5.70	8.10	4.64	1340.67	1607.68	610
206	9.25	9.60	9.00	1970.72	2050.56	900

Appendix C. Image Display Software

The following is the listing of the source code of the image display software written in Turbo PASCAL version 3.1.

```
PROGRAM DIGICAM;

(*$I TYPEDEF.SYS *)      (* Routines of the Turbo-Graphix Toolbox *)
(*$I GRAPHIX.SYS *)
(*$I KERNEL.SYS *)

CONST STPT                = $0318; (* Camera Status Port *)
      DTPT                = $0319; (* Data Port Camera  *)
      MaxBytes            = 1024;

TYPE ByteArray            = ARRAY[1..1024] OF BYTE;(* 64*128 Pixels *)

VAR Storage               : TEXT;
      Filename            : STRING[14];
      Save_or_not        : BOOLEAN;
      Main_Array_Counter,X_direction : Integer;
      Y_direction,PixelCounter : Integer;
      PixelCounter2,PictureCounter,Ct,I : Integer;
```

```

Values                : ByteArray;
ErrorCounter,ErrorCt  : Integer;
ControlVal,BYT        : Byte;
Area, SampleCounter   : Integer;
Answer,ch              : Char;

```

(* ----- *)

PROCEDURE RECEIVEIMAGE;

```

var cb : byte;
Label Next,NEXT1;

```

BEGIN

```

controlval := 0;
Ct := 0;
ErrorCounter := 0;
ErrorCt := 0;

```

```

repeat until (port[stpt] and 64) = 64; (* A COMMAND MAY BE SEND TO DCAM *)
  Port[dtpt] := $5B; (* SOAK and SEND *)
  Delay(73); (* Exposure Time *)

```

```

repeat until (port[stpt] and 64) = 64; (* A COMMAND MAY BE SEND TO DCAM *)
  Port[dtpt] := $5B; (* SOAK and SEND *)
  INLINE($FA); (* turn interrupts off *)
  (* avoid trouble with timer-interrupt *)

```

FOR I := 1 TO MaxBytes DO

BEGIN

Repeat

```

  Ct := SUCC(Ct); (* successor of CT *)
  If ct > 10000 then Goto Next; (* avoid endless Loop *)
  cb := PORT[STPT];

```

(* if the Status-Port > 192 then a Bit was lost during transmission *)

```

    until cb > 64;
    Values[I] := PORT[DTPT]          (* Datas -> Array *)
END;

Next:          (* Jump to this Label if to many Errors *)

INLINE($FB);          (* turn interrupts on *)

end;

(* ----- *)

PROCEDURE SET_GRAPHIC;

begin
  InitGraphic;
  DefineWindow(1,0,0,XMaxGlb,YMaxGlb);          (* Maximum Window *)
  DefineWorld(1,128,0,0,200);          (* Camera-Array 64*128 Pixels *)
  SetClippingOn;
  SelectScreen(2);          (* Select the invisible Screen to draw on *)
  SelectWorld(1);
  SelectWindow(1);
  SetLineStyle(0);
end;

(* ----- *)

PROCEDURE MAKE_BOX_DRAW_TEXT; (* # of pictures, Pixels and Area Writer *)

var PixelText : STRING[5];

begin
  DrawLine(0,0,128,0);          (* Draw Box *)
  DrawLine(128,0,128,64);          (* Toolbox's Procedure *)
  DrawLine(128,64,0,64);
  DrawLine(0,64,0,0);
  DrawLine(32,0,32,64);

```

```

DrawLine(96,0,96,64);

DrawTextW(80,150,2,'To Continue');
DrawTextW(84,120,2,'Press Any Key !');
STR(PictureCounter,PixelText);
DrawTextW(120,98,1,'Number of Pictures = ');
DrawTextW(90,100,2,PixelText);          (* # of Pictures taken *)
STR(PixelCounter,PixelText);
DrawTextW(60,98,1,'Number of Pixels = ');
DrawTextW(30,100,2,PixelText);          (* # of Pixels counted *)
Area := Round(0.00*PixelCounter);      (* Area & Pixel's Relationship *)
STR(Area,PixelText);
DrawTextW(60,78,1,'Area = ');
DrawTextW(30,80,2,PixelText);          (* The corresponding Area *)
DrawTextW(12,78,1,'mm square');
end;

```

```
(* ----- *)
```

```
PROCEDURE BYTE_PLOT;
```

```

begin
for I:= 1 to 8 do
begin
(* check if highest Bit is set *)
if (BYT and 128) < > 128 then
begin
DrawPoint(X_direction,Y_direction);
PixelCounter := SUCC(PixelCounter);      (* save later *)
end;
X_direction := SUCC(X_direction);
BYT := BYT SHL 1;      (* shift left 8 times to scan the whole Byte *)
end;
end;

```

```
(* ----- *)
```

```

PROCEDURE PIXELS_COUNTER;

Var Row, Column : INTEGER;

begin
  X_direction := 32;          (* Reset Counters *) (* X-Direction *)
  PixelCounter := 0;         (* Pixels set *)
  for Row := 1 to 64 do
    begin
      Y_direction := Row;
      for Column := 5 to 12 do
        begin
          Main_Array_Counter := Column + 16*(Row - 1);
          BYT := Values[Main_Array_Counter];
          BYTE_PLOT;
        end;
      X_direction := 32;
    end;
  end;

  (* ----- *)

PROCEDURE WRITE_TO_FILE;          (* Store Data into File *)

Var AreaStore, AreaStore2 : real;
    Row, Column          : Integer;

begin
  PixelCounter := 0;          (* Pixels set *)
  Writeln;
  Write('Enter the Sample Number = ');
  Read(SampleCounter);
  RECEIVEIMAGE;

  for Row := 1 to 64 do
    begin

```

```

Y_direction := Row;
for Column := 5 to 12 do
begin
  Main_Array_Counter := Column + 16*(Row - 1);
  BYT := Values[Main_Array_Counter];
  for I := 1 to 8 do
  begin
    if (BYT and 128) < > 128 then PixelCounter := SUCC(PixelCounter);
    BYT := BYT SHL 1;
  end;
end;
end;
AreaStore := 0.00*PixelCounter;

ClrScr;
Filename := 'DISPLAY1.OUT';
ASSIGN(Storage,Filename);
APPEND(Storage);
WriteLn(Storage,SampleCounter:5,PixelCounter:10,AreaStore:20:5);
CLOSE(Storage);
end;

(* ----- *)

begin          (* MAIN *)
  ClrScr;

  PORT[STPT] := $C0;  (* Master Reset *)
  PORT[STPT] := $28;

  REPEAT
    PictureCounter := 1;
    Write('Save the Data ( Y/N ) ? ');
    Read(ch);
    if upcase(ch) = 'Y' then Save_or_not := TRUE else Save_or_not := FALSE;
    if Save_or_not then WRITE_TO_FILE;
    SET_GRAPHIC;

```

```
REPEAT
  RECEIVEIMAGE;
  PIXELS_COUNTER;
  MAKE_BOX_DRAW_TEXT;
  SwapScreen;
  ClearScreen;
  PictureCounter := SUCC(PictureCounter);
UNTIL (keypressed);
LeaveGraphic;
write('Another Test ( Y / N ) ? ');
Read(Answer);

Writeln;
UNTIL upcase(Answer) = 'N';
end.                                (* MAIN *)
```

Appendix D. System Software

The following is the listing of the system software written in Turbo PASCAL version 4.0.

```
PROGRAM DIGICAM;

uses Crt;

CONST STPT           = $0318; (* Camera Status Port *)
      DTPT           = $0319; (* Data Port Camera  *)
      MaxBytes       = 1024;  (* (64*128)/8 = 1024 Bytes *)

TYPE ByteArray      = ARRAY[1..1024] OF BYTE;(* 64*128 Pixels *)
      VolumeArray   = ARRAY[1..10] OF INTEGER;
      SizeArray     = ARRAY[1..10] OF STRING[20];

VAR True_Or_False   : BOOLEAN;
      Image_Data    : ByteArray;
      BYT           : Byte;
      Volume        : VolumeArray;
      Size          : SizeArray;
      Main_Array_Counter,PixelCounter : Integer;
      Ct,I,Image_No,Oyster_No,Detect : Integer;
```

```

ErrorCounter,ErrorCt,ControlVal   : Integer;
Row,Column,Row_No,ExSmall        : Integer;
Standard,Select,Large,ExLarge    : Integer;
KeyPress                           : Char;

```

```
(* ----- *)
```

```
PROCEDURE RECEIVEIMAGE;
```

```
var cb : byte;
Label Next;
```

```

BEGIN                                     (* begin ReceiveImage *)
controlval := 0;
Ct := 0;
ErrorCounter := 0;
ErrorCt := 0;
Repeat until (port[stpt] and 64) = 64; (* A COMMAND MAY BE SEND TO DCAM *)
Port[dtpt] := $5B;                       (* SOAK and SEND *)
INLINE($FA); (* turn interrupts off, avoid trouble with timer-interrupt *)
for I := 1 to MaxBytes do                 (* 70 millisecc *)
begin
Repeat
Ct := SUCC(Ct);                          (* successor of CT *)
If ct > 10000 then Goto Next;             (* avoid endless Loop *)
cb := PORT[STPT];                        (* if the Status-Port > 192 *)
                                        (* then a Bit was lost during transmission *)
until cb > 64;
Image_Data[I] := PORT[DTPT];              (* Data -> Array *)
end;

Next:                                     (* Jump to this Label if to many Errors *)

INLINE($FB);                             (* turn interrupts on *)
end;

```

```
(* ----- *)
```

PROCEDURE DRAW_BOX;

```
Var Top1,Top2,Bottom1,Bottom2      : Char;  
    LineTop,LineSide,BarT1,BarT2   : Char;  
    Inbox1,Inbox2,Inbox3           : Char;  
    SBox1,SBox2,SBox3,SBox4,SBox5,SBox6 : Char;  
    TBar1,TBar2,Tbar3,Tbar4,Tbar5   : Char;
```

```
Begin      (* This procedure is to draw display graphic *)  
    Top1 := #201;  
    Top2 := #187;  
    Bottom1 := #200;  
    Bottom2 := #188;  
    LineTop := #205;  
    LineSide := #186;  
    BarT1 := #204;  
    BarT2 := #185;  
    Inbox1 := #254;  
    Inbox2 := #222;  
    Inbox3 := #221;  
    SBox1 := #192;  
    Sbox2 := #217;  
    Sbox3 := #218;  
    Sbox4 := #191;  
    SBox5 := #179;  
    SBox6 := #196;  
    TBar1 := #197;  
    Tbar2 := #193;  
    Tbar3 := #194;  
    TBar4 := #180;  
    Tbar5 := #195;  
    GotoXY(1,1);Write(Top1);  
    For I := 1 to 77 Do write(LineTop);  
    GotoXY(78,0);Write(Top2);  
    For I := 2 to 25 Do Begin GotoXY(1,I);Write(LineSide);End;  
    For I := 2 to 25 Do Begin GotoXY(79,I);Write(LineSide);End;
```

```

GotoXY(1,25);For I := 1 to 78 Do write(LineTop);
GotoXY(1,25);Write(Bottom1);
GotoXY(79,25);Write(Bottom2);
GotoXY(1,23);Write(BarT1);
GotoXY(2,23);For I := 1 to 77 Do Write(LineTop);
GotoXY(79,23);Write(BarT2);
GotoXY(25,2);For I := 1 to 30 do Write(InBox1);
GotoXY(25,7);For I := 1 to 30 do Write(InBox1);
GotoXY(25,2);For I := 1 to 4 do Begin Gotoxy(25,2 + I);Write(Inbox2);End;
GotoXY(54,2);For I := 1 to 4 do Begin Gotoxy(54,2 + I);Write(Inbox3);End;
GOTOXY(33,3);Write('OYSTER SORTER');
GotoXY(38,4);Write('By');
GotoXY(35,5);Write('T. W. Awa');
GotoXy(37,6);Write('1988');
GotoXY(29,9);Write('OYSTER NO:   SIZE');
For I := 1 to 5 Do begin GotoXY(33,10 + I);Write(I);End;
GotoXY(7,17);write('Total Number of Oysters in each Category :');
GotoXy(7,19);Write('Very Small');
GotoXy(22,19);Write('Standard');
GotoXy(37,19);Write('Select');
GotoXy(48,19);Write('Extra Select');
GotoXY(64,19);Write('Extra Large');
GotoXY(4,18);Write(SBox3);
GotoXY(4,22);Write(SBox1);
GotoXY(76,18);Write(SBox4);
GotoXY(76,22);Write(SBox2);
GOtoXy(5,18);For I := 1 to 71 Do Write(SBox6);
GOtoXy(5,20);For I := 1 to 71 Do Write(SBox6);
GOtoXy(5,22);For I := 1 to 71 Do Write(SBox6);
For I := 1 to 3 do begin GotoXY(4,18 + I);Write(SBox5);End;
For I := 1 to 3 do begin GotoXY(18,18 + I);Write(SBox5);End;
For I := 1 to 3 do begin GotoXY(32,18 + I);Write(SBox5);End;
For I := 1 to 3 do begin GotoXY(46,18 + I);Write(SBox5);End;
For I := 1 to 3 do begin GotoXY(61,18 + I);Write(SBox5);End;
For I := 1 to 3 do begin GotoXY(76,18 + I);Write(SBox5);End;
GotoXY(18,20);write(Tbar1);GotoXy(18,18);write(Tbar3);
GotoXy(18,22);write(Tbar2);

```

```

GotoXY(32,20);Write(Tbar1);GotoXy(32,18);write(Tbar3);
GotoXy(32,22);write(Tbar2);
GotoXy(46,20);Write(Tbar1);GotoXy(46,18);write(Tbar3);
GotoXy(46,22);write(Tbar2);
GotoXY(61,20);write(Tbar1);GotoXy(61,18);write(Tbar3);
GotoXy(61,22);write(Tbar2);
GotoXy(4,20);write(Tbar5);Gotoxy(76,20);write(Tbar4);
GotoXY(25,24);Write('TO CONTINUE - Press Any Key !');

```

End;

```
(* ----- *)
```

```
PROCEDURE PICTURE_DETECTOR(Row_Detect : Integer);
```

```
Begin (* This procedure is to detect the existing of a good picture *)
```

```
PixelCounter := 0;
```

```
For Column := 3 to 10 do
```

```
Begin
```

```
Main_Array_Counter := Column + 16*(Row_Detect-1);
```

```
If Image_Data[Main_Array_Counter] < > 255
```

```
Then PixelCounter := SUCC(PixelCounter);
```

```
end;
```

```
True_Or_False := PixelCounter = 0
```

```
End;
```

```
(* ----- *)
```

```
PROCEDURE PIXEL_COUNTER;
```

```
Begin (* This procedure is to count the number of dark pixels *)
```

```
PixelCounter := 0;
```

```
Image_No := SUCC(Image_No);
```

```
For Row := 1 to 64 Do (* Total number of rows = 64 *)
```

```
For Column := 3 to 10 do (* Total number of column used = 7 bytes *)
```

```
begin
```

```
Main_Array_Counter := Column + 16*(Row - 1);
```

```
BYT := Image_Data[Main_Array_Counter];
```

```

For I := 1 to 8 do
begin
  If (BYT and 128) < > 128 Then PixelCounter := SUCC(PixelCounter);
  BYT := BYT SHL 1
end
end;
Volume[Image_No] := PixelCounter;
If Image_No = 5 Then          (* To grade 5 oysters at a time *)
Begin
  For I := 1 to 5 Do
  Begin
    Oyster_No := SUCC(Oyster_No);          (* Oyster's Categories *)
    If Volume[I] < 309 Then
    Begin
      Size[I] := 'Very Small  ';
      ExSmall := SUCC(ExSmall)
    End;
    If (Volume[I] > = 309) and (Volume[I] < 569) Then
    Begin
      Size[I] := 'Standard  ';
      Standard := SUCC(Standard)
    End;
    If (Volume[I] > = 569) and (Volume[I] < 849) Then
    Begin
      Size[I] := 'Select  ';
      Select := SUCC(Select)
    End;
    If (Volume[I] > = 849) and (Volume[I] < 1144) Then
    Begin
      Size[I] := 'Extra Select  ';
      Large := SUCC(Large)
    End;
    If Volume[I] > = 1144 Then
    Begin
      Size[I] := 'Extra Large  ';
      ExLarge := SUCC(ExLarge)
    End;
  End;
End;

```

```

    GotoXY(22,10 + I);Write(Oyster_NO:5,' ',Size[I],Volume[I],' ');
    GotoXY(10,21);Write(ExSmall);
    GotoXY(25,21);Write(Standard);
    GotoXY(40,21);Write(Select);
    GotoXY(55,21);Write(Large);
    GotoXY(70,21);Write(ExLarge);
    GotoXy(54,24)
End;
Image_No := 0;
End
End;

(* ----- MAIN ----- *)

Begin

PORT[STPT]:= $C0;                (* Master Reset *)
PORT[STPT]:= $28;

ClrScr;
ExSmall := 0;
Standard := 0;
Select := 0;
Large := 0;
ExLarge := 0;
Oyster_No := 0;
Image_No := 0;
DRAW_BOX;
REPEAT
    RECEIVEIMAGE;
    True_Or_False := TRUE;
    PICTURE_DETECTOR(1);
    If True_Or_False = TRUE Then
        Begin
            PICTURE_DETECTOR(64);
            If True_Or_False = TRUE Then
                Begin

```

```

PICTURE_DETECTOR(15);
CASE True_Or_False of
  FALSE : PIXEL_COUNTER;
  TRUE  : Begin
    PICTURE_DETECTOR(30);
    CASE True_Or_False of
      FALSE : PIXEL_COUNTER;
      TRUE  : Begin
        PICTURE_DETECTOR(45);
        If True_Or_False = FALSE Then PIXEL_COUNTER;
      End
    End
  End
End
End
End;
UNTIL KeyPressed;
End.                                (* MAIN *)

```

Appendix E. System Calibration Data

The following is the data collected for system calibration at stationary position and at four different motor speeds.

Obs	Stationary	Motor Speed (Revolutions per Minute)				Actual Area (mm ²)
		7.5 RPM	10 RPM	15 RPM	20 RPM	
1	809	652	588	454	349	1867.63
2	810	652	592	450	370	1867.63
3	810	647	590	450	365	1867.63
4	808	645	586	446	372	1867.63
5	811	642	590	447	358	1867.63
6	816	641	577	447	350	1867.63
7	819	629	575	454	361	1867.63
8	819	634	567	451	346	1867.63
9	817	628	576	452	346	1867.63
10	819	635	575	452	346	1867.63
11	835	665	593	480	383	1881.65
12	834	659	592	482	384	1881.65
13	835	660	581	480	382	1881.65
14	832	665	583	475	378	1881.65
15	831	656	594	475	392	1881.65
16	825	661	583	455	375	1881.65

17	827	653	578	460	370	1881.65
18	829	658	590	454	358	1881.65
19	828	651	585	462	368	1881.65
20	827	652	584	451	374	1881.65
21	392	313	285	218	157	1020.08
22	392	314	286	212	156	1020.08
23	392	312	279	218	148	1020.08
24	392	309	276	212	153	1020.08
25	392	324	284	212	153	1020.08
26	393	312	261	208	131	1020.08
27	394	307	263	192	123	1020.08
28	392	304	272	194	122	1020.08
29	395	305	262	181	136	1020.08
30	396	310	263	191	129	1020.08
31	674	521	496	390	312	1554.22
32	674	515	491	376	302	1554.22
33	672	519	482	380	303	1554.22
34	671	514	489	384	306	1554.22
35	673	520	487	374	298	1554.22
36	666	524	480	364	286	1554.22
37	664	518	473	357	293	1554.22
38	667	521	470	362	290	1554.22
39	666	523	470	354	285	1554.22
40	667	528	473	362	290	1554.22
41	734	587	537	410	338	1700.50
42	736	591	533	416	329	1700.50
43	735	581	522	407	328	1700.50
44	734	594	528	408	324	1700.50
45	736	586	538	409	330	1700.50
46	736	577	518	394	309	1700.50
47	735	579	522	388	312	1700.50
48	737	574	520	390	325	1700.50
49	738	578	519	392	311	1700.50
50	735	576	523	392	318	1700.50
51	990	781	707	537	455	2228.43
52	989	785	699	545	451	2228.43
53	990	775	695	557	469	2228.43

54	990	776	694	555	452	2228.43
55	990	777	688	553	452	2228.43
56	1002	773	706	538	446	2228.43
57	1004	768	693	540	436	2228.43
58	1004	778	699	524	444	2228.43
59	1002	774	689	542	435	2228.43
60	1004	769	688	540	439	2228.43
61	380	294	256	186	124	945.83
62	376	290	259	189	119	945.83
63	377	295	259	187	125	945.83
64	377	290	255	172	117	945.83
65	374	292	257	178	119	945.83

Appendix F. Cross Validation Data

The following is the cross validation data for the calibrated area-pixel equation at motor speed of 15 RPM.

Metal Target no.	Pixels	Actual Area mm²	Predicted Area mm²
1	476	1867.63	1951.65
	483	1867.63	1975.84
	481	1867.63	1968.93
	483	1867.63	1975.84
	487	1867.63	1989.66
	483	1867.63	1975.84
	484	1867.63	1979.30
	482	1867.63	1972.39
	484	1867.63	1979.30
	481	1867.63	1968.93
	2	475	1881.65
484		1881.65	1979.30
488		1881.65	1993.12
488		1881.65	1993.12
490		1881.65	2000.03
480		1881.65	1965.47
491		1881.65	2003.49
477		1881.65	1955.11

	497	1881.65	2024.22
	485	1881.65	1982.75
3	218	1020.08	1060.11
	224	1020.08	1080.84
	219	1020.08	1063.56
	223	1020.08	1077.38
	227	1020.08	1091.21
	219	1020.08	1063.56
	218	1020.08	1060.11
	219	1020.08	1063.56
	226	1020.08	1087.75
	219	1020.08	1063.56
4	396	1554.22	1675.20
	402	1554.22	1695.94
	402	1554.22	1695.94
	395	1554.22	1671.75
	408	1554.22	1716.67
	402	1554.22	1695.94
	404	1554.22	1702.85
	404	1554.22	1702.85
	406	1554.22	1709.76
	400	1554.22	1689.03
5	419	1700.50	1754.68
	425	1700.50	1775.42
	431	1700.50	1796.15
	416	1700.50	1744.32
	438	1700.50	1820.34
	417	1700.50	1747.77
	431	1700.50	1796.15
	426	1700.50	1778.87
	428	1700.50	1785.78
	419	1700.50	1754.68

Appendix G. Calibration Data with 6.5 mm Lens

The following is the data collected for digital camera with 6.5 mm C-mount Lens.

Obs	Actual Area (mm ²)	Pixels
1	3825.36	1762
2	1881.65	855
3	1881.65	840
4	1881.65	840
5	1010.75	427
6	1010.75	427
7	1010.75	428
8	1010.75	428
9	1096.41	449
10	1096.41	455
11	1096.41	462
12	1096.41	450
13	1704.08	733
14	1704.08	748
15	1704.08	751
16	782.83	291
17	782.83	275
18	458.06	171
19	458.06	171

Vita

The author, Teck Wah Awa, son of Sing Awa and Sun Ying, was born in Seremban, Negeri Sembilan, Malaysia, on September 23, 1962. He received his Malaysia Certificate of Education in December 1979. The author went to Canada in January of 1980. He attended Park Avenue Academy, Toronto, Ontario, Canada and completed his Ontario Secondary School Honour Graduation Diploma in Summer 1980. He then enrolled to University of Guelph, Guelph, Ontario, Canada and received his Bachelor of Science Degree in Agricultural Engineering in Spring 1985. In Fall 1986 he enrolled at Virginia Polytechnic Institute and State University as a graduate student in Agricultural Engineering Department.